Exploration of geothermal resources in the Alberta Basin, Canada

vorgelegt von
Diplom Geologe
Simon Weides
geb. in Köln

von der Fakultät VI – Planen Bauen Umwelt
der Technischen Universität Berlin
zur Erlangung des akademischen Grades

Doktor der Ingenieurwissenschaften
- Dr. Ing. -

genehmigte Dissertation

Promotionsausschuss:

Vorsitzender: Prof. Dr. Uwe Tröger
Gutachter: Prof. Dr. Wilhelm Dominik
Gutachterin: Prof. Dr. Inga Moeck (University of Alberta)

Tag der wissenschaftlichen Aussprache: 14. Juli 2014

Berlin 2014

Preface

This work is presented as cumulative doctoral thesis and is related to the Helmholtz–Alberta Initiative (HAI), an independent research collaboration between the Helmholtz Association of German Research Centres and the University of Alberta.

This thesis is based on four scientific articles, which either have already been published in a scientific peer reviewed journal, or are ongoing submitted for publication:

1) Weides, S., Moeck, I., Majorowicz, J., Palombi, D., and Grobe, M. (2013): "Geothermal exploration of Paleozoic formations in central Alberta", Canadian Journal of Earth Sciences, 2013, 50(5): 519–534, doi: 10.1139/cjes-2012-0137 (Chapter 2 of this thesis).

2) Weides, S., Moeck, I., Majorowicz, J., and Grobe, M. (2014): "The Cambrian Basal Sandstone Unit in central Alberta—an investigation of temperature distribution, petrography and hydraulic and geomechanical properties of a deep saline aquifer", Canadian Journal of Earth Sciences, 2014, 51: 783–796, doi: 10.1139/cjes-2014-0011 (Chapter 3 of this thesis)

3) Chapter 4: Weides, S., Moeck, I., Schmitt, D. and Majorowicz, J. (2014): "An integrative geothermal resource assessment study for the siliciclastic Granite Wash unit, northwestern Alberta (Canada)", Environmental Earth Sciences, published online first 10 May 2014, doi: 10.1007/s12665-014-3309-3. (Chapter 4 of this thesis)

4) Chapter 5: Weides, S., and Majorowicz, J. (2014): "Implications of spatial variability in heat flow for geothermal resource evaluation in large foreland basins: the case of the Western Canada Sedimentary Basin", Energies, 2014, 7(4), 2573–2594, doi: 10.3390/en7042573. (Chapter 5 of this thesis).

Permeability in this thesis is given in m². In petroleum engineering and geology, the units *darcy* (D) and *millidarcy* (mD) are widely used. 1 *darcy* is equivalent to 9.869233×10^{-13} m^2.

The term porosity is used in this thesis to describe the effective porosity of rocks.

Acknowledgements

I would like to thank several people without whom this thesis would not have been possible.

First of all I would like to express my gratitude to my scientific supervisors *Prof. Wilhelm Dominik* from the Technical University of Berlin and *Prof. Inga Moeck* from the University of Alberta for their support and encouragement during the last 4 years.

I wish to thank *Prof. Ernst Huenges* and all colleagues from section 4.1 at the German Research Center for Geosciences for providing an excellent and enjoyable working environment. Special thanks to my colleagues *Fiorenza Deon, Andrea and Hans-Jürgen Förster, Anna Jentsch, Egbert Jolie, Stefan Klapperer, Ben Norden* and *Mochamad Nukman* from the exploration geology cluster.

I would like to thank our project partners *Prof. Martyn Unsworth, Prof. Doug Schmitt, Jacek Majorowicz* and *Hannes Hofmann* from the University of Alberta, and *Matthias Grobe, Dan Palombi* and *Gordon Jean* from the Alberta Geological Survey for the great and fruitful cooperation within the Helmholtz-Alberta Initiative.

Last but not least, special thanks to *Susa*, and to my family and all friends who supported me throughout the PhD thesis.

This research was funded by the Helmholtz Association's Initiative and Networking Fund, the participating Helmholtz Centres and by the Government of Alberta through Alberta Environment's ecoTrust program.

Abstract

Geothermal energy is the thermal energy that is stored and produced in the Earth, and that can be used as clean and renewable energy source. In general, geothermal systems can be categorized based on the type of heat transport and the geologic controls of the heat source, heat transfer mechanism and storage capacity of the system. With regard to these criteria, the Alberta Basin belongs to the conduction-dominated "foreland basin play type". The Alberta Basin has a long tradition of hydrocarbon exploration and production with more than 300,000 wells drilled in the last decades. However, only few studies focused on exploration of geothermal resources, and until to date no geothermal production site exists in Alberta. This thesis analyzes the geothermal conditions of the Alberta Basin and delineates the favorable locations for further geothermal prospection in Alberta. It demonstrates specific exploration methods that can be applied in a situation where a large amount of geological and geophysical data is publicly available and has to be re-evaluated and re-interpreted for geothermal exploration.

The Western Canada Sedimentary Basin (WCSB)—of which the Alberta Basin represents the central part—consists of a north-eastward tapering sedimentary wedge that unconformably overlies the Precambrian crystalline basement. The sedimentary succession thickness is > 5 km close to the Rocky Mountains in the southwest and thins towards the northeast, where it is terminated by erosion or non-deposition.

The thermal state of the WCSB basin was mapped using a large thermal database. Results show that the heat flow and the geothermal gradient of the WCSB range from 30–100 mW/m^2 and 20–55 °C/km, respectively, with an average of 60 mW/m^2 and 33 °C/km, respectively. Thickness, depth, extent and reservoir properties of potential geothermal target formations were investigated in two regional exploration studies focusing on the central Alberta Basin around Edmonton (160 km × 200 km) and the northwestern Alberta Basin around Peace River (70 km × 90 km). The applied methods include 3D structural geological modeling based on well log and seismic data, geostatistical mapping of porosity and permeability data from core tests, and the analysis of the stress state of faults. Six formations were identified as favorable for geothermal applications: the Cambrian Basal Sandstone Unit (BSU) and four Devonian carbonate formations (central Alberta), and the Devonian Granite Wash Unit (northwestern Alberta). The BSU as the most promising geothermal target formation was further investigated by petrographic analysis and porosity-, permeability- and geomechanical testing of BSU core samples.

Zusammenfassung

Die in der Erde gespeicherte Wärmeenergie –geothermische Energie–kann als saubere und erneuerbare Energiequelle genutzt werden. Geothermische Systeme lassen sich anhand der geologischen Kontrollfaktoren bezüglich der Wärmequelle, der Wärmetransportmechanismen und der Speicherfähigkeit des Untergrundes unterscheiden und kategorisieren. Das Alberta Becken wird dabei zum „Vorlandbecken-typus“ gezählt, der durch konduktiv-dominierten Wärmetransport charakterisiert ist.

Aufgrund seiner großen Öl-, Gas- und Kohle- Lagerstätten gehört das Alberta Becken in West–Kanada mit über 300,000 abgeteuften Bohrungen zu den geologisch am intensivsten erkundeten Gebieten der Welt. Dennoch widmeten sich nur vereinzelte Studien dem geothermischen Potential des Beckens, das bisher ungenutzt bleibt.

In der vorliegenden Dissertation werden die geothermischen Bedingungen des Alberta Beckens untersucht, und Gebiete mit besonders günstigen Bedingungen zur weiteren Erkundung ausgewiesen. Dabei wird aufgezeigt, wie existierende Daten aus der Kohlenwasserstofferkundung, die im Falle des Alberta Beckens in großer Zahl vorliegen, für die geothermische Exploration neu interpretiert und genutzt werden können.

Die thermischen Bedingungen des westkanadischen Sedimentbeckens (WCSB), dessen zentraler Teil vom Alberta Becken eingenommen wird, wurden mithilfe einer großen Menge an Temperaturdaten kartiert. Die Ergebnisse zeigen, dass der Wärmefluss und der geothermische Gradient zwischen 30–100 mW/m^2 bzw. 20–55 °C/km liegen, mit Mittelwerten von 60 mW/m^2 bzw. 33 °C/km. Die Eigenschaften von potentiellen geothermischen Reservoirhorizonten wurden in zwei Regionalstudien in Zentral- und Nordwest Alberta untersucht. Zur Analyse von Mächtigkeit, Tiefe, und räumlicher Erstreckung der Horizonte wurden (struktur-) geologische 3D Modelle aus Bohrlochlogdaten und seismischen Daten entwickelt. Der Spannungszustand an geologischen Trennflächen wurde mit der „slip-tendency“ Methode untersucht, und die räumliche Verteilung von Gesteins-Porosität und -Permeabilität (basierend auf Kerntest-Daten) mit geostatistischen Methoden kartiert. Sechs Gesteinsformationen konnten als potentiell geothermisch nutzbar identifiziert werden: der Kambrische „Basal Sandstone“ (BSU), vier Devonische Karbonat-Formationen (alle in Zentral-Alberta), sowie der Devonische „Granite Wash“- Sandstein (in NW Alberta). Der BSU als vielversprechendster der sechs Horizonte wurde mithilfe von petrographischen Analysen und Porositäts-, Permeabilitäts- und Geomechanik-Tests detailliert untersucht.

Abbreviations

AGS	Alberta Geological Survey
APP	Annual Pool Pressure test
B.C.	British Columbia
BHT	Bottom Hole Temperature measurement
BSU	Basal Sandstone Unit
DST	Drill Stem Test
EGS	Enhanced geothermal system
HDR	Hot Dry Rock
GHG	Greenhouse gas
IDW	Inverse Distance Weighting
k	Conductivity
Kmax	Maximum horizontal permeability
Khor	Horizontal permeability
NWT	Northwest Territories
MW_{el}	Megawatt electrical
MW_{th}	Megawatt thermal
Q	Heat flow
P_p	Pore pressure
PRA	Peace River Arch
S.D.	Standard deviation
S_{Hmax}	Maximum horizontal stress
S_{Hmin}	Minimum horizontal stress
S_V	Vertical stress
UCS	Unconfined compressive strength
μ	Coefficient of sliding friction
WCSB	Western Canada Sedimentary Basin

Table of contents

List of figures

List of tables

Chapter 1

Introduction

In times of climate change and discussion about environmental aspects of energy consumption, green energy resources get into the focus of interest. Besides solar and wind, geothermal energy is one of these green alternative energies that could be applied in order to reduce the amount of greenhouse gases emitted to the atmosphere. Geothermal energy is a technology which is in particular dependent on geologic conditions, and positioning the geothermal wells at the right location may decide success or failure of a project. To date no geothermal production site exists in the Alberta Basin, and only few studies on the geothermal potential of the Alberta Basin were conducted. The goal of this thesis is to assess the geothermal resources of the Alberta Basin and to delineate favorable settings for geothermal development in Alberta.

1. What is geothermal energy?

The term geothermal energy describes the use of the thermal energy that is produced and stored in the solid Earth as a clean and renewable energy source. The thermal energy of the crust originates from the decay of radiogenic isotopes such as uranium (^{238}U and ^{235}U), thorium (^{232}Th) and potassium (^{40}K), and from primordial heat from the formation of the planet 4.5 billion years ago. While in earlier studies (e.g. Turcotte & Schubert 2002) radiogenic decay was assumed to be the major contributor to the Earth heat flux, results from a recent study by Gando et al. (2011) indicate that only about a half of the total heat flux can be assigned to radiogenic decay, while the other half can be assigned to primordial heat of the Earth.

Generally, the use of geothermal energy is most efficient (and economic) in regions with a high surface heat flow, where a large amount of thermal energy reaches the shallow subsurface or even the surface. But also in regions where the surface heat flow is in the range of the global average, or even below, it is possible to use the Earth`s heat. In the last decade, under the impression of climate discussion, declining fossil fuel reserves and rising energy costs, renewed efforts have been undertaken to explore and use the geothermal resources of the Earth.

1.1 Categorization of geothermal resources

Different schemes exist to categorize geothermal resources, the majority of them dividing the resources into different classes based on the temperature–respectively the enthalpy–of the geothermal fluids which store and transport the heat from the reservoir to the surface (e.g. from Muffler and Cataldi (1978), Haenel et al. 1988, Hochstein 1988, or Sanyal 2005; see also Williams et al. 2011). Because these schemes were defined by authors working in different geothermal systems all over the world, they differ in the temperature ranges used for categorization. The United States Geological Survey (USGS) (as an example) uses the categorization scheme of Muffler and Cataldi (1978) which divides geothermal systems into low temperature- (< 90 °C), intermediate temperature- (90–150 °C) and high temperature resources (> 150 °C). In contrast, Hochstein (1988) proposed a categorization which uses also three classes, but at significantly higher temperature levels: low temperature (< 125 °C), intermediate temperature (125–225 °C) and high temperature (> 225 °C). Other authors define low temperature as < 100 °C (Benderitter and Cormy 1990), < 150 °C (Nicholson 1993) or 190 °C (Axelsson and Gunnlaugsson 2000). Besides the lack of general agreement on one scheme, the categorization of geothermal resources based on the temperature does not allow for field analog comparisons or the development of appropriate exploration strategies, because a certain temperature can be found in all kinds of geological environments at various depths (Moeck and Beardsmore 2014).

Geothermal resources can also be categorized by the type of heat transport and the geologic controls of the heat source, heat transfer mechanism and storage capacity of the system as proposed by Moeck (2014) and Moeck and Beardsmore (2014) in the „geothermal play type“ catalog. A geothermal play is defined by the reservoir unit, the heat charge system, the regional topseal or caprock, the timely relationship and the play fairway (Moeck and Beardsmore 2014). At the system scale geothermal plays can be separated into two large groups referring to heat transport, which can either be dominated by convection leading to accumulated heat, or the heat transport is dominated by conduction leading to distributed heat (Moeck 2014). Convection-dominated geothermal play types include all known high temperature (> 200 °C) geothermal reservoirs shallower than 3,000 m. According to the nature of the dominant heat source and tectonic settings, convection dominated plays are grouped into „magmatic“-, „plutonic“- and „fault-controlled in extensional domains“- types (Moeck 2014; Moeck and Beardsmore 2014). In convection-dominated geothermal systems the temperature often exceeds 150 °C at shallow depth in

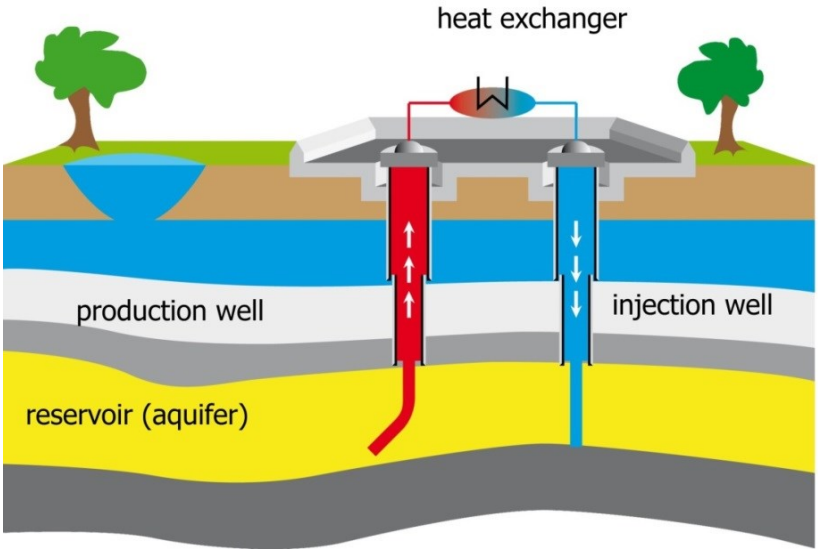

Fig. 1: Geothermal loop for utilization of a low- to intermediate enthalpy reservoir (modified after Blöcher, personal communication).

less than 2 km. In this case the hot fluid can be used directly to power a turbine, which drives a generator to produce electricity. Prominent examples for electricity production from convection dominated geothermal plays are found in New Zealand („intrusive magmatic play“), Iceland („extrusive magmatic play“), Italy (Larderello, „plutonic play with recent volcanism“), California (The Geysers, „plutonic play without recent volcanism“) or Nevada (Great Basin, „extensional domain geothermal play“).

Geothermal play types in conduction-dominated systems are grouped into „intracratonic basin plays“, orogenic belts with adjacent foreland basins“ and crystalline rock/basement plays“ (Moeck and Beardsmore 2014). The geothermal fluids commonly found in conduction dominated systems have temperatures below 150 °C in a depth range of 3–5 km. These resources can either be exploited by direct heat use for heating of buildings or for industrial processes, or to produce electricity using an Organic Rankine cycle (ORC) or a Kalina cycle. The subsurface installations are the same for both direct use and electricity production. Typically, two wells—a producer and an injector—are drilled into the reservoir, which is commonly located at a depth of 2–5 km (Fig. 1). From the production well the warm fluid is pumped through a heat exchanger, where the heat is transferred to a second fluid cycle. The cold fluid is then reinjected into the reservoir. Examples for geothermal electricity production for conduction-dominated geothermal plays are found in the North German Basin (Neustadt-Glewe, „intracratonic basin play“), in the Bavarian Molasse Basin (Unterhaching, „foreland basin play type“) or in the Australian Cooper Basin (Habanero, „crystalline rock play“).

The Alberta Basin, the focus area of this study, can be categorized as „foreland basin play type“ (Moeck 2014; Moeck and Beardsmore 2014).

1.2 Direct use of geothermal heat

In comparison with electricity production from geothermal energy, direct heat utilization has several advantages, such as much higher energy efficiency (50–70 %) as opposed to conventional (5–20 %) or binary cycle geothermal power plants (10–13 %) (Fridleifsson 1998, DiPippo 2012). Generally, the development time for a project is much shorter, and typically much less capital investment is involved (Fridleifsson 1998). A combination of power and heat production and cascaded use, meeting different temperature requirements from a single source, offers the potential for maximum energy extraction and economics (Fridleifsson 1998). However, other than electricity hot fluid cannot be transported over long distances from the geothermal production site. Therefore direct use of geothermal heat is very site specific for the market, as the consumer for the heat needs to be available close to the geothermal site.

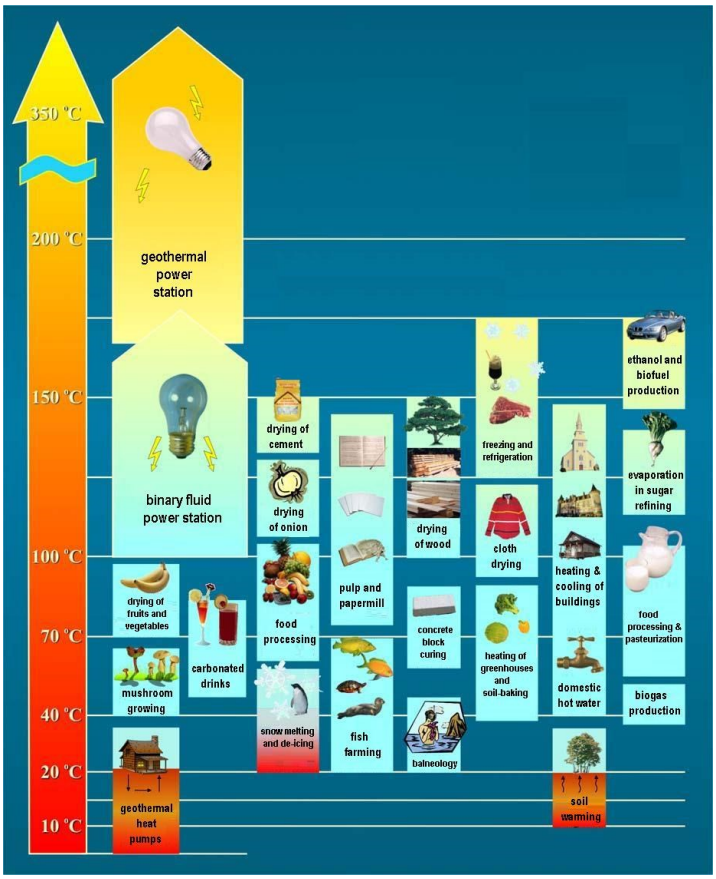

Fig. 2: Typical utilization forms for direct use of geothermal energy (after Líndal 1973).

Depending on the temperature, a wide variety of utilization exists for the direct application of geothermal energy (Fig. 2). Typically, the agricultural and aquatic uses require the lowest temperatures, with values from 20–95 °C. Bathing and therapeutic sites need temperatures from 20–45 °C. For domestic hot water provision temperatures above 40 °C are needed, while space heating requires temperatures above 70 °C. Refrigeration, drying, and most industrial processes normally require temperatures above 100 °C. By applying heat-pumps, the extent for space heating and warm water provision can be extended down to 5 °C (Lund 2010). Good examples of direct use of geothermal heat for district heating from low- and intermediate enthalpy resources are found in the Paris Basin (Laplaige et al. 2000; Lopez et al. 2010) and the German Molasse Basin (Schellschmidt et al. 2010).

1.3 History of geothermal energy

Geothermal fluids as a source of energy are known and used since more than 2000 years. In the Roman Empire, as well as in ancient China or in the Ottoman Empire, thermal baths fed by warm springs were centers of human activity and public life. In China, warm fluids were used in agriculture in the 4th to 6th century to increase the number of rice harvests per year (Stober and Bucher 2012).

The increase of temperature with depth—the geothermal gradient—was discovered by Alexander von Humboldt in 1791 by measuring temperatures in a mining area in the Ore Mountains near Freiberg. First deep wells, drilled in the 19th century to a depth of up to 1700 m, confirmed that the average geothermal gradient in Germany is 30 °C/km (Stober and Bucher 2012). In 1939 the first measurement of the terrestrial heat flow was conducted by Benfield (1939).

The utilization of geothermal energy in Europe started in the 19th century in Larderello, in the Tuscany region of central Italy. It was in 1827 when Francesco Larderel placed bricks above a hot pool thereby building a low pressure steam generator. Besides providing heat for mineral recovery (boron), the steam was also used to perform mechanical work with a steam engine. In 1904 the first electrical energy from geothermal sources was produced in Larderello by coupling a steam engine with a generator. The first power plant in Larderello started to produce electricity in 1913 with an electrical power of 250 kW. Today, the power plants in Larderello have a capacity of about 583 MW_{el} (Bertini et al. 2006).

The first large scale direct heat use of geothermal sources began in Iceland in the 1920s, when large systems for heating of domestic houses and greenhouses were installed in the city of Reykjavik. Today, geothermal heat is the source for heating and warm water

provision of 90 % of Iceland`s households, and 53 % of the countries 'primary energy need is fed by geothermal sources (Stober and Bucher 2012).

In the 1950s and 1960s other countries such as New Zealand, Mexico and the USA followed the example of Iceland and Italy, and began to develop their geothermal resources. It was in 1960 when one of the world´s most famous geothermal project—"The Geysers"—was initiated north of San Francisco. Nowadays "The Geysers" is the largest geothermal complex in the world, consisting of 22 power plants (and more than 350 wells) with an installed capacity of 1517 MW_{el} and an average production factor of 63 % (Lund et al. 2005).

In Germany the development of geothermal resources began in 1984 with the geothermal heating plant of Waren (Müritz) in the North German Basin. Today, after an extensive modernization, the plant has a capacity of 3.6 MW_{th} and produces 60 °C warm fluid from a 1.6 km deep sandstone reservoir at a flow rate of 17 L/s (ITG 2014). The first German geothermal power plant was established in 2003 in Neustadt–Glewe in the North German Basin. Other electrical power plants followed in the Upper Rhine Valley in Landau (2007) and Bruchsal (2009). However, due to the low efficiency (10–13 %) of electric power production from low temperature fluids (< 150°C), the largest potential for geothermal energy from these resources is the direct use of heat. The most promising region for a geothermal development in Germany is the southern Molasse Basin, due to the highly permeable Upper Jurassic carbonate rock aquifer (Malm) which is located at a depth of 2200 m (central Munich) to more than 5000 m south of Munich. In the Austrian village of Altheim, located 120 km east of Munich, geothermal heat is produced from the Upper Jurassic aquifer since 1990, followed by the first electricity production (ORC cycle) in the Molasse Basin in 2000 (Oberösterreichischer Energiesparverband 2014). The largest German geothermal power plant (50 MW_{th}) was established in Unterhaching in 2007, parallel producing heat for district heating (enough for 5000 households) and electricity (up to 3.4 MW_{el}) in a Kalina power cycle station (Geothermie Unterhaching 2013). In 2013 two large heat plants followed (Sauerlach and Dürrnhaar), and several more are being constructed or planned for the next years.

1.4 Worldwide status quo of geothermal energy utilization

Geothermal energy is currently used for base load electric generation in 24 countries, with an estimated 67.8 GWh/yr of supply provided in 2011 (IEA 2013). In six of these countries geothermal energy serves more than 10 % of the electricity demand (IPCC 2011).

Category	Installed Capacity (MW_{th})							Utilization (TJ/yr)						
	1995	2000	2005	2007	2008	2010#	2011	1995	2000	2005	2007	2008	2010#	2011
Geothermal heat pumps	1,854	5,275	15,384	-	-	33,134	-	14,617	23,275	87,503	-	-	200,149	-
Space heating	2,579	3,263	4,366	-	-	5,394	-	38,230	42,926	55,256	-	-	63,025	-
Greenhouse heating	1,085	1,246	1,404	-	-	1,544	-	15,742	17,864	20,661	-	-	23,264	-
Aquaculture pond heating	1,097	605	616	-	-	653	-	13,493	11,733	10,976	-	-	11,521	-
Agricultural drying	67	74	157	-	-	125	-	1,124	1,038	2,013	-	-	1,635	-
Industrial uses	544	474	484	-	-	533	-	10,120	10,220	10,868	-	-	11,745	-
Bathing and swimming	1,085	3,957	5,401	-	-	6,700	-	15,742	79,546	83,018	-	-	109,410	-
Cooling/snow melting	115	114	371	-	-	368	-	1,124	1,063	2,032	-	-	2,126	-
Others	238	137	86	-	-	42	-	2,249	3,034	1,045	-	-	955	-
Worldwide Total (Lund)	8,664	15,145	28,269	-	-	48,493	-	112,441	190,699	273,372	329,270	329,880	423,830	-
Worldwide Total (GIA)	-	-	-	-	-	-	54,200©	-	-	-	-	-	-	459,000©

Tab. 1: worldwide direct use categories and their development 1995, 2000, 2005 and 2010 (from Lund et al., 2011) and incorporating updates for GIA Member countries for 2011 (from IEA 2013).

Worldwide, the geothermal electric energy sector is a rapidly growing business, especially in the last decade. While from 1980–2005 the installed capacity grew at an average rate of 200 MW_{el}/yr, the trend intensified from 2005, now growing at 350 MW_{el}/yr (IEA 2013). The majority of the worldwide capacity of 11,079 MW_{el} (IEA 2013) is installed in convection-dominated regions where steam or hot liquids exceeding 225 °C can be used directly in the turbines. However, in the last years more and more projects were developed in conduction-dominated regions, producing electricity with ORC- (e.g. Birdsville, Australia; Altheim, Austria) or Kalina plants (Unterhaching, Germany).

Today, in 78 countries geothermal energy is used directly for heating and cooling, generating 459,000 TJ/yr of thermal energy in 2011 (including ground heat pumps which represent 47 %; IEA 2013). The total installed capacity has doubled every 5 years since 1995 and is currently at 54,200 MW_{th} (IEA 2013) (Tab. 1).

2. Geology of the Alberta Basin

The Alberta Basin is the central part of the Western Canada Sedimentary Basin (WCSB), which sits on a stable Precambrian platform and elongates along the eastern edge of the Rocky Mountains from British Columbia through Alberta and Saskatchewan into Manitoba (Porter et al. 1982, Bachu 1995) (Fig. 3). Basically, the WCSB comprises a wedge of sedimentary rocks increasing in thickness from zero at the Canadian Shield in the northeast to more than 6 km in the southwest (Porter et al. 1982, Bachu 1995) (Fig. 3). The WCSB was initiated during the late Proterozoic by rifting of the North American Craton (Bachu 1995). Two major basin stages can be distinguished in the evolution of the WCSB:

a passive margin period, which ranged from Late Proterozoic to Middle Jurassic, and foreland basin period beginning in the Middle Jurassic (Porter et al. 1982). During the passive margin phase, thermal contraction led to transgressive onlap of the cratonic platform (Bachu 1995). Deposition of shallow water carbonates, evaporites and shales characterize this period. In the Middle Jurassic the second basin period was initiated. During the Columbian and Laramide orogenies allochtonous terranes were subsequently accreted to the western margin of North America, resulting in isostatic flexure of the lithosphere which formed the foreland basin. From the Middle Jurassic to early Cretaceous, westward dipping of the passive-margin succession led to extensive erosion of eastwardly progressively older strata, which subcrop along the pre-Cretaceous unconformity (Bachu 1995). During the active margin phase in the Cretaceous and early Tertiary, synorogenic clastics (mainly shales) from the emerging Cordillera filled the basin. From Tertiary to recent, erosion has removed from up to 3800 m of sediments in the southwest to only 1000 m in the north (Bachu 1995). Present day topography of the basin ranges from close to 1200 m elevation in the southwest at the edge of the thrust and fold belt to slightly less than 200 m in the northeastern corner of the basin near the Canadian Shield (Bachu 1995).

3. Current state of geothermal exploration in the Western Canada Sedimentary Basin

Investigation of the geothermal state of the WCSB started with the study by Garland and Lennox (1962) who performed the first measurements of heat flow in two wells near Edmonton. With the sudden rise in the price of oil in 1973, and the popular perception that the supply of oil was approaching a decline, the Government of Canada initiated a geothermal energy research program which ran from 1974 to 1986 with a total budget of 6 million CAD. In the beginning of the program geological knowledge was accumulated to delineate the Canadian resources. Two reports on the geothermal energy potential of the WCSB were published in this initial phase (Sproule Associates Limited 1976, 1977). During the geothermal energy research program two major projects were developed, one in the volcanic terrain of the Cordillera (Meager Mountain) and one in the WCSB of eastern Saskatchewan (Regina). After a feasibility study (Vigrass et al. 1978) a well was drilled into the depth of 2214 m at the Campus of the University of Regina (Vigrass 1979; Jessop and Vigrass 1989). Tests showed an excellent geothermal potential, but unfortunately the large sports building that was intended to be the load for the well was not built, so the well has only been used as a research facility (Jessop 2008).

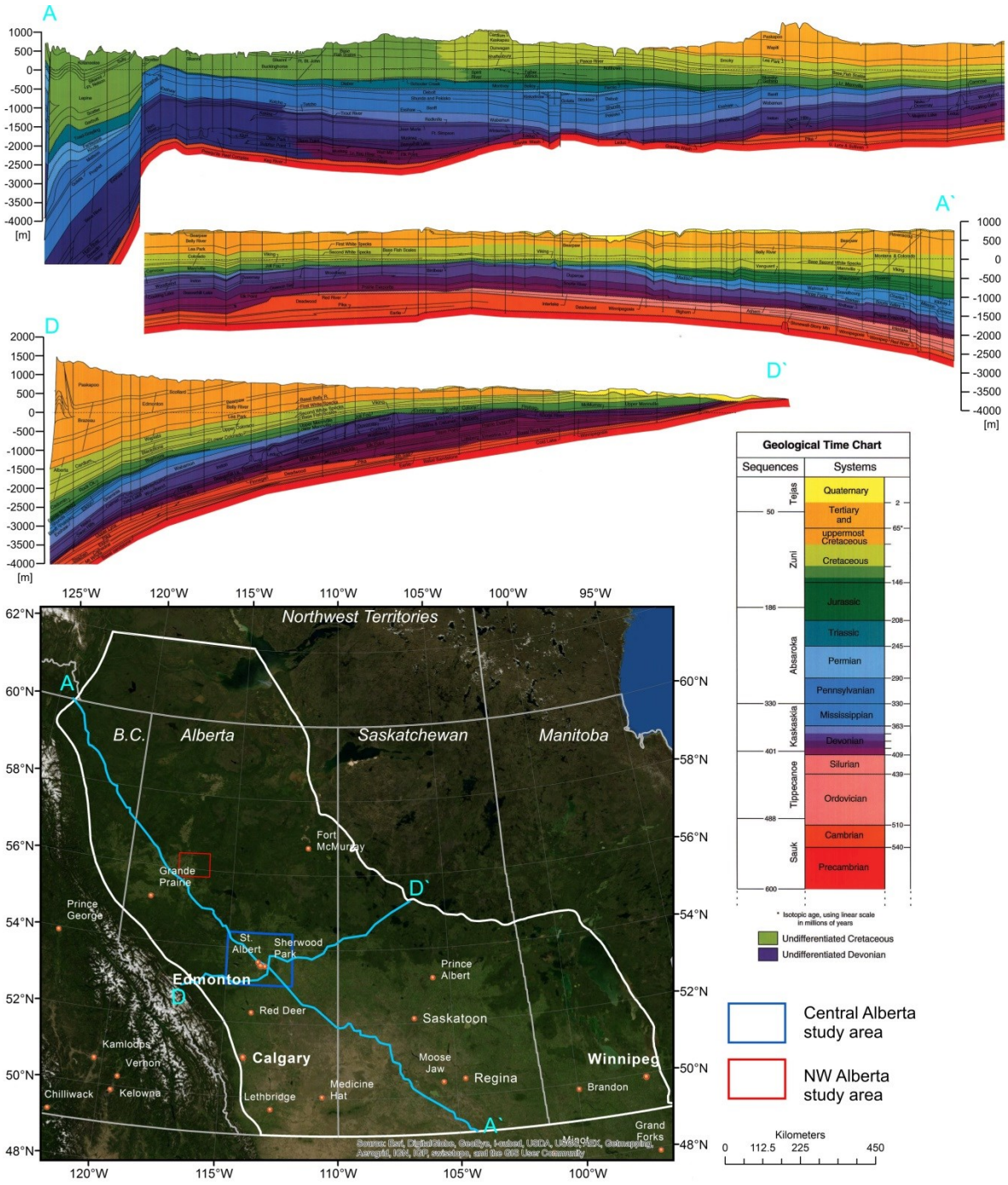

Fig. 3: *Upper part*: Two cross sections cutting through the Western Canada Sedimentary Basin; A–A` strikes perpendicular and D–D` parallel to the main dip direction of the basin. *Lower part*: Location of the cross sections and the two study areas. Cross sections are modified from Wright et al. (1994).

The first regional scale geothermal study in the WCSB was published by Jones et al. (1985) who predicted and mapped the temperature at the depth of the Paleozoic erosional surface and the Precambrian surface for the whole Alberta basin. After the discovery of a geothermal anomaly around the towns of Hinton and Edson in western Alberta, Lam and Jones (1985) investigated the geothermal potential of the area. Due to the combination of the relatively high gradient of approx. 36 °C/km and the thick sedimentary succession

(4–6 km), the Hinton-Edson area was seen as a possible geothermal energy source. Aquifer porosity, aquifer thickness, water chemistry and water recovery were examined with petroleum exploration data. The authors concluded that the Mississippian and Upper Devonian carbonate rocks appear to present aquifers with good geothermal potential because of their depth, thickness, wide spatial extent and good water recovery (Lam and Jones 1985). In a second study Lam and Jones investigated the potential for geothermal energy recovery in the Calgary area in southern Alberta (Lam and Jones 1986). In this area the geothermal gradient is rather low (24 °C/km). However, due to the relatively thick sedimentary succession (4 km) and the substantial population of the city, the authors concluded that the Calgary area is an attractive location for geothermal recovery and use. Following their approach of the Hinton-Edson study (Lam and Jones 1985), different aquifer properties were examined with petroleum exploration data. The largest potential for geothermal purposes again was found in Upper Devonian and Mississippian carbonate rocks.

Since the end of the geothermal energy program in 1986 only little research on geothermal questions was conducted, with the exception of the studies published by Bachu and Burwash in the early 1990`s, who investigated and mapped heat flow, geothermal gradient and temperature at Precambrian surface for the whole WCSB (Bachu and Burwash 1991; Bachu 1993; Bachu and Burwash 1994).

In the beginning of the millennium the hydrocarbon industry came up with a new potential application for geothermal utilization. In 2007 the industry consortium GeoPos (Geopowering the oil sands) began to investigate the technical and economic feasibility of using geothermal sources to supply the heat for energy and greenhouse-gas intensive oil sands extraction and processing (Airwaterland 2007). However, due to the economic crisis in 2008, the consortium stopped its work. In 2010 the Helmholtz Alberta Initiative, a research collaboration between the University of Alberta and the German Helmholtz Association of Research Centres, took up the idea of providing geothermal energy for oil sands in northeastern Alberta and, beyond that, focused also on the exploration of the geothermal potential of the deeper Alberta basin (as presented in this PhD thesis). In 2011 the Geological Survey of Canada published a report (Grasby et al. 2011), which synthesizes previous geothermal studies and delineates the potential of the different geothermal resource types in Canada. A major finding of the report is that the highest geothermal potential (for electricity production) exists in the volcanic belts of the Cordillera and in parts of the WCSB (northeastern British Columbia, northern Alberta and

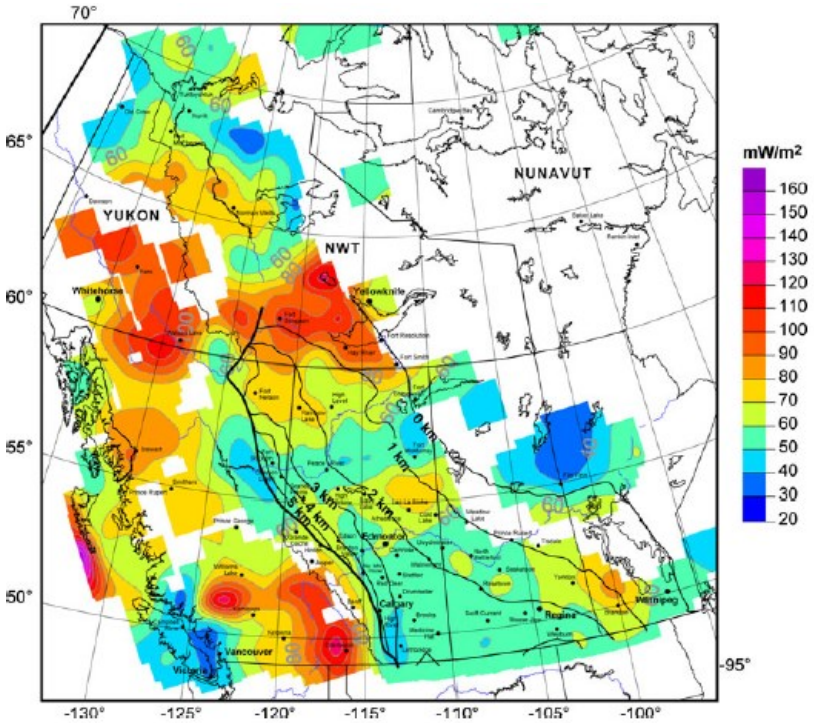

Fig. 4: Map showing averaged heat flow in western Canada. Major communities and contours of total sediment thickness of the Western Canada Sedimentary Basin are shown (from Majorowicz and Grasby 2010b).

southern Northwest Territories). The report describes the other deeper parts of the WCSB as very large resource for direct heat use. In 2013 the British Columbia Ministry of Energy and Mines assessed the geothermal resource at the geothermal anomaly of the Clarke Lake gas field in northeastern British Columbia (Walsh 2013) by using the volume method (Williams 2007). Ferguson and Grasby (2014) studied the geothermal potential of the Basal Clastics in eastern Saskatchewan. Numerous studies have investigated heat flow and temperature at depth of the WCSB (Majorowicz and Jessop 1981; Jessop et al. 1984; Majorowicz et al. 1985; Majorowicz 1996; Majorowicz et al. 1999; Jessop et al. 2005; Grasby et al. 2009; Majorowicz and Grasby 2010a,b;) and North America (Blackwell and Richards 2004). The heat flow in the southern and central part of the WCSB generally ranges from 30–80 mW/m^2, while values up to 100 mW/m^2 and higher were measured in the northern part (see Fig. 4). The geothermal gradient in the southern and central parts of the WCSB ranges from 20–40 °C/km (Fig. 5). In the northern part of the WCSB gradients > 50 °C/km were measured.

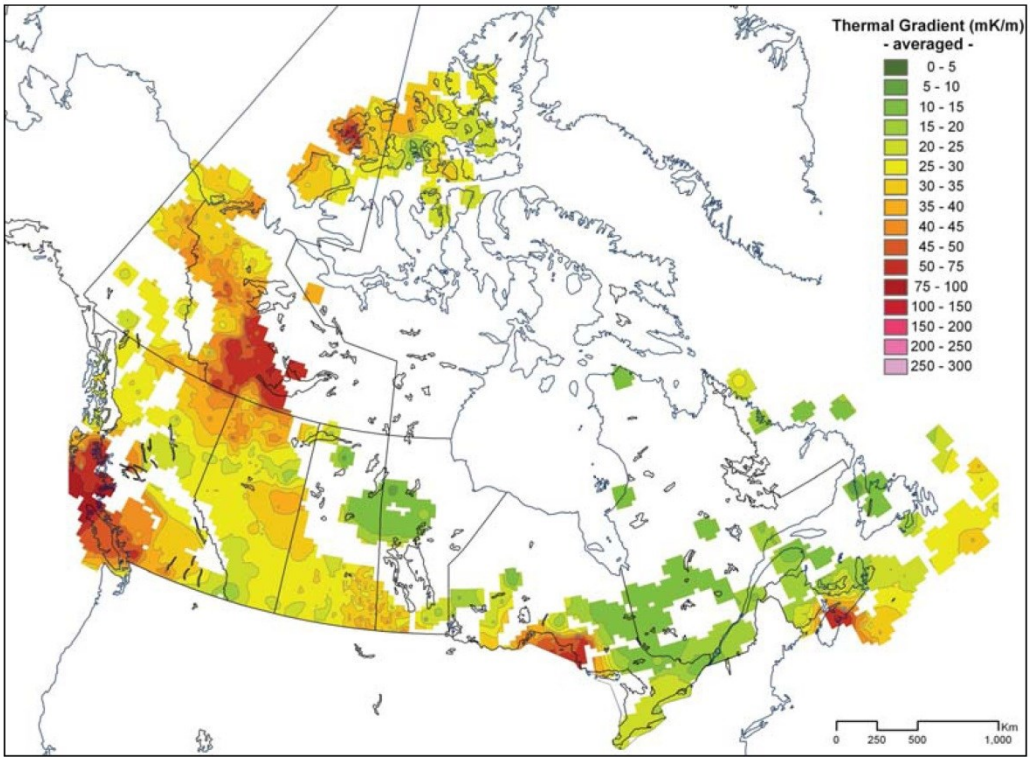

Fig. 5: Distribution of the geothermal gradient in Canada (from Grasby et al. 2011).

4. The concept of geothermal assessment

The verb "to assess" means to estimate or to judge the value or character of something (Dictionary.com). In the context of geothermal exploration, the aim of an assessment is to evaluate the geothermal potential of the subsurface, and to identify the formations which would be the primary goal for the development of a geothermal reservoir. Several approaches have been applied for geothermal assessment in the past. The USGS has defined geothermal resource assessment in their Circular 790 (Muffler 1979) as the "estimation of the amount of thermal energy that might be extracted from the Earth and used economically at some reasonable future time". The key element of the USGS assessment studies (and of other assessment studies, e.g. Kohl et al. 2005, Blackwell et al. 2006, Lee et al. 2010, Walsh 2013) is the volumetric method which is used to estimate the total thermal energy within a reservoir volume. The main values required for this calculation are the reservoir temperature and volume, furthermore surface temperature and the volumetric specific heat of the reservoir rock (Williams 2007; Williams et al. 2008). The volumetric approach provides a reasonable estimate of the total heat content of the reservoir, but it does not predict the thermal energy which is available at the wellhead. To estimate this energy a reservoir factor is applied, which ranges between 0.1 and 0.25 for

sedimentary basin reservoirs (Williams 2007; Williams et al. 2008). The recovery factor directly incorporates an estimation of the effective porosity of the reservoir. A drawback of this volumetric method is that is does not account for permeability, which is a key reservoir property. If the reservoir permeability is too low, the geothermal heat production from a well can become uneconomic or even unfeasible, because the flow rate will be too low. The outcome of the volumetric method is therefore of low practical value, because it only gives an estimation on the total amount of thermal energy which can be extracted from the reservoir, without considering the technical practicability. For this reason the volumetric method was not applied in this thesis.

A more practical approach for assessing the geothermal potential of a region is to analyze and map the properties which influence the quality of a geothermal reservoir, which are temperature, depth, thickness, extent, porosity and permeability. With help of these maps the geothermal sweet spots—the areas where positive anomalies of the different properties coincide—can be identified. These are the spots which are most favorable for geothermal utilization.

Generally the assessment process of geothermal resources can be subdivided into two phases, similar to the assessment of hydrocarbon systems (Fig. 6). In the initial phase the "chance of discovery" is assessed, and favorable geothermal resources are delineated. The second phase, which follows the first drilling and well testing activities, examines the "chance of development" and investigates whether the favorable resources of the initial phase are suitable for geothermal production and how these suitable reservoirs can be developed (Moeck and Beardsmore 2014).

This thesis covers the first phase of the geothermal assessment in Alberta by analyzing and mapping properties of potential geothermal target formations and delineating the favorable geothermal resources. The goals and objectives of this thesis, the focus areas, the data base, and the methods which were applied are described in the next paragraph.

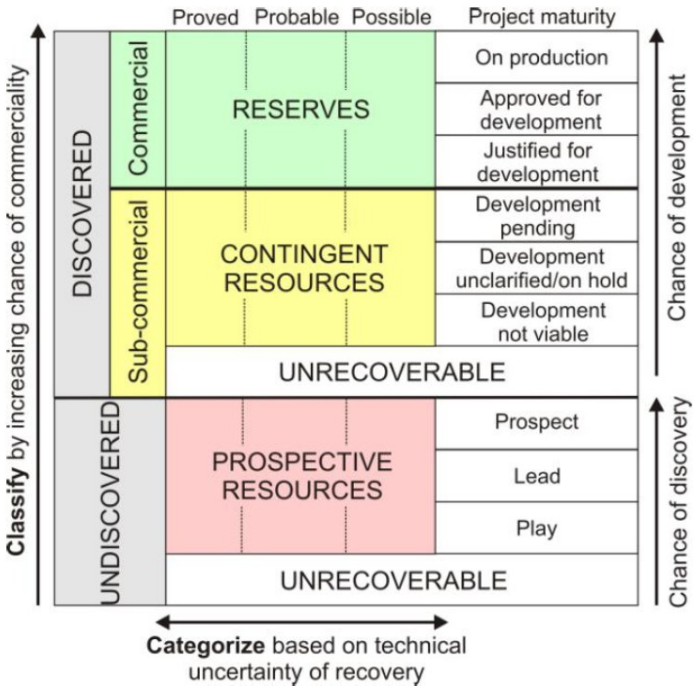

Fig. 6: Classification of risk (vertical axis) and categorization of uncertainty (horizontal axis) for hydrocarbon systems according to the Petroleum Resources Management System (SPE-PRMS 2007). The play is the lowest class in this scheme and therefore a fundamental part of the assessment process (from Moeck and Beardsmore 2014).

5. Goals and objectives of this thesis

This thesis aims is to assess the geothermal resources of the Alberta Basin and to delineate the spots which are favorable for the development of a first geothermal site in Alberta. As assessing the geothermal conditions of the whole Alberta Basin (which is larger than Germany) would exceed the scope of a PhD thesis, it was decided to focus on two representative regions of the basin. The first study area is located in central Alberta around the city of Edmonton, while the second study area is located in northwestern Alberta around the town of Peace River (Fig. 3). Both areas differ from each other not only in respect to their geology and their geographic location, but also in respect to the heat demand and the potential application of geothermal heat production. In central Alberta the application for geothermal heat would be the provision of heat for district heating and for warm water supply in the densely populated Edmonton metropolitan area. In northwestern Alberta a huge heat demand exists for industrial (in-situ oil sands exploitation) and agricultural processes (heating of greenhouses).

The key questions addressed in this study are:

- What is the extension and thickness of potential geothermal target formations in the Alberta basin and in the two study areas?
- What is the porosity and permeability of the potential geothermal target formations, and how are these rock properties distributed?
- How are heat flow and geothermal gradient distributed in the Alberta Basin, and what temperatures can be expected in the potential geothermal target formations?
- Which are, according to the previous points, the best spots for a geothermal development?
- What kind of geological structures exist in the subsurface, and how are the structures oriented in the current stress field? What is reactivation potential of existing faults during production or injection of geothermal fluids?

To answer these questions, a wide range of different methods was applied, including 3D structural geological modeling based on well log data and 2D seismic data, geostatistical mapping of hydraulic parameters and temperature data, hydraulic and geomechanical testing and thin section analysis. Application of data intensive methods like 3D modeling and geostatistical mapping was only possible due to the extensive well data base which is publically available in Alberta. Thanks to the long tradition of hydrocarbon exploration and production in Alberta, more than 300,000 wells were drilled in the Alberta Basin until today. Temperature data from more than 26,000 of these wells were used to investigate the thermal state of the WCSB. Geological modeling and analysis of hydraulic parameters in the two study areas were conducted with stratigraphic information and core test results from more than 10,000 wells.

In the Peace River study, the in-situ stress field was estimated from literature data, and the reactivation potential of faults was assessed using the slip tendency method (Morris et al. 1996). The most suitable geothermal aquifer in central Alberta—the Cambrian Basal Sandstone Unit—was investigated by thin section analysis, core analysis and geomechanical testing.

Structure of the thesis

Chapter 2 explores the Paleozoic formations of the central Alberta Basin, focusing on thickness and extension of four Devonian and one Cambrian formation. Porosity, permeability and temperature distribution is mapped from core test and well log data with geostatistical methods. In Chapter 3, the petrography, mineralogy, porosity, permeability and geomechanical parameters of the Cambrian Basal Sandstone Unit—the deepest geothermal formation in central Alberta—are analyzed. The temperature distribution in the Basal Sandstone Unit is mapped with help of an extensive thermal database. Chapter 4 investigates the geothermal potential of the siliciclastic Granite Wash Unit in northwestern Alberta. Besides extent and thickness of the formation, the chapter focusses on the distribution of hydraulic parameters and temperature. Geological structures in the subsurface are interpreted and modelled from seismic data. The stress state of these structures in the current stress field is analyzed by applying the slip tendency method. In Chapter 5, heat flow and geothermal gradient of the sedimentary succession of the WCSB are analyzed and mapped based on a large thermal database. The most important aquifers of the WCSB are discussed with regard to their geothermal potential, and regional temperature distribution within these aquifers is mapped. Chapter 6 synthesizes the key findings of the four previous chapters and discusses potential next steps in the assessment process and future geothermal development in the Alberta Basin.

Chapter 2

Originally published in the *Canadian Journal of Earth Sciences, 2013, 50 (5): 519–534*

Geothermal Exploration of Paleozoic formations in central Alberta

Simon Weides, Inga Moeck, Jacek Majorowicz, Dan Palombi, Matthias Grobe

Abstract

This study explores the distribution of Paleozoic formations in the central Alberta Basin and investigates rock properties with regard to their usability as geothermal reservoirs. The study area of this regional scale investigation is about 160 km × 200 km in size and located around Edmonton where the basin depth ranges between 1.8 km and 3.5 km. A 3D geological model was developed based on stratigraphic tops from about 7000 wells from the database of the Alberta Geological Survey (AGS). Spatial distribution and thickness of deep formations were established in the 3D geological model.

Porosity and permeability of four Devonian carbonate formations— Cooking Lake, Leduc, and Nisku formations, and Wabamun Group—were investigated using data from more than 50,000 core analyses. Average porosity of the Devonian strata in the study area ranges from 4.5 % (Nisku) to 8.7 % (Wabamun), average permeability is between 3.5×10^{-15} m^2 (Wabamun) and 26×10^{-15} m^2 (Leduc). The distribution of both parameters was analyzed using geostatistical methods. Based on an average geothermal gradient and the geometry of formations from the 3D modeling study, an estimation of formation temperatures for the Paleozoic formations is presented. Temperature in the Cambrian Basal Sandstone Unit ranges from 62 °C in the shallower northeast (1.8 km) to 122 °C in the deeper southwest (3.5 km); temperature in the Devonian strata ranges from 22 °C to 87 °C. With these new results potential geothermal reservoirs can be delineated in the Alberta Basin around Edmonton, enabling future detailed exploration and field development.

1. Introduction

Alberta is known for its resources of oil, gas and coal. Recently, renewed efforts to develop renewable energy technologies as part of Alberta's future energy plan has rekindled interest in Alberta's geothermal energy potential (Majorowicz and Moore 2008; Bell and Weis 2009; Grasby et al. 2011). With an average geothermal gradient of 25–35 °C/km and a heat flow of 50–70 mW/m^2, central Alberta has been characterized as a low enthalpy region (Majorowicz and Grasby 2010b; Grasby et al. 2011;). Considering Alberta's climatic conditions with long cold winters (average annual temperature in Edmonton is 2.4 °C, average temperature in January is -13.5 °C; from National Climate Data and Information Archive 2000) in combination with it being a low enthalpy region, its demand for geothermal energy would likely be focused on heat provision rather than electricity

production (Grasby et al. 2011). Geothermal energy could play a role in replacing some fossil-fuel generated heat energy used within industrial processes and/or as an energy source for district heating. Potential customers in the Edmonton area are private residences, office buildings, and public and commercial buildings, such as universities, hospitals or shopping centers. Industrial sites with a high heat demand such as refineries and upgraders exist in northeastern Edmonton and Fort Saskatchewan. For a successful utilization of the geothermal resource in this area the development of Enhanced Geothermal Systems (EGS) is required. The concept of EGS emphasises an integration of engineering and geosciences, aiming to adapt subsurface conditions to surface technology (Huenges 2010). Only with help of an integrated geothermal exploration concept, which is dependent on the state of investigation that the basin has undergone before, can the resource be exploited efficiently.

1.1 Focus of the study

This study is the first detailed investigation of the geological-geothermal subsurface conditions of an area in central Alberta. It demonstrates the specific exploration methods that can be applied in a situation where a large amount of geological and geophysical data is publicly available and has to be re-evaluated and re-interpreted for geothermal exploration.

The area of investigation, approx. 160 km × 200 km in size, is located around the city of Edmonton (Fig. 7). In this area, the thickness of the sedimentary succession of the Alberta Basin from ground surface to the top of the Precambrian crystalline basement is between 1.8–3.5 km, and the depth to the top of the Paleozoic sediments is ranging from 600 m to 2300 m. The study area was chosen in consultation with staff at the Alberta Geological Survey (AGS) and coincides with the study area of the AGS Saline Aquifer Mapping project.

The aim of geothermal exploration is to delineate potential geothermal reservoirs and to describe the distribution of relevant rock parameters that are necessary to quantify the producible geothermal energy in place. Important parameters are porosity, permeability, reservoir rock thickness and temperature to estimate flow rate and temperature gain. Ongoing geothermal projects in other low-enthalpy regions demonstrate the approach from exploration, reservoir access and utilization with installed geothermal technology. The geothermal test site of Gross Schönebeck in the North German Basin extracts hot water from a 4.2 km deep Permian sandstone reservoir that has an average porosity of

9.8–18.3 % and an average permeability of 3–100 × 10^{-15} m^2 (0.1–17 × 10^{-15} m^2 at in-situ conditions, from Trautwein and Huenges 2005). In the south Bavarian Molasse Basin the largest geothermal power plant in Germany is installed in a reservoir formation of karstic reef limestone that has an average permeability of 100–1000 × 10^{-15} m^2 (Birner et al. 2009). Zones with high porosity and permeability are favourable for geothermal application; however, it is possible to increase permeability by stimulation treatments to obtain higher flow rates. Besides the hydraulic properties of the reservoir, the reservoir temperature and the end-user demand is important for consideration. Líndal (1973) describes different applications for different temperature ranges. For district heating a fluid with a temperature of 70–80 °C is needed, for warm water provision temperatures higher than 40 °C are sufficient (Líndal 1973).

The study presented here is a first assessment of the geothermal potential of the deeper central Alberta Basin at a regional scale. This includes the analysis of hydrothermal systems and the identification of formations that could be potentially utilized for geothermal applications. The term "hydrothermal" is used here to describe a system where water which is more or less in temperature equilibrium with the surrounding rock mass is moving through a sedimentary formation. This is in contrast to Hot Dry Rock (HDR) systems, where no large amount of natural formation fluid exists and water has to be injected in the reservoir for geothermal utilization as demonstrated in Soultz (France) (Tischner et al. 2006). HDR systems are considered for low permeable granitic or crystalline rock which is represented in the study area by crystalline basement rocks underlying the Alberta Basin. The development of a 3D geological model, based on stratigraphic information from the database of the Alberta Geological Survey (AGS), enables the analysis of geometry, spatial distribution and thickness of the deep formations. Porosity and permeability of the formations are investigated with the help of core analysis data from the Alberta general well data file. The spatial distribution of these parameters is analysed through geostatistical methods. An estimation of temperature in the subsurface is given based on a geothermal gradient analysis for the Paleozoic formations analysed in the 3D modeling study.

1.2 Heat demand of Alberta

The province of Alberta has a high demand for heat which is mainly provided by the utilization of fossil fuels. The major part of this heat is used in industrial processes and for space heating of residential, commercial and institutional buildings. The largest energy

consumer in Alberta´s industrial sector is the rapidly growing mining industry with a share of 65.5 % of Alberta´s total industrial energy consumption (727.6 PJ in 2009, increase of 273 % from 1990; Natural Resources Canada, 2009). A large part of this energy is used in oil sands mining extraction processes where heated water is used to separate highly viscous bitumen from the host sediments. In surface mining this water is taken from the Athabasca River at a temperature of 7 °C (annual median temperature from Hebben, 2009) and heated up to temperatures from 40–55 °C with natural gas. In oil sands in situ extraction, steam is produced at temperatures ranging from 250 °C in Steam Assisted Gravity Drainage (SAGD) to 300–340 °C in Cyclic Steam Stimulation (Ko and Donahue 2011). Most of the heat consumed by the mining industry is provided by natural gas (398.2 PJ in 2009, increase of 773 % from 1990; Natural Resources Canada, 2009), which has led to a concomitant increase in greenhouse gas emissions (GHG). In 2009, 41.9 Mt of CO_2 were emitted from the oil sands industry which represents 37.1% of GHG emissions of the Alberta´s industrial sector (Government of Alberta 2011) or almost 18 % of Alberta´s total emissions (Environment Canada 2011).

The share of residential, commercial and institutional sectors sums up to 19 % of Alberta´s total energy use (Natural Resources Canada 2009; 2011). Geothermal energy has the potential to decrease Alberta´s fossil fuel consumption and its related GHG emissions. A standard geothermal doublet system that produces a modest 40 °C temperature gain at a flow rate of 15 L/sec would have a thermal energy of 2.5 MW_{th} and produce 72 TJ per year for 8000 full load hours. 300 of these standard geothermal doublet systems would produce 21.6 PJ per year and save 1.2 Mio t of CO_2 emissions compared to burning of natural gas (IPCC 2006).

2. Geological setting

2.1 Alberta Basin

The Alberta Basin consists of a northeastward tapering sedimentary wedge that unconformably overlies the Precambrian crystalline basement. The sedimentary succession reaches a thickness of over 5 km close to the Rocky Mountains in the southwest and thins towards the northeast, where it is terminated by erosion or non-deposition. In the evolution of the basin two major periods of basin evolution can be distinguished: (1) A passive margin period, which ranged from Late Proterozoic to Middle Jurassic and was dominated by the deposition of carbonates, shales and evaporites (Porter et al. 1982; Price 1994);

(2) A foreland basin period, beginning with the rise of the Rocky Mountains in the Middle Jurassic and characterised by siliciclastic deposits filling the basin foredeep (Porter et al. 1982; Price 1994).

2.2 Paleozoic strata and hydrostratigraphy

The aim of this study is to investigate the Paleozoic sedimentary strata and assess their usability for geothermal applications. In the study area the Paleozoic sediments are known in a depth range between 610 m to 3530 m (Mossop and Shetsen 1994a). Depending on their porosity and permeability, geological layers can be classified into aquifers, aquitards and aquicludes. An aquifer stores and yields water in sufficient quantities, and transmits water relatively easily (Subramanya 1994). An aquitard significantly impedes the flow of water, to the effect that only limited seepage is possible, and an aquiclude is essentially impermeable to the flow of water (Subramanya 1994). This classification of hydrostratigraphic units often comprises one or more geological units that are in contact and exhibit similar characteristics with regard to fluid flow, and are usually defined at the local scale (Bachu 1995). Hydrostratigraphic systems are complex groups of hydrostratigraphic units that exhibit common overall characteristics at a regional scale,

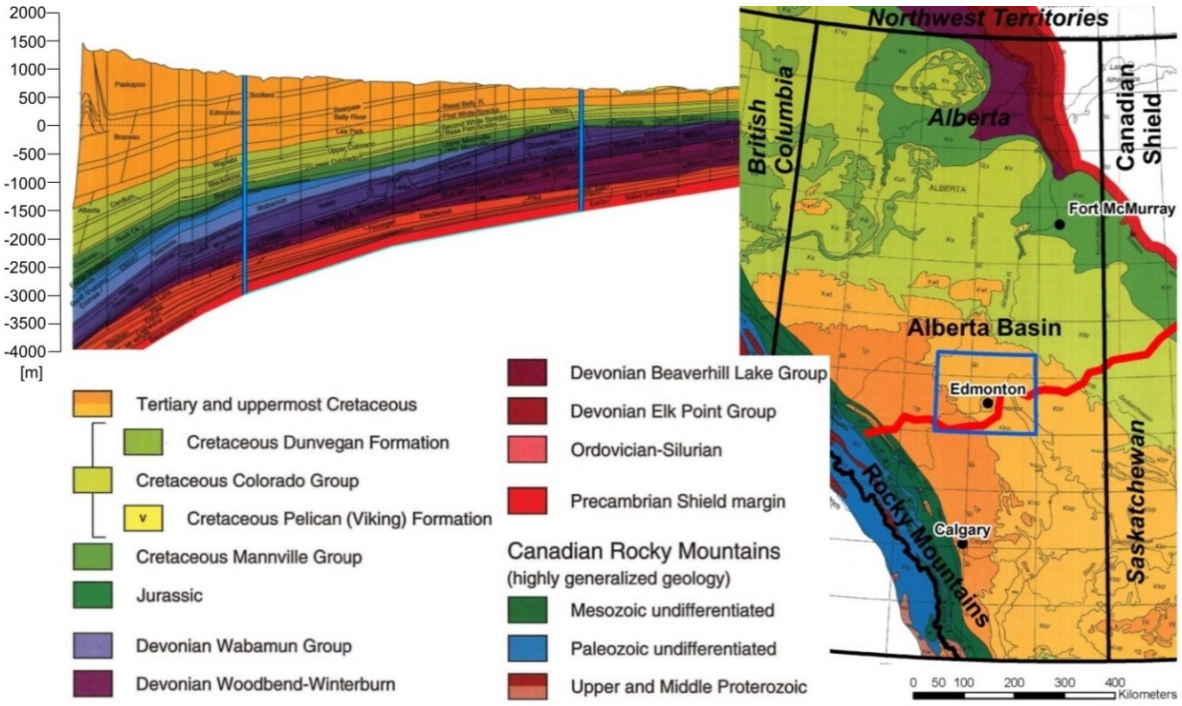

Fig. 7: Location of study area with geological map and cross-section (modified from Mossop and Shetsen 1994a; Wright et al. 1994); study area is approx. 160 × 200 km in size; basin depth is between 1.8–3.5 km. The two vertical blue bars on the cross section represent the borders of the study area.

present (Bachu 1995). The major regional hydrostratigraphic systems in the Paleozoic succession of the study area, as identified by several hydrogeological studies, are described in the following paragraph (after Bachu 1995) and are illustrated in Fig. 8. The average thickness of the hydrostratigraphic systems in the study area were taken from cross-sections published in the Atlas of the Western Canadian Sedimentary Basin (Mossop and Shetsen 1994b). The Precambrian crystalline basement is considered as an aquiclude consisting mainly of granite, quartz diorite, rhyolite and metamorphic rocks (Burwash et al. 1994) overlain by fine to coarse grained Middle Cambrian sandstones of the Basal Sandstone aquifer with a thickness of 35 m to 45 m (Slind et al. 1994). At the top this aquifer is confined by the Middle to Upper Cambrian aquitard, consisting of 220 m to 350 m of interbedded shales, siltstones and carbonates (Slind et al. 1994). Unconformably overlying siliciclastics, carbonates and minor salt deposits of the Devonian Lower Elk Point Group form the 70 m to 160 m thick Elk Point aquitard system (Meijer Drees 1994). The carbonates of the Winnipegosis Formation comprise the westward thinning Winnipegosis aquifer (15–70 m), which is confined at the top by 60 m to 120 m of evaporites of the Prairie aquiclude–aquitard system (Meijer Drees 1994). The overlying platform carbonates and associated reefs of the Beaverhill Lake Group, the Cooking Lake Formation and the Leduc Formation form the Middle to Upper Devonian aquifer system. Extensive dolomitization and probably associated increased porosity occurs at the western margin of the platform carbonates of the Cooking Lake Formation over a width of 10–30 km, and the reefal buildups of the Leduc Formation at the Rimbey-Meadowbrook trend and on the western part of the Redwater reef (Andrichuk 1958a, 1958b; Switzer et al. 1994; Wendte 1994). On average the Middle to Upper Devonian aquifer system has a thickness of 270 m to 330 m, in the central part of the study area in the north–south trending Leduc Formation reefal carbonates the thickness can reach up to 450 m (Oldale and Munday 1994; Switzer et al. 1994). This aquifer is overlain by 70 m to 180 m of shale of the Ireton Formation forming the Ireton aquitard (Switzer et al. 1994). The overlying platform carbonates of the Winterburn and Wabamun groups, particularly the partly dolomitized Nisku Formation and Wabamun Group (Stoakes 1988; Switzer et al. 1994) form the Upper Devonian aquifer system with a thickness of 170 m to 190 m (Halbertsma 1994). In the central and eastern part of the study area the Upper Devonian aquifer system subcrops at the pre-Cretaceous unconformity and is partly eroded (Halbertsma 1994). In the western part, overlying Exshaw Formation shales and the shaly lower part of the Banff Formation form the Exshaw-Banff-aquitard.

2.3 Potential geothermal reservoirs and controlling geologic factors

Potential geothermal reservoirs in the Alberta Basin are part of hydrostratigraphic units in a depth range between 1–5 km where fluid temperatures are ranging from about 40–150 °C (Líndal 1973; Majorowicz and Moore 2008). These units are the Cambrian Basal Sandstone Unit, and the Devonian carbonates of the Cooking Lake-, Leduc-, and Nisku formations and Wabamun Group (Fig. 8).

Positive porosity and permeability domains in sediments are controlled by facies, diagenesis and structural inventory. During diagenesis porosity is reduced by mechanical compaction, chemical compaction (pressure solution) and cementation (Marfil et al. 1996). Permeability in sandstones can be reduced by alteration of feldspars to clay (Marfil et al. 1996). Formation of dolomite in limestones through diagenetic processes can result in an increase of porosity and permeability (Machel 2004). Faults and fractures can create pathways for fluid flow, in particular in low-porosity carbonate rocks where also karst channels contribute to high permeability domains (Aydin 2000; Graham et al. 2005). In fractured carbonate rock, the fault damage zone rather than the fault core is a zone of elevated permeability due to a dense and interconnected fracture pattern (Agosta et al. 2007). Detailed studies about hydraulic conditions of fault damage zones in reservoir rocks of the studied area are not available.

Porosity and permeability of the Cambrian Basal Sandstone Unit may be mainly affected by the distribution of facies and diagenesis, however detailed studies on this formation in

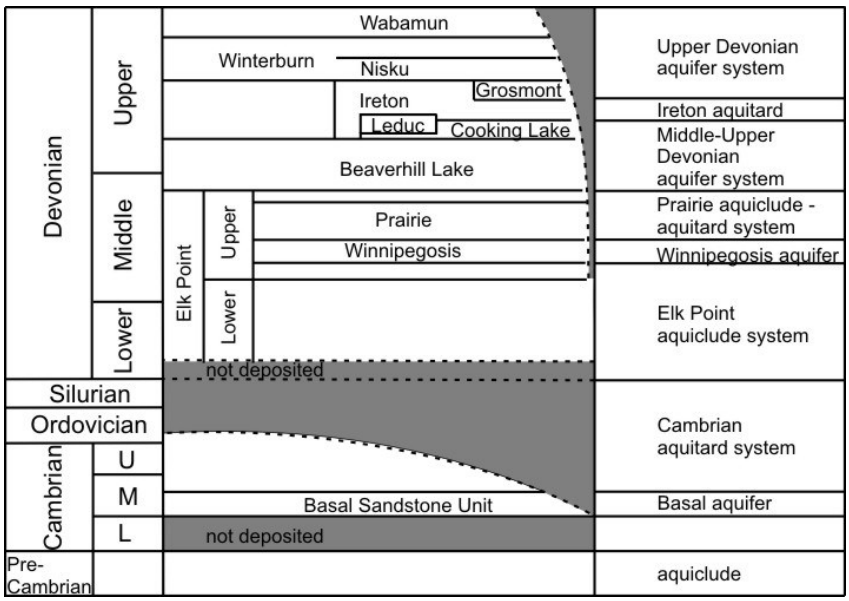

Fig. 8: Relevant basin-scale stratigraphic and hydrostratigraphic Paleozoic units (modified from Bachu 1995).

the studied area are lacking. Reservoir properties of the four Devonian carbonate formations are controlled mainly by dolomitization and occurrence of fractures.

3. 3D geological modeling study

A 3D geological model (Fig. 9) was developed for analysis of the spatial distribution of the potential geothermal reservoir units in the study area. With the developed 3D geological model it is possible to identify the regional thickness variation of the five Paleozoic formations representing potential geothermal aquifers ranging in depth between 610 m and 3531 m (Fig. 9). The aquitards and aquicludes were integrated into the 3D geological model in order to constrain the top and bottom boundaries of the five hydrostratigraphic units of interest. Finally, the spatial distribution of all formations of this geosystem needs to be investigated to develop an accurate model and to achieve a consistent result from ground level to basin floor. In the following paragraphs the modeling technique is described before results from the 3D model are analyzed in detail.

3.1 Data set and approach

The model is based on the stratigraphy identified by numerous well logs from the AGS database. In total, stratigraphic tops from 6916 wells were used to build the model. This database is extensive, but it is also biased towards hydrocarbon-rich strata and areas, since most of the data comes from hydrocarbon exploration and production wells. A high amount of data exists for the Mesozoic succession (> 6500 wells in the Lower Cretaceous) and hydrocarbon–bearing Upper Paleozoic strata (> 2000 wells in the Upper Devonian). In contrast, only a small number of wells have been drilled in the strata below the Upper Devonian carbonates. In the study area, 72 wells have reached the top of the Middle Devonian Elk Point Group, of which 16 wells were drilled into the Cambrian strata, with 13 penetrating the top of the Precambrian basement in a depth between 1769 m and 3533 m.

Due to the large areal extent of this study, and the expense that would be required to purchase industry seismic data, no seismic information was used in the development of the 3D model; therefore, no information on faults was integrated into the model. However, as a result of the significant amount of stratigraphic data available, information from all regions in the study area exists for the majority of formations, which enables the development of a detailed lithostratigraphic 3D geological model, sufficient for analysis of formation related temperature distribution.

The 3D geological model was developed with EarthVision® modeling software (Dynamic Graphics Inc.). The datasets for the formations were visualized individually in three-dimensional space to identify outliers by analysis of the spatial position of the stratigraphic tops. Effectively, few stratigraphic tops were identified as outliers as their spatial position differed markedly in relation to stratigraphic tops from other wells in the vicinity (in some cases the z-value differed more than 100 m from other stratigraphic tops in the direct surrounding of less than 5 km). These obvious data errors which probably result from wrong kelly bushing elevations are removed from the dataset. The calculation of the formation top surface grids was carried out by minimum tension gridding, which is an interpolation algorithm that is based on the nearest neighbour weighted average method (Dynamic Graphics Inc. 2009). Since the focus of this study is on the geothermal potential of deep formations, all formations of interest in the Paleozoic succession were characterized, and modelled separately, while Mesozoic and Cenozoic formations have been grouped to form units of greater thickness. Due to the large scale of the model (the study area is approx. 160 km × 200 km), only regionally extensive formations have been modelled. For this particular 3D model a minimum formation thickness of about 30 m was required to calculate a surface grid in the 3D model that is consistent over the study area. The 3D model has a grid spacing of 250 m in the horizontal direction, and a vertical discretization of 5 m. The final lithostratigraphic 3D model comprises 20 different geological units, of which 14 are in the Paleozoic strata and six are in the Mesozoic- and Cenozoic-aged strata (Fig. 9).

3.2 Results of the 3D modeling study

Based on the 3D geological model, the spatial distribution and thickness of the Paleozoic formations representing the deep aquifer systems were analyzed. The total thickness of the Phanerozoic succession in the study area ranges between 1769 m and 3533 m. The Paleozoic strata dip towards the southwest with an average of 0.4 °.

The Cambrian Basal Sandstone Unit is the deepest sedimentary unit in the study area (Fig. 9). It lies unconformably on the Precambrian basement and is distributed over the whole study area. Its thickness ranges from 28 m to 45 m in the northeast with an average thickness of 38 m. The depth to the surface of the Cambrian Basal Sandstone Unit is

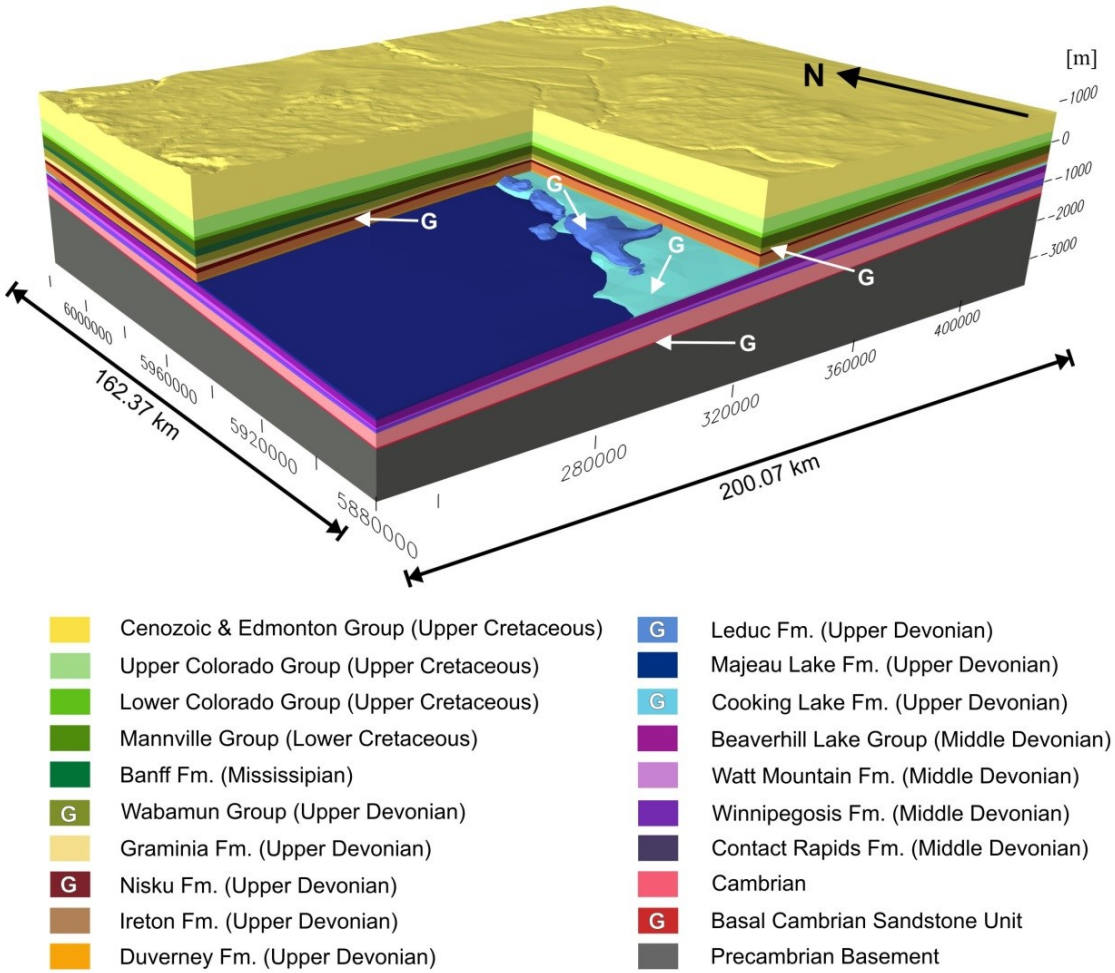

Fig. 9: Three dimensional geological model of the study area. The model is based on stratigraphic picks from about 7000 wells and potential geothermal reservoir units are indicated by the letter “G”.

form the 85 m to 515 m thick sedimentary succession of the Elk Point Group. This group is overlain by 150 m to 280 m of carbonates and shales of the Upper Devonian Beaverhill Lake Group. The four carbonate units investigated in this study are found in the Upper Devonian Woodbend, Winterburn and Wabamun groups. The platform carbonates of the Cooking Lake Formation were deposited in the eastern half of the study area and terminate in the vicinity of the 114 ° meridian west. The Cooking Lake Formation has an average thickness of 57 m. The overlying Leduc Formation reefal carbonates form a north-south trending chain in the central part of the study area reaching a maximum thickness of 300 m. The rocks of the Cooking Lake and Leduc formations are overlain by the shales of the Duvernay and Ireton formations, which reach a maximum thickness of 300 m gradually thinning out to 115 m above the Leduc reef trend. The strata of the Nisku Formation and Wabamun Group are distributed over the majority of the study area, thinning out towards the eastern margin where the strata have been removed by erosion. The average thickness

of the Nisku Formation is 75 m, the carbonates of the Wabamun Group are 113 m thick on average.

4. Porosity and permeability analysis of Paleozoic formations

The parameterization of reservoir rocks plays a major role in EGS exploration. Porosity is the main parameter to detect zones within a rock formation that potentially contain warm fluids in quantities large enough to be utilized for geothermal heat production. Permeability of the formation controls the flow in the reservoir and hence directly influences well positioning and production rate of a geothermal system. The ideal case for a geothermal site is to have a reservoir with both high porosity and permeability. However, in zones with high porosity but low permeability EGS treatments can be employed, in which permeability is enhanced to increase productivity and ultimately to bring a formerly non-economic reservoir to be economic.

4.1 Data set

For this study, porosity and permeability of the Paleozoic aquifers were investigated by utilizing core analysis data from the Alberta general well data file. In total, information from 51 617 Paleozoic rock samples (plugs) from more than 975 wells was used for this study. As described earlier, most of the data in the Alberta general well data file comes from the hydrocarbon industry, and therefore the majority of the core samples exist from the Leduc and Nisku formations while comparatively little information is available from the Cooking Lake Formation and Wabamun Group. No core analysis data for the Cambrian Basal Sandstone Unit in the study area was available. Earlier studies of the Cambrian Basal Sandstone in central and southern Alberta described good (15–20 %) to excellent (20–25 %) porosity except in a band south and southeast of Edmonton where the sandstone is cemented with kaolin and porosity is poor (5–10 %; Levorsen 1967; Pugh 1971; Nowlan et al. 1995).

Porosity and maximum (horizontal) permeability (Kmax) were assessed for each of the formations that appeared to have favourable geothermal conditions. The porosity and permeability values obtained from core analyses represent volume-averaged values corresponding to the sample size. In general, they represent matrix properties and not larger scale features such as fractures or vugs. Nevertheless, some individual core analyses show very high Kmax values (> 10 D) that seem to reflect flow through these features. The core analysis data in the Alberta general well file comes from various companies and the

analyses were performed by various laboratories from the 1950s until today. Measurement and data entry errors are likely present in the dataset, and only little information on the sample and measurement quality of individual core tests is available. Conducting an individual examination and culling of analyses is not possible with a dataset of this large size, and no clear criteria for automatic culling could be developed.

4.2 Upscaling of core analysis data

Individual results from core analyses are only representative on the cm-scale and porosity and permeability of rocks may vary within short distances both vertically and laterally. Given the variations at a small scale and the inherent heterogeneity of carbonate rocks, data trends can still be identified at a larger scale. To investigate regional-scale (km-scale) trends in the data, a scaling-up process must be applied to the small-scale core analysis data (Bachu and Underschultz 1992). This process of upscaling is analogous—and identical in a mathematical sense—to filtering a signal to remove short-wavelength noise in order to detect existing long-wave trends (Cushman 1984; Bachu and Underschultz 1992). Since there are several orders of magnitude between the plug scale and the regional scale, a sequential approach should be used by which the values of the parameter of interest are successively scaled up (Cushman 1984). Therefore, the plug-scale values were scaled up first to well scale, and then the well scale values were scaled up to average values representing the regional scale. However, it has to be emphasized that these scaled-up values still do not reflect large scale features such as vugs and fractures.

Variation of permeability of consolidated sediments is best characterized by a lognormal frequency distribution (Dagan 1989). One possibility to estimate a representative value of horizontal permeability at the well scale in each formation is to calculate the geometric average of the plug-scale maximum permeability values in a core (Bachu and Underschultz 1992).

Local-scale porosity may be described by a normal probability density function and has a much smaller variance (Dagan 1989). The variance of normalized log permeability exceeds the variance of normalized porosity by a factor of 1.2 (Wabamun Group) to 6.1 (Nisku Formation). The porosity value at the well scale in each formation is given by the arithmetic average of the plug-scale values of the sampled interval. Up-scaling to regional-scale values was conducted by calculation of the geometric average of the well-scale values. The 51,617 plug-scale values were scaled up to well-scale by individual stratigraphic unit, resulting in 1035 porosity and 1013 Kmax values for the four formations

of interest. These values are unevenly distributed: more than 400 well scale values exist for the Leduc- and Nisku formations, while few values exist for the Wabamun Group (83) and for the Cooking Lake Formation (10, Tab. 2) Well scale porosity and permeability relationships of the four Devonian carbonate formations are shown in Fig. 10.

4.3 Porosity and permeability variation

The lowest regional scale porosity was found in the Nisku Formation at 4.5 % (Tab. 2). Regional scale porosity of the Leduc Formation was 6.7 % and tests performed on samples from the Cooking Lake Formation have a regional scale porosity of 8.2 %. The highest regional scale porosity in the Devonian carbonates was found in samples from the Wabamun Group with a value of 8.7 %. The well-scale porosity of the individual formations is highly variable: e.g., for the Wabamun Group it ranges from 0.4–28.3 %. The box plots shown in Fig. 11 graphically display the median, quartiles, interquartile range

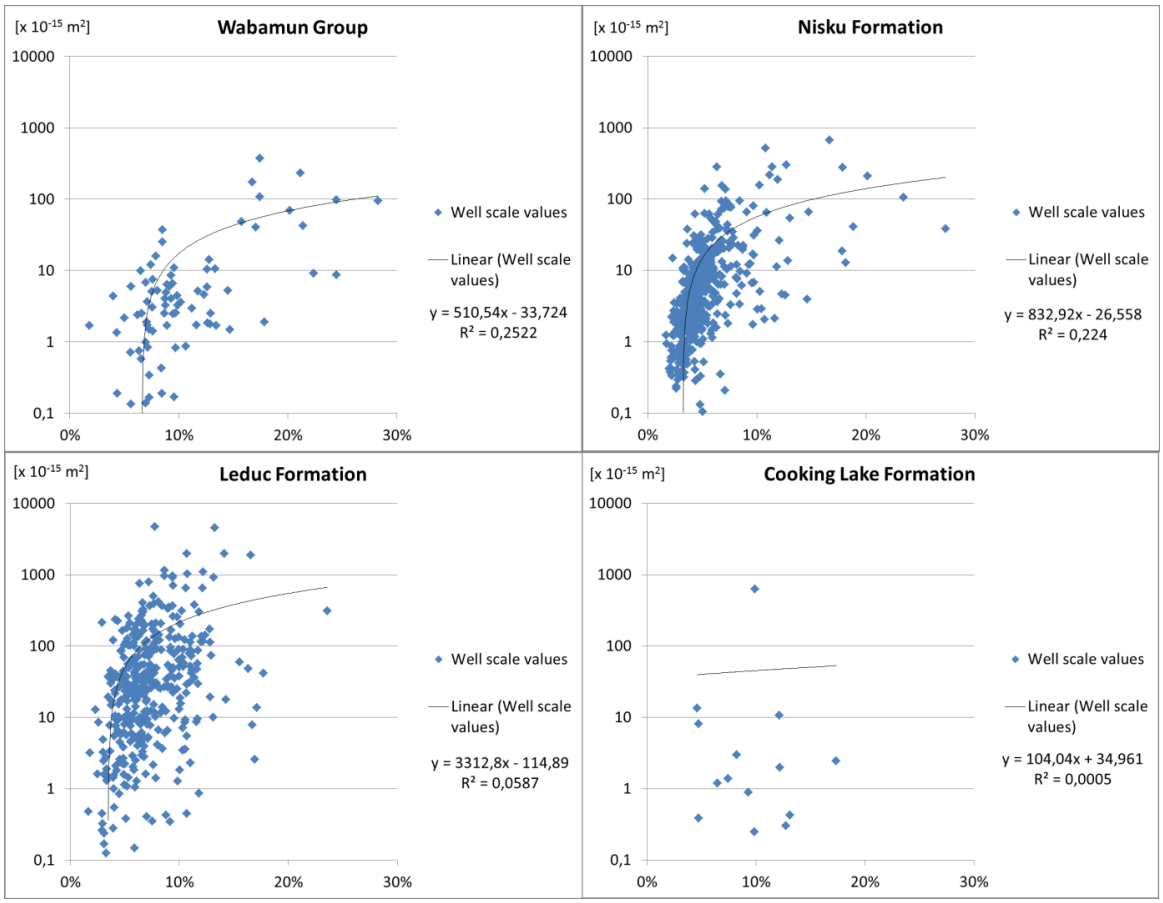

Fig. 10: Log permeability and porosity relationships of the four Devonian formations, based on upscaled conventional core analysis data.

Stratigraphic unit	No. of well scale values	Porosity (%)			Maximum horizontal permeability ($\times 10^{-15}$ m^2)		
		Average	Minimum	Maximum	Average	Minimum	Maximum
Wabamun	83	8.7	0.4	28.3	3.5	0.05	405.0
Nisku	536	4.5	1.4	18.1	4.9	0.02	4560.0
Leduc	404	6.7	0.6	23.6	26.0	0.01	4709.3
Cooking Lake	10	8.2	4.6	17.3	3.9	0.4	628.0

Tab. 2: Well-scale porosity and permeability from core analysis data.

and extreme values of the data, and give a good pictorial representation of the variability. To explain this wide range of well-scale values, different factors have to be taken into consideration. Naturally, the lithology of the individual formations changes laterally and with depth leading to different well-scale values. In addition to these large-scale variations, carbonate systems have an inherent variability and heterogeneity in comparison to siliciclastic systems. Furthermore do local features such as vugs and fractures have a strong impact on the test result of an individual sample and lead to very high porosity values. Samples from clay lenses, as they appear in carbonate facies such as mudstones and wackestones which are related to finer grained material, will have very low porosity in contrast. The number of samples taken from a well also influences the calculated well-scale value. In a dataset with a large number of samples, local features leading to anomalously high or low core analysis results will compensate each other, while in a set with only few samples one or two extreme values will have a high influence on the calculated well-scale value. On average, one well-scale value for a specific formation is based on 53 individual core analysis results. The highest regional scale Kmax of 26.0×10^{-15} m^2 is found in the Leduc Formation. The strata of the Cooking Lake and Nisku formations have a regional scale Kmax of 3.9×10^{-15} m^2 and 4.9×10^{-15} m^2, while the lowest regional scale Kmax was found in the Wabamun Group with 3.5×10^{-15} m^2 respectively (Tab. 2). The variability of well-scale Kmax is high, as presented in the box plot of well-scale Kmax (Fig. 12). For the Leduc and Nisku formations Kmax ranges from 0.01×10^{-15} m^2 (which represents the lower measurement limit on the core analysis data) and more than 4500×10^{-15} m^2.

4.4 Regional distribution of porosity and permeability

The regional distribution of porosity and permeability in the four Devonian stratigraphic units was mapped using the ordinary kriging algorithm. With kriging, unbiased estimates

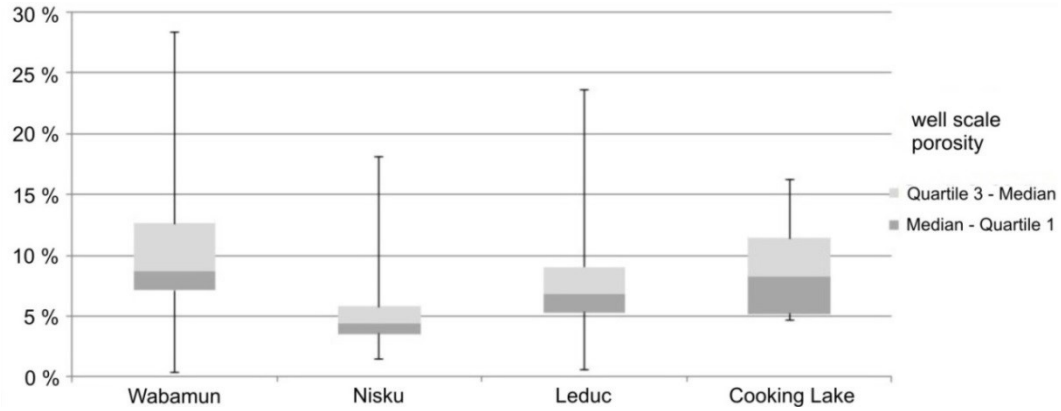

Fig. 11: Box plots of well-scale porosity from core analysis data.

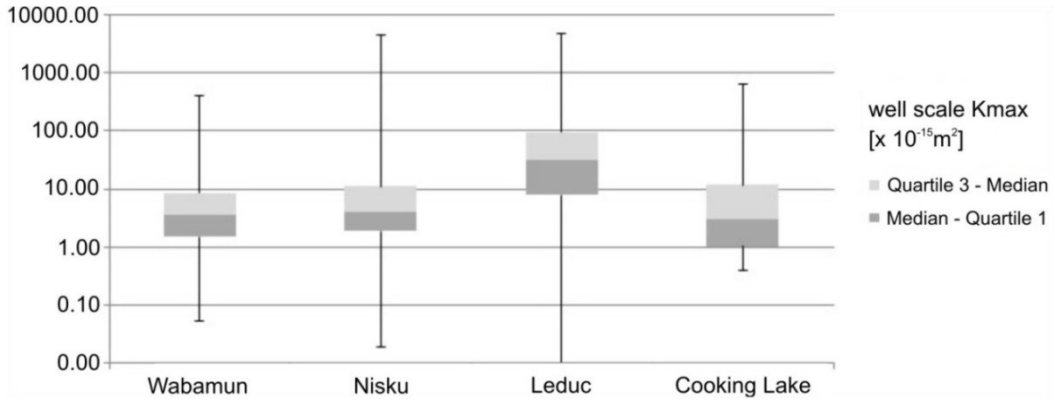

Fig. 12: Box plots of well-scale maximum horizontal permeability from core analysis data.

the semivariogram and the initial set of data values (David 1977). Ordinary kriging has been called the "anchor algorithm of geostatistics" and it is the most commonly used kriging algorithm for mapping topography and property data (Deutsch and Journel 1998). A detailed discussion of the ordinary kriging method can be found in Isaaks and Srivastava (1989). The property mapping was performed with upscaled core analysis data (i.e., well-scale) values using the "Geostatistical Analyst" extension of the ArcGIS® 9.3 software. The resulting maps (Fig. 13, Fig. 14) show a NE–SW trend of decreasing porosity and permeability for the Cooking Lake and Nisku formations, and Wabamun Group. This trend can be explained by higher compaction of the strata due to increasing burial depth in this direction (Ahr 2008). For the Nisku Formation and Wabamun Group, increased porosity and permeability in the northeast may also be related to the development of karst at the sub-Cretaceous unconformity (Dembicki and Machel 1996). However, this trend of decreasing porosity and permeability towards the SW is not found in the Leduc Formation.

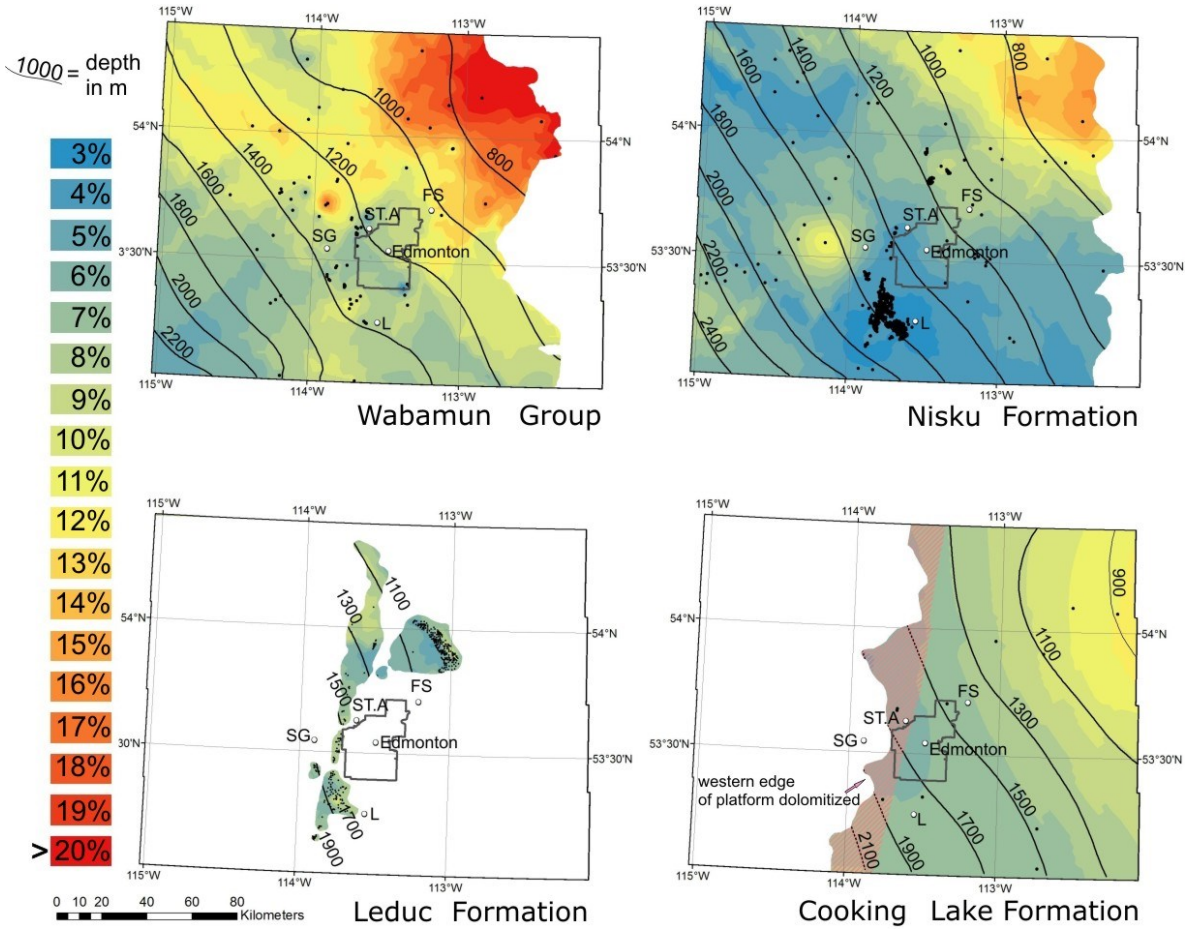

Fig. 13: Porosity distribution in the Devonian Cooking Lake, Leduc and Nisku formations and Wabamun Group. Estimates of porosity are based on upscaled core analysis data and mapped using the ordinary kriging method. The approximated area of dolomitization at the edge of the Cooking Lake platform is indicated by a hatched pattern (from Switzer et al. 1994). Contour lines indicate the depth from surface to formation top in meters. Formation extents are interpreted within the 3D geological model. FS = Fort Saskatchewan, St.A = St. Albert, L = Leduc, SG = Spruce Grove.

The distribution of high porosity and permeability zones in the Leduc Formation is controlled by depositional facies variations, dolomitization and the presence of locally existing moldic and vuggy porosity (Walls and Burrowes 1990; Amthor et al. 1994). The carbonate depositional model produced for the Redwater Leduc reef by Bachu et al. (2011) identified the reef flat, reef margin, and upper fore-slope facies to contain higher porosity and permeability, while in the tidal flat/lagoon facies the porosity and permeability are lower. Amthor et al. (1994) found that dolomitization of Leduc reefs resulted in a decrease in porosity at shallow depths, while at greater depths dolomitized carbonates were able to withstand compaction better, and thereby retained more porosity than limestones at the same depth. As a result of depositional facies and compaction, several zones of higher porosity and permeability exist in the Leduc Formation, e.g., the northeastern side of the Redwater reef and the northern part of the Rimbey-Meadowbrook reef trend in the study

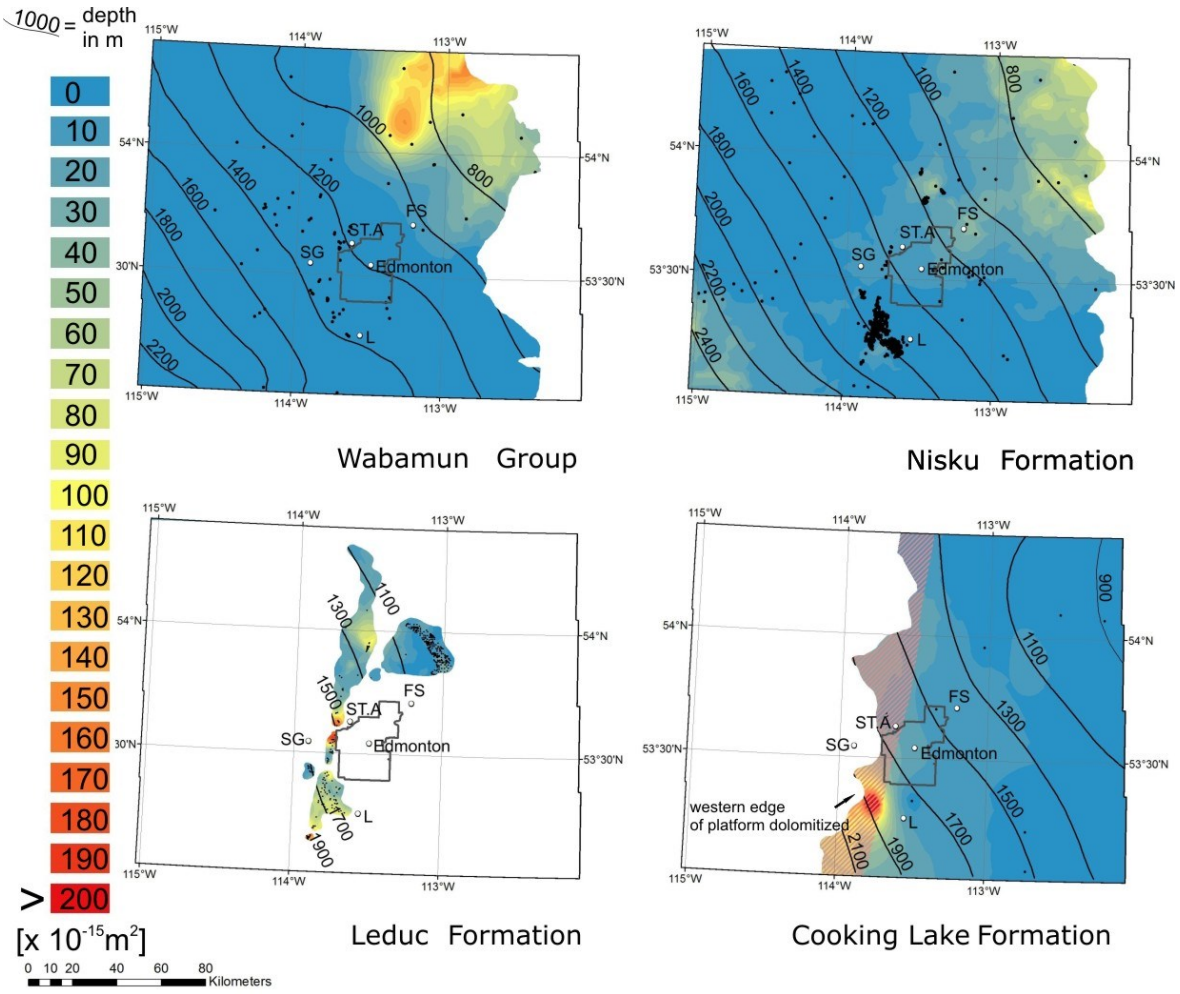

Fig. 14: Distribution of maximum horizontal permeability (Kmax) in the Devonian Cooking Lake, Leduc and Nisku formations and Wabamun Group. Estimates of permeability are based on upscaled core analysis data and mapped using the ordinary kriging method. The approximated area of dolomitization at the edge of the Cooking Lake platform is indicated by a hatched pattern (from Switzer et al. 1994). Contour lines indicate the depth from surface to formation top in meters. Formation extents are interpreted within the 3D geological model. FS = Fort Saskatchewan, St.A = St. Albert, L = Leduc, SG = Spruce Grove

area, but also further south, e.g., between the town of Spruce Grove and the city of St. Albert (Fig. 13, Fig. 14). The carbonates of the Cooking Lake Formation are thick and extensively dolomitized at the western platform margin beneath the Rimbey-Meadowbrook Leduc reef trend resulting in zones of increased porosity and permeability (Switzer et al. 1994; Wendte 1994). In the core analysis dataset from the Alberta General well file, only data from one well is located in this zone which makes geostatistical interpolation difficult. In the map (Fig. 13, Fig. 14) this zone at the western margin of the Cooking Lake platform is indicated by a hatched area coloured pink (from Switzer et al. 1994).

5. Temperatures of Paleozoic formations

Knowledge of subsurface fluid temperatures is important in geothermal exploration. (Gray et al. 2012) estimated the average geothermal gradient (GradT) for the Phanerozoic succession in northern Alberta to be 32 °C/km using bottom hole temperature (BHT) data and temperature data from drill-stem tests (DST). Gray et al. (2012) corrected the BHTs for drilling circulation disturbance. Majorowicz and Jessop (1981) estimated that the effective thermal conductivity in central Alberta is > 2 W/(mK) and the heat flow is > 64 mW/m^2 considering thermal conductivity (TC) measurements of the rocks, net rock mineralogical composition data and porosity estimates from well logs. This estimate came closer to earlier precise heat flow measurements in wells near Leduc and Redwater around Edmonton (Garland and Lennox 1962). These first heat flow determinations in Alberta in wells with precise equilibrium temperature logs and measured thermal conductivity on cores have been the only high precision heat flow data until new measurements were performed in a deep well in northeastern Alberta near the city of Fort McMurray in 2011 (Majorowicz et al. 2012). All other heat flow determinations for the area are from estimates based on single point industrial measurements of temperature (DST, BHT, etc.) and thermal conductivity approximations. The heat flow measurements of Garland and Lennox (1962) were both made at depths less than 1000 m (some as shallow as 300 m). Their values for Leduc and Redwater are 67 mW/m^2 and 61 mW/m^2, respectively. Applying a paleoclimatic correction (Gosnold et al. 2011; Majorowicz et al. 2012; Majorowicz et al. 2013) would bring these values up by 12 % to 75 mW/m^2 and 68 mW/m^2, respectively. These values are much higher than the 59 mW/m^2 determined from the deep well in northeast Alberta (Majorowicz et al. 2012).

The heat flow estimate of > 69 mW/m^2 for central Alberta by (Majorowicz and Jessop 1981) is slightly higher than the average heat flow of Canada which is 64 mW/m^2 with a standard deviation of 16 mW/m^2 (Majorowicz and Grasby 2010b). It is also close to the precise measurement of heat flow by Garland and Lennox (1962) after application of a paleoclimatic correction (75 mW/m^2 and 68 mW/m^2 for Leduc south of Edmonton and Redwater north of Edmonton). These quite elevated heat flow values in the Edmonton area may be related to elevated heat generation of the Precambrian basement (> 2 μW/m^3 acc. to Jones and Majorowicz (1987). While these are not the highest heat flow values in Alberta (heat flow as high as 90 mW/m^2 has been observed in northwestern Alberta), they are considered elevated for the Precambrian cratonic basement and likely related to hotter upper crustal Precambrian rocks of the Churchill province (Jones and Majorowicz 1987).

5.1 Estimation of geothermal gradient and mean ground temperature

Recent work on the thermal field in Alberta was done by Gosnold et al. (2011), Majorowicz et al. (2012) and Gray et al. (2012) and covered most of central and northern Alberta. The thermal field studies are based on an extensive data base, which included BHTs, temperatures taken during DSTs and annual pressure and temperature (P/T) tests. 1480 corrected temperature values from this data base were extracted for this study (Fig. 15) and statistically approximated resulting in a geothermal gradient of 34.6 °C/km (Fig. 16). The standard deviation of this geothermal gradient is 5.7 °C/km. Compiled plots of individual temperature records coming from large numbers of wells for this study area are bounded by a large standard error of estimate of statistical temperature vs. depth linear regression as shown by Lam and Jones (1985). Their southern Alberta study based on 33,652 BHTs from 18,711 wells shows that the standard error of estimate of temperature vs. depth plots varies regionally from 3–6 °C in the Alberta plains to 8-14 °C in the Rocky Mountain Foothills. In our study the standard error of estimate of the corrected temperature data (Fig. 15) is not larger than 4 °C. This variability is partly due to non-determined uncertainty in the industrial data pool (e.g. measuring errors) as well as variability of lithology of variable thermal conductivity with depth and space. These factors are almost impossible to distinguish due to low quality of the industrial temperature data. Continuous equilibrium logs would be required to narrow this uncertainty, which at the present are not available for the study area.

An assumption on the mean ground temperature is needed to calculate temperature at depth from the known geothermal gradient. The temperature records taken at a depth of a few hundred meters are closer to equilibrium with recent millennial temperature than present climatically elevated temperatures at surface (Majorowicz et al. 2013). In contrast, temperatures measured below a depth of 1500 m appear to be in equilibrium with surface temperatures from the Wisconsin glaciation, which is about -1 °C to -4 °C (Jessop 1990; Gosnold et al. 2011; Majorowicz et al. 2012; Majorowicz et al. 2013). This has been accommodated in assigning a ground surface mean temperature correction in relationship to default 0 °C with an uncertainty of 2 °C.

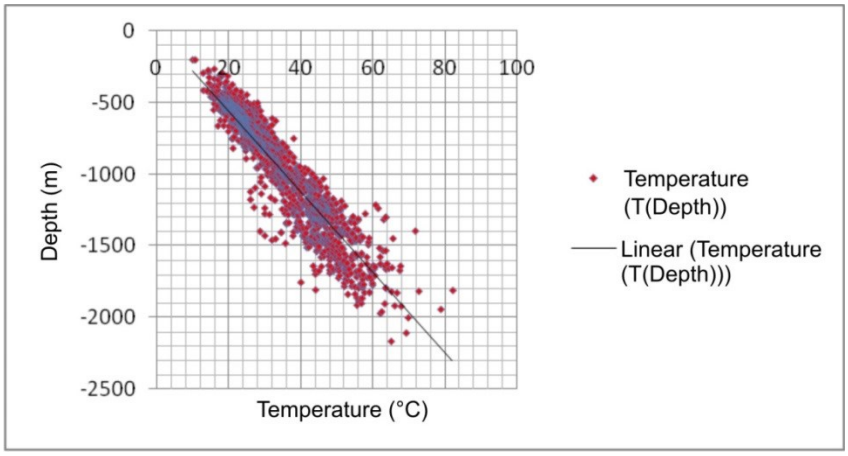

Fig. 15: Variation of corrected temperature data vs. depth for wells in the study area.

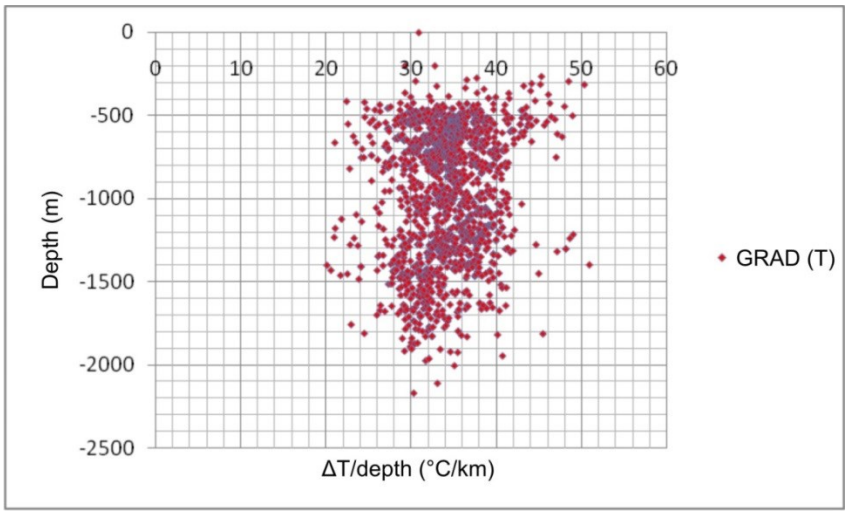

Fig. 16: Variation of geothermal gradient for wells in the study area.

5.2 Regional distribution of subsurface temperatures

Based on the average temperature gradient of 34.6 °C/km, the assumed ground surface mean temperature of 0 °C was used to calculate the temperatures at the top of the aquifer units combined with information about depth of the five stratigraphic units from well data. The average geothermal gradient was multiplied with the measured total vertical depth from ground surface to the top of the individual stratigraphic unit, resulting in five datasets of temperatures at top a stratigraphic unit, which were interpolated with local polynomial interpolation. The lateral extent of the formations was derived from the 3D geological model. Temperature ranges for the subsurface were estimated for the entire study area, particularly for the units beneath the city of Edmonton (Fig. 17, Tab. 3). Due to the

southwest dip of the strata, the temperature generally increases towards the southwestern corner of the study area.

The highest temperature is found in the Cambrian Basal Sandstone Unit with temperatures ranging from 62 °C in the NE to 122 °C in the SW. The temperature in the Devonian stratigraphic units ranges from 21 °C in the Wabamun Group in the NE of the study area to 88 °C in the Nisku Formation in the SW. Beneath Edmonton, the temperature in the Cambrian Basal Sandstone Unit is estimated to be between 81–89 °C, and between 36–59 °C in the Devonian units.

Temperature distribution at formation tops results from the average geothermal gradient, the mean ground surface temperature and the depth of the formation tops relative to the ground level. The uncertainty in temperature calculations depends mainly on the geothermal gradient, which has a standard deviation of 5.7 °C/km. The uncertainty of the mean ground surface temperature is 2 °C. The standard prediction error of the formation depth is ranging from 0.5 % for areas with high data density (e.g. Nisku Formation for most of the study area) and more than 5 % for areas with low data density (e.g. Cambrian Basal Sandstone Unit in the outer parts of the study area). The stratigraphic tops from well logs used for 3D geological modeling have a precision of ± 10 m (Mossop and Shetsen 1994b).

We assume conductive heat transfer for the study area; however, this assumption will not affect the calculations as these result from statistically established geothermal gradient based on the 1840 temperature records for the study area. A possible influence of a convective component of heat transfer is not included in the temperature calculations as this is not measured in this study. This method of statistically approaching temperature

Period	Stratigraphic unit	Depth in study area	Estimated temperature in study area	Depth beneath Edmonton	Estimated temperature beneath city of Edmonton
Devonian	Wabamun	610–2290 m	21–79 °C	1050–1295 m	36–44 °C
	Nisku	650–2542 m	22–88 °C	1185–1435 m	41–50 °C
	Leduc	985–1905 m	34–66 °C	not deposited	-
	Cooking Lake	813–2220 m	28–77 °C	1465–1715 m	51–59 °C
Cambrian	Basal Sandstone	1785–3531 m	62–122 °C	2365–2575 m	81–89 °C

Tab. 3: Estimated temperatures at the top of stratigraphic units in the study area.

records for establishing a single geothermal gradient for the study area has been chosen rather than calculating temperature from estimates of heat flow and estimates of thermal conductivity based on conductive heat transfer. In the area only two heat flow values exist which are based on actual measurements (precise temperature logs and measured thermal conductivity) taken above 1 km depth by from Garland and Lennox (1962). All other heat flow values reported in previously published literature are estimates which are bounded by large uncertainties and estimated errors are sometimes larger than regional variability in the study area.

6. Discussion

The porosity and permeability of four Devonian formations was investigated with existing core analysis data from the Alberta General well file. Analysis of the data shows that these formations have average well-scale matrix porosity values between 4.7–8.7 % and average well-scale matrix permeability values of 5–142 $\times$ 10^{-15} m^2. Investigation of cores from the study area has shown that in parts of the Devonian formations, particularly the Leduc Formation, porosity comprises locally vuggy and moldic porosity, which is also known from various previous studies, e.g., Walls and Burrowes (1990) and Amthor et al. (1994). Porosity and permeability of these local features is high, and their influence on regional scale permeability is not fully represented by the core analysis data. In the Wabamun Group and Nisku Formation, and also in the Cooking Lake Formation except at its western edge, a trend of decreasing porosity and permeability with depth was recognized, which can be explained by higher compaction of the strata. Elevated porosity and permeability at the western dolomitized edge of the Cooking Lake platform is indicated by core analysis results from one well only. Further data is required to confirm this finding and to map this zone of higher porosity and permeability with higher accuracy. Increased porosity and permeability in the northeast for the Nisku Formation and Wabamun Group may be related to the development of karst at the sub-Cretaceous unconformity (Dembicki and Machel 1996). The estimates presented in this study are representative of matrix properties, therefore it is likely that porosity and permeability could be substantially higher in localized areas. Also, influence of faults and fractures on fluid flow cannot be investigated by core analysis data. With these restrictions upscaling of core analysis data to the regional scale is an appropriate and opportune method to analyze rock properties and their spatial distribution in the first phase of EGS exploration, especially in regions as Alberta where a large amount of data is publicly available. The geostatistical method used in this study for

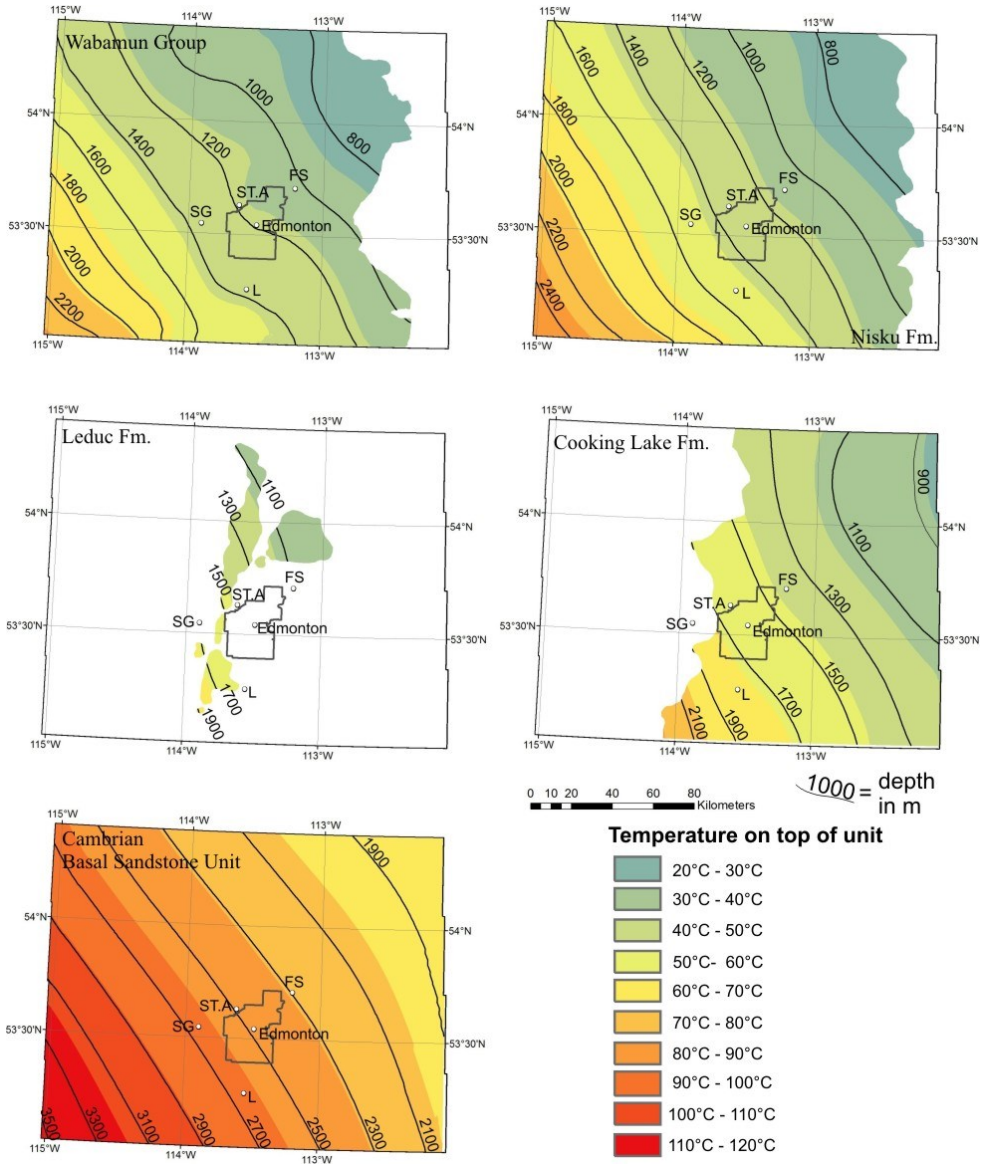

Fig. 17: Estimated temperature at the top of the Wabamun Group, Nisku, Leduc, Cooking Lake formations, and Cambrian Basal Sandstone Unit. Temperatures were calculated using an average geothermal gradient for the Phanerozoic succession of 34.6 °C/km. Contour lines indicate the depth from surface to formation top in meters. Formation extents are interpreted within the 3D geological model. FS = Fort Saskatchewan, St.A = St. Albert, L = Leduc, SG = Spruce Grove.

interpolation of core analysis data was ordinary kriging. For future studies Sequential Gaussian Simulation should be applied instead, which is based on kriging, but has several advantages, as this method accounts for the spatial variability of rock properties, it yields a measure for the involved uncertainty and provides many models of the subsurface instead of one. Besides rock properties such as porosity and permeability, the temperature of the potential geothermal reservoirs was estimated. Naturally, the temperature in the formations increases with depth. The characteristics of the Paleozoic formations in the study area were

compared in four regions of different location and depth (Fig. 18). Region 1 is located in the shallower portion of the study area in the northeast, while region 2 is located in the deeper part toward the southwest. Regions 3 and 4 are located in the middle of the study area around the town of Leduc (3) and around the urban area of Edmonton (4) (Fig. 18). Ranges for porosity, permeability, and formation temperatures of these stratigraphic units for the individual areas are presented in Tab. 4. When comparing the regions 1 and 2—the shallowest and the deepest parts of the basin in the study area, respectively—the differences in rock properties and temperatures of the formations in both areas are striking. The Paleozoic formations in the shallow northeast (region 1) have the highest porosities and permeabilities, but also the lowest temperatures (Tab. 4). In contrast the formations in the deeper southwest (region 2), obtain the lowest porosities and permeabilities, but the highest temperatures (Tab. 4). The best place for applying geothermal technology naturally would be a region where the formation has a high porosity and permeability, and where temperatures are in a higher range. In regions 3 and 4, located in the center of the study area (Fig. 18), both hydraulic rock properties and formation temperatures converge. The highest porosity in these regions is found in the Wabamun Group (7–12 %), whereas the Cooking Lake Formation (up to 170 × 10^{-15} $m^{2)}$ and Leduc Formation (up to 230 × 10^{-15} $m^{2)}$ have the highest permeabilities. The temperature ranges from 37–66 °C in the Devonian formations and from 79–95 °C in the Cambrian Basal Sandstone Unit. Porosity and permeability of the Cambrian Basal Sandstone Unit in central Alberta have not been investigated, yet. Earlier studies of the Cambrian Basal Sandstone in central and

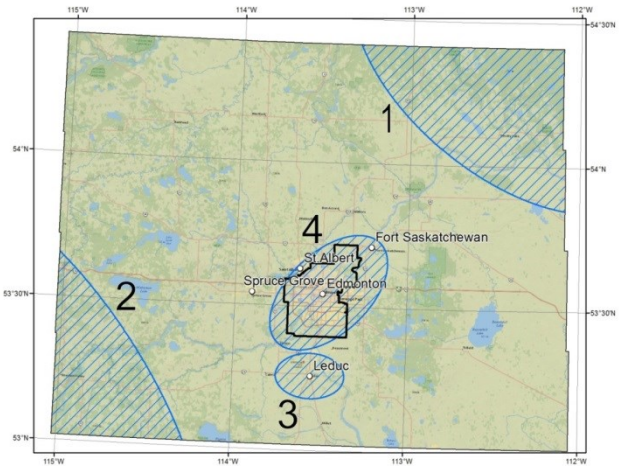

Fig. 18: Location of four regions selected for comparison of formation properties and subsurface temperatures to evaluate geothermal resource potential; Characteristics of the specific stratigraphic unit in the respective area are listed in Tab. 4.

regions in central Alberta and in western Saskatchewan, except in a band south and southeast of Edmonton where the sandstone is cemented with kaolin and porosity is poor (5–10 %) (Levorsen 1967; Pugh 1971; Dixon 2008; Nowlan et al. 1995). Its potential to store CO_2 is currently investigated for the Shell Quest CCS project in the northeastern part of the study area (Shell 2010b).

Since no seismic data was used in the 3D geological modeling process, no information on subsurface structures was integrated into the model. The spatial distribution of stratigraphic tops and the geometry of the modelled horizons were analyzed in the 3D software, but no regional-scale structures could be identified with this method. Regional analysis of Paleozoic formations has shown that the potential geothermal reservoirs in central Alberta are controlled by depositional and diagenetic facies rather than by geological structures. The 3D geological model developed in this study in combination with the geostatistical

Region	Stratigraphic unit	Porosity [%]	Permeability [$\times 10^{-15}$ m^2]	Temperature [°C]	Measured depth to surface [m]
1	Wabamun	17–28 (not deposited in corner)	70–150	22.0–23.8	610–688
	Nisku	13–18	15–150	22.5–27.8	650–804
	Leduc	not deposited	not deposited	not deposited	not deposited
	Cooking Lake	9–13	2–9	28.1–39.5	813–1141
	Basal Sandstone Unit	no data	no data	62.1–67.3	1796–1944
2	Wabamun	5–8	0.5–6	64.7–79.2	1870–2290
	Nisku	4–9	2–50	69.8–88.0	2018–2542
	Leduc	not deposited	not deposited	not deposited	not deposited
	Cooking Lake	not deposited	not deposited	not deposited	not deposited
	Basal Sandstone Unit	no data	no data	107.3–122.2	3100–3531
3	Wabamun	7–10	2–10	44.9–50.0	1299–1445
	Nisku	3–5	2–4	49.0–55.7	1417–1611
	Leduc	5–11 (only in W)	30–100	54.7–58.3	1581–1686
	Cooking Lake	6–8	10–170	58.9–65.5	1701–1892
	Basal Sandstone Unit	no data	no data	88.2–94.9	2550–2743
4	Wabamun	7–12	2–13	38.4–46.7	1111–1351
	Nisku	3–8	2–50	37.1–52.2	1071–1508
	Leduc	7–9 (only in SW)	20–230 (only in SW)	52.0–56.0	1504–1619
	Cooking Lake	6–9	10–120	47.3–63.4	1367–1832
	Basal Sandstone Unit	no data	no data	78.9–92.5	2280–2674

Tab. 4: Ranges of porosity, permeability, temperature and depth to surface for the five Paleozoic formations in the four areas identified for comparison of geothermal resource potential within the study area (see Fig. 18).

mapping based on core analysis data allows an adequate analysis of these facies-controlled potential geothermal systems.

7. Conclusions

Regional analysis of rock properties shows that the five deep formations investigated in this study are potentially useable for geothermal applications. The Cambrian Basal Sandstone Unit seems the best suitable horizon for geothermal applications in central Alberta due to its depth and its distribution throughout the whole study area. However, since no core analysis data for this horizon from the study area exists in the Alberta general well data file, a detailed investigation of the properties of the Cambrian Basal Sandstone Unit is necessary, including porosity and permeability tests, geomechanical tests and thin section analysis.

A possible application for geothermal heat production is district heating, for which a geothermal fluid with a temperature of 70–80 °C is needed (Líndal 1973). For the Cambrian Basal Sandstone Unit, temperatures above 70 °C are estimated throughout the majority of the study area except for the northeastern corner (region 1 in Fig. 18). In the region around the city of Edmonton, temperatures between 81–89 °C are expected. In the Devonian strata temperatures above 70 °C are predicted only for the Nisku Formation in the southwestern corner of the study area. Temperatures above 40 °C can be used for heating of greenhouses and domestic water provision (Líndal 1973; Laplaige et al. 2000). Fluids above 40 °C are estimated for all Devonian strata in the western half of the study area, including the region around Edmonton. Furthermore, fluids of all temperature ranges can be used as preheated feedwater for various applications.

The 3D model presented in this study was developed without seismic data; it is based on stratigraphic tops from wells. As a large amount of well data is publicly available in Alberta, this approach allows the development of a 3D lithostratigraphic model that is detailed sufficiently for analysis of stratigraphic unit thicknesses and geometries for temperature estimation and rock property modeling. However, for a detailed exploration study at a local scale, prior to the development of a specific geothermal site, seismic data must be integrated into the modeling process to obtain information about existing structures in the subsurface. Faults and fractures are potential fluid pathways and information on their occurrence and style is crucial in geothermal exploration. The next step in exploration for a specific site would include an investigation of stress states and reactivation potential of fractures and faults by applying the slip tendency technique on the

3D structural geological model (Morris et al. 1996; Moeck et al. 2009b). Knowledge of the reactivation potential of faults is a critical issue in the development of EGS reservoirs where hydraulic stimulation treatments are applied to enhance permeability thereby increasing productivity. Matrix porosity and permeability of the reservoir rock can be analyzed by existing core analysis data from the Alberta General well file supplemented with new samples. In addition, investigation and analysis of existing well logs from the Alberta general well file can help to determine formation properties at the well- and regional-scales.

Acknowledgements

Well data was provided by ERCB/AGS.

The 3D geological model was processed with EarthVision®, Dynamic Graphics Inc. (DGI).

The maps were created using ArcGIS® software by Esri Inc.

This study is part of the Helmholtz–Alberta Initiative (HAI), which is research collaboration between the Helmholtz Association of German Research Centres and the University of Alberta.

Chapter 3

Submitted to the *Canadian Journal of Earth Sciences (under revision)*

The Cambrian Basal Sandstone Unit in central Alberta—an investigation of temperature distribution, petrography and hydraulic and geomechanical properties of a deep saline aquifer

Simon Weides, Inga Moeck, Jacek Majorowicz, Matthias Grobe

Abstract

Recent geothermal exploration indicated that the Cambrian Basal Sandstone Unit (BSU) in central Alberta could be a potential target formation for geothermal heat production, due to its depth and extent. Although several studies showed that the BSU in the shallower Western Canada Sedimentary Basin (WCSB) has good reservoir properties, almost no information exists from the deeper WCSB. This study investigated the petrography of the BSU in central Alberta with help of drill cores and thin sections from six wells. Porosity and permeability as important reservoir parameters for geothermal utilization were determined by core testing. The average porosity and permeability of the BSU is 10 % and less than 1×10^{-14} m^2, respectively. A zone of high porosity and permeability was identified in a well located in the northern part of the study area. This study presents the first published geomechanical tests of the BSU, which were obtained as input parameters for the simulation of hydraulic stimulation treatments. The BSU has a relatively high unconfined compressive strength (up to 97.7 MPa), high cohesion (up to 69.8 MPa) and a remarkably high friction coefficient (up to 1.22), despite a rather low tensile strength (less than 5 MPa). An average geothermal gradient of 35.6 °C/km was calculated from about 2000 temperature values. The temperature in the BSU ranges from 65 °C to 120 °C. Results of this study confirm that the BSU is a potential geothermal target formation, though hydraulic stimulation treatments are required to increase the permeability of the reservoir.

1. Introduction

The Cambrian Basal Sandstone Unit (BSU) is distributed in the eastern and central part of the Western Canada Sedimentary Basin (WCSB) and unconformably overlies the Precambrian basement (Fig. 19). Due to the lack of hydrocarbon resources in the BSU and its position at the base of the sedimentary succession, information and knowledge about the BSU in the deeper WCSB is scarce. New interest in the BSU in central Alberta has arisen because it is being considered as a target reservoir for underground storage of CO_2 (Shell 2010a, 2011) and as a potential target formation for geothermal heat production (Weides et al. 2013; Hofmann et al. 2014).

The aim of this study was to improve the understanding of the temperature regime in central Alberta and the reservoir characteristics of the BSU (i.e. petrography, porosity, permeability, geomechanical properties) to assess its suitability for geothermal heat production. In the portion of central Alberta, desrcibed in this study (Fig. 20), two general requirements for siting a geothermal project are fulfilled: (1) a high heat demand (in the Edmonton metropolitan area) and (2), the temperatures in the BSU are high enough (60–120 °C) to be used for applications such as warm water provision or district heating and meet this heat demand (Weides et al. 2013). Besides temperature, the porosity, permeability and thickness of the reservoir rock are important parameters because they control the flow rate of a geothermal well. In areas of moderate heat flow like central Alberta, high flow rates must be achieved to extract enough heat from the subsurface, which is often a problem in the development of a geothermal project. Furthermore knowledge of the geomechanical properties of the reservoir rock is required to predict the behavior of the reservoir during extraction and injection of fluids (in geothermal production or CO_2 sequestration), or during stimulation treatments which might be conducted to increase the reservoir permeability (see Hofmann et al. 2014). Injection (or extraction) of fluids changes the in situ stress state of the reservoir, which could induce tensile or shear fractures in the rock, or lead to movement on fault planes and related seismicity.

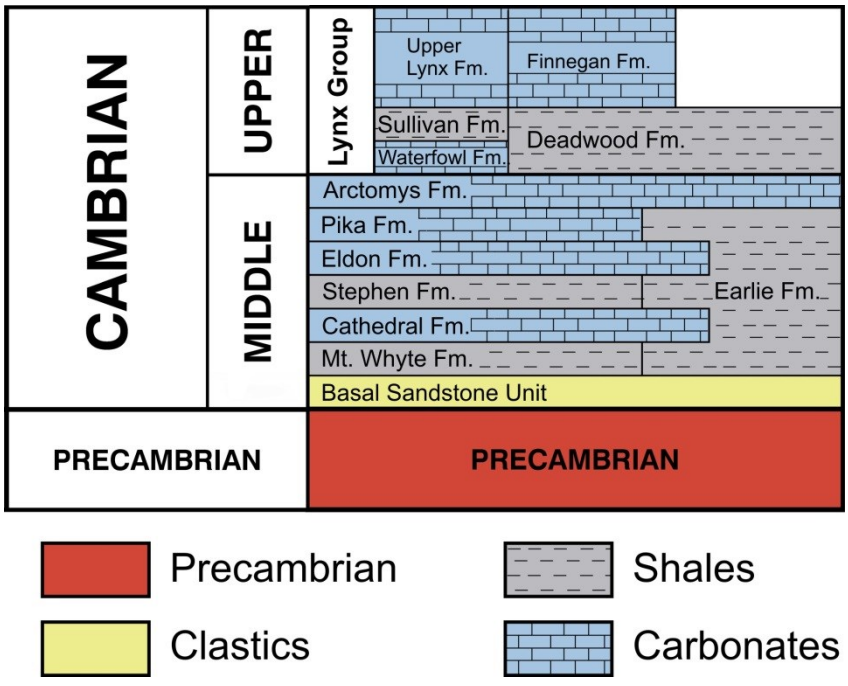

Fig. 19: Cambrian stratigraphy in central Alberta (modified from Energy Resources Conservation Board 2009).

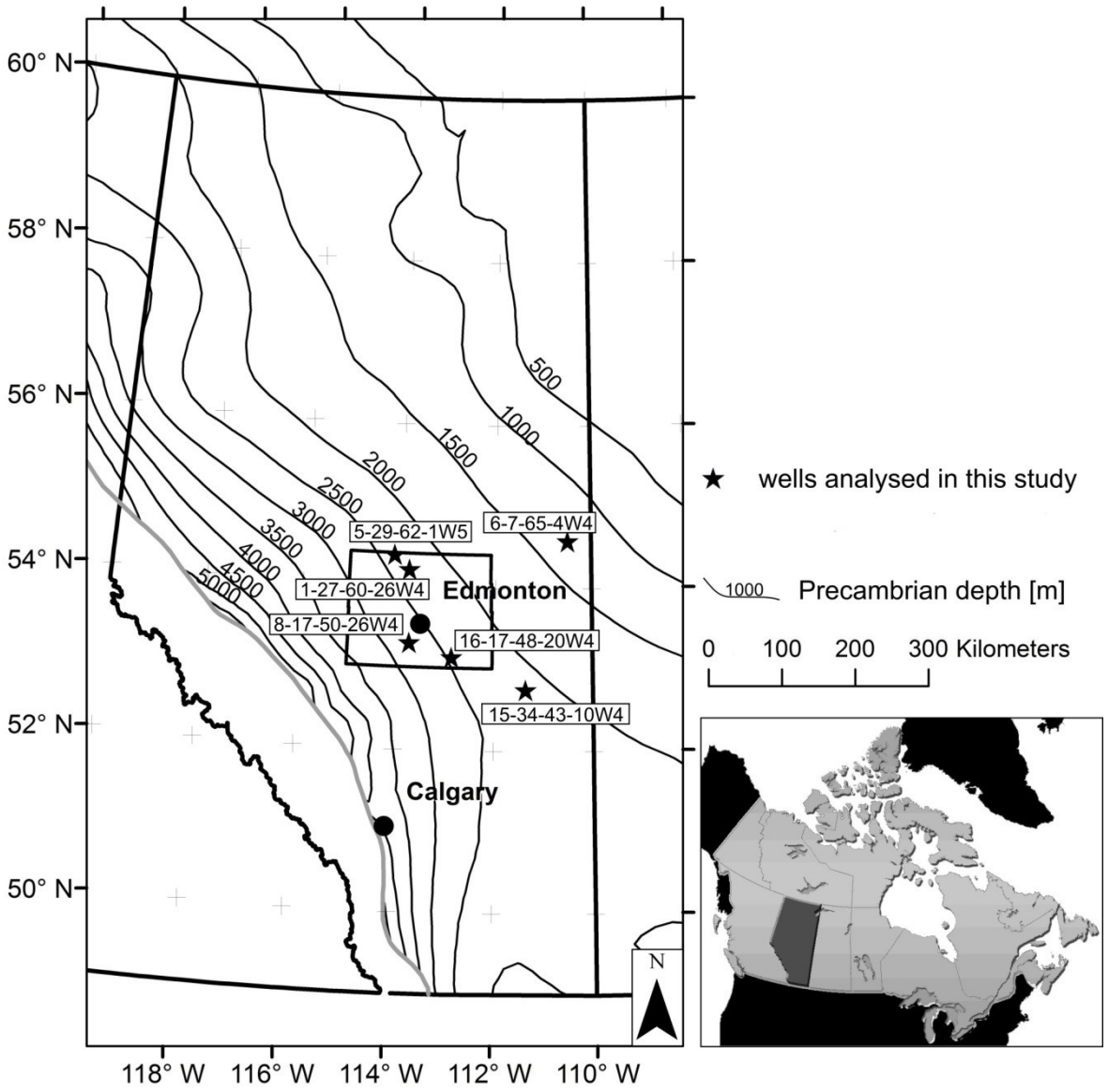

Fig. 20: Location of the study area and of the 6 wells with Basal Sandstone Unit (BSU) core material analyzed in this study. Contours show the depth of the top of the Precambrian basement in this region.

With regard to heat transfer, the central Alberta part of the WCSB belongs to the conduction dominated geothermal systems (applying the "geothermal play type" catalog from Moeck and Beardsmore 2014). Within this category it can be classified as "foreland basin" type, whose typical geothermal reservoirs are characterized by high porosity and preferably high permeability (Moeck and Beardsmore 2014). Geothermal conditions similar to the central WCSB exist, for example, in the German Molasse Basin, where geothermal wells were produce heat at temperatures of 100–140 °C from carbonate reservoirs at depths of 3–4 km (Geothermie Unterhaching 2014). Siliciclastic reservoir rocks similar to the BSU which are used as geothermal reservoirs are, for example, the Triassic sandstones (Buntsandstein) at the geothermal site of Landau (Upper Rhine graben,

Germany) (Geox 2014) and the Permian sandstone (Rotliegend) at the geothermal site of Gross Schönebeck in the Northeast German Basin (Moeck et al. 2009a).

1.1 Previous studies

Cambrian strata in the Alberta Basin were first recognized in a few deep hydrocarbon exploration wells drilled in the early 1950s. The lithological term Basal Sandstone Unit was introduced by Aitken (1968) for medium- and coarse-grained Cambrian sandstones with excellent (20–25% according to the classification after Levorsen, 1967) porosity in some wells. The thickness of the BSU in the wells studied by Aitken (1968) ranges between 27 m and 45 m. Pugh (1971, 1973) described the BSU in Alberta as a deposit of mainly coarse-grained sandstones, composed of rounded and poorly to very poorly sorted quartz grains, with good (15–20 %) to excellent (20–25 %) porosity. As an exception he describes a band south and southeast of Edmonton where the sandstone is cemented with kaolin and porosity is poor (5–10 %; Pugh, 1971). In the wells studied by Pugh (1971, 1973) the thickness of the BSU ranges from 17 m in the southeast and northwest to 115 m at the eastern border to Saskatchewan in the Lloydminster area. Slind et al. (1994) presented a synthesis of Cambrian stratigraphy and palaeography that included cross-sections and a brief descriptive text on the BSU. Coskun et al. (1995) analyzed porosity and permeability of the BSU in the shallower basin (1000–1500 m) of east-central Alberta from 143 core samples (from 4 wells), resulting in an average porosity value of 17 % and an average permeability value of more than 1×10^{-13} m^2.

The first detailed sedimentological study of the BSU was presented by Dixon (2008) for the eastern, shallower part of the WCSB in Saskatchewan, where the BSU is up to 290 m thick. According to Dixon (2008), the BSU and the overlying shales of the Early Formation represent the first of two two major transgressive-regressive sequences between the Middle Cambrian and the earliest Ordovician (Fig. 19).

The feasibility of large scale CO_2 storage in the BSU is being investigated in the Shell Quest project located northeast of Edmonton (Shell 2010a, 2011). Further work focusing on the CO_2 storage potential of the BSU has been conducted by Alberta Innovates and partners (Government of Canada 2010; Hauck et al. 2012; Huang et al. 2012; Rebscher et al. 2012).

The geochemical effects of storing CO_2 in the BSU were investigated by Talman et al. (2013).

Weides et al. (2013) identified the BSU as the most suitable horizon for geothermal applications in in central Alberta. Hofmann et al. (2014) performed thermo-hydraulic reservoir simulations and simulated hydraulic fracture stimulations for geothermal heat production from the BSU using the results of this present study as input parameters.

The geothermal potential of the basal clastics in Saskatchewan (which is an Upper Cambrian siliciclastic unit similar to the BSU) was studied by Jessop and Vigrass (1989), Vigrass (2007) and Ferguson and Grasby (2014). The authors concluded that direct geothermal use of the basal clastics could be quite successful, mainly due to the good hydraulic properties which should provide flow rates necessary for geothermal production with minimal or no stimulation (Ferguson and Grasby 2014).

Several studies investigated the heat flow, geothermal regime and radiogenic heat production of the WCSB during the last decades (Garland and Lennox 1962; Majorowicz and Jessop 1981; Jessop et al. 1984; Majorowicz et al. 1985; Burwash and Burwash 1989; Bachu 1993; Bachu and Burwash 1994; Jessop et al. 2005; Majorowicz 1996; Majorowicz et al. 1999; Grasby et al. 2009; Majorowicz and Grasby 2010a, Majorowicz et al. 2014). The heat flow of the WCSB ranges from 30–100 mW/m^2 (average of 60.4 mW/m^2), and the geothermal gradient is between 20 °C/km and more than 55 °C/km (average of 33.2 °C/km; Weides and Majorowicz 2014).

2. Methods

A variety of different methods was used to investigate the petrography of the BSU and the parameters that are relevant in geothermal exploration which are porosity, permeability and geomechanical properties, as well as depth, thickness and temperature distribution. For this study about 50 m of BSU core material from six wells was available for analysis, with four of these wells located within the study area (wells 5-29-62-1W5, 1-27-60-26W4, 8-17-50-26W4, 16-17-48-20W4), and two wells (15-34-43-10W4, 6-7-65-4W4) located approximately 50 km southeast and 75 km northeast of the study area, respectively (Fig. 20). The depth of the BSU in wells 5-29-62-1W5, 1-27-60-26W4, 8-17-50-26W4, 16-17-48-20W4 and 15-34-43-10W4 ranges from 2108 m (15-34-43-10W4) to 2730 m (8-17-50-26W4) (see Fig. 20), while well 6-7-65-4W4 is located in the shallower basin and penetrates the BSU at a depth of 1320 m.

2.1 Petrographic analysis of core material

For the petrographic description of the BSU the core material was visually analyzed (Figs. 21, 22, 23, 24). The mineral composition of the BSU was investigated by conducting a modal analysis (area percentage) on thin sections from 32 rock samples (from wells 5-29-62-1W5, 1-27-60-26W4, 8-17-50-26W4, 16-17-48-20W4 and 15-34-43-10W4; Fig. 19) using an optical microscope (Fig. 25). The grain size of 10 of these samples was analyzed using the image analysis software *JMicroVision* developed by Roduit (2008). Grain roundness was studied on 10 samples using visual comparators developed after Pettijohn et al. (1987). The degree of grain sorting was analyzed by applying the Folk and Ward (1957) formula on the graphic representation of the grain size data, and by using visual comparators as they were developed by Jerram (2001).

2.2 Helium pycnometry

Porosity was calculated from grain volumes and bulk volumes of 10 plug samples (from wells 5-29-62-1W5, 1-27-60-26W4, 8-17-50-26W4 and 15-34-43-10W4; Fig. 26; Tab. 5). The bulk volumes were determined with a caliper gauge, assuming a perfect cylindrical shape of the plug samples. Grain volume and density of the samples were measured using a MicroMeritics AccuPyc 1330 helium pycnometer. The pycnometer operates on Archimedes' principle of gas displacement. Density and volume of the sample are determined by measuring the pressure change of helium in a calibrated volume. A detailed description of the method can be found in Chang (1988).

2.3 Probe permeametry

Permeability was measured directly on cores using a Temco MP-401 Mini–Permeameter. With probe-permeametry the permeability of rock can be determined by measuring the flow-rate and pressure of nitrogen gas as it follows an unconfined flow path through the rock. Mini-permeametry is a rapid, inexpensive, nondestructive method to determine permeability of a rock sample (Halvorsen and Hurst 1990). The estimates of permeability obtained from probe permeametry are at least as accurate as Hassler–sleeve estimates (Halvorsen and Hurst 1990). However, it should be noted that with this method only matrix permeability of very small rock volumes of up to 1 cm^3 is measured. The probe tip used in this study had an inner diameter of 0.125 in. 96 measurements were conducted on cores from wells 5-29-62-1W5, 1-27-60-26W4, 8-17-50-26W4, 16-17-48-20W4 and 15-34-43-10W4 (Tables 5 and 6; Fig. 27). All measurements were performed perpendicular to the direction of drilling, hence subparallel to bedding. For comparison

with the porosity values which were measured on plug samples, 9 of these 96 measurements were taken at the location from which core plugs were taken.

2.4 Geomechanical testing

The geomechanical properties of the BSU were determined in uniaxial, triaxial, and diametral compression tests (Tab. 7). In total, 10 tests were conducted on core plugs which were all taken in the direction of drilling, hence subvertical to bedding. The tests were conducted using a servo controlled MTS 4,600 kN high stiffness loading frame, a 1,000 kN load cell (class 1) and servo controlled oil driven confining pressure system with a total capacity of 200 MPa. For diametral compression testing (Brazilian disk) a loading device was used that introduces the load on the required diametral sectors. The axial loading rate on the specimen was 0.1–0.2 mm/min. All geomechanical tests were conducted at room temperature.

Three samples (from wells 1-27-60-26W4 and 8-17-50-26W4) were tested under unconfined compression. The uniaxial compression test is conducted on cylindrical test specimens with a length to diameter ratio of 2:1. The specimens used had a long axis parallel to the axis of the drill core, a length of 5 cm, and a diameter of 2.5 cm. The ends of each test specimen were lapped so that they were perpendicular to the long axis. The specimens were axially loaded, and the load was increased in displacement mode until the peak load was reached. The unconfined compressive strength (UCS) was calculated from peak load. The Young's modulus is calculated from the linear part of the stress-strain diagram at 50 % of the strength (Tobias Backers, personal communication).

Six samples (from wells 5-29-62-1W5, 1-27-60-26W4, 8-17-50-26W4, and 15-34-43-10W4) were subjected to a multiple failure state test in a standard triaxial testing cell. In a triaxial test configuration, the rock specimen is subjected to a homogeneous state of stress in which two of the principal stresses are of equal magnitude (Jaeger et al. 2007). All stresses are compressive, with the unequal stress more compressive than the two equal stresses, so that $\sigma_1 > \sigma_2 = \sigma_3 > 0$. The triaxial stress state is achieved by subjecting the cylindrical rock specimen to uniaxial compression in the presence of hydrostatic compression applied by a pressurized fluid (Jaeger et al. 2007). The confining stress and the axial stress (or differential stress) are measured during the test. The initial confining pressure is isostatically applied to the specimen. Then the axial load on the specimen is increased at a constant displacement rate. At the onset of failure, i.e., at zero inclination of the load-displacement diagram, the axial loading is stopped. The confining pressure is

subsequently increased to a higher level. The axial stress is then increased further until failure occurs, and in this way the test continues at a multiple of confining stress levels (Fjar et al. 2008). With this test the parameters of a Mohr failure envelope can be derived from just one sample.

The tensile strength of two rock specimens (from wells 5-29-62-1W5 and 1-27-60-26W4) was determined by the Brazilian test. In this test, a thin circular disk is diametrically compressed to failure. The compression induces tensile stresses normal to the vertical diameter, which are essentially constant over a region around the center (Li and Wong 2013). The indirect tensile strength is typically calculated based on the assumption that failure occurs at the point of maximum tensile stress, i.e. at the center of the disc. At peak load a fracture is introduced from the center of the specimens and propagates outwards. If the fracture is initiated at the mantle surface the test is not valid. From the geometrical measures and the peak load the indirect tensile strength is determined.

2.5 Mapping of depth, thickness, thermal gradient and temperature

The depth to the top of the Precambrian (which is equal to the base of the BSU) and the thickness of the BSU were mapped with Inverse Distance Weighting (IDW) using data from 15 wells (from IHS 2012) (Fig. 28a, b).

The geothermal gradient was calculated from 2005 temperature values from 615 wells. The temperature data were derived from bottom hole temperature measurements (BHTs), temperature measurements from drill stem tests (DSTs) and annual pressure and temperature tests in shut in wells. This data set was compiled from data published in Majorowicz and Moore (2008), Majorowicz and Grasby (2010a), Gray et al. (2012), Majorowicz et al. (2012) and Weides and Majorowicz (2014). Where information about circulation times was available, the data from BHTs were corrected using the Horner method (Lachenbruch and Brewer 1959). The rest were corrected using the standard AAPG Harrison correction (Harrison et al. 1983). The distribution of the thermal gradient in the sedimentary succession was mapped using the simple kriging method (Fig. 28c). With kriging, unbiased estimates of regionalized variables at unsampled locations are made using the structural properties of the semivariogram and the initial set of data values (David 1977). The raster of the thermal gradient map was then multiplied with the raster of the Precambrian depth map (Fig. 28a), resulting in a temperature map for the top of the Precambrian (i.e., the base of the BSU) (Fig. 28d).

3. Results

3.1 Sedimentology and petrography

The succession of the BSU consists of thin to thick beds of fine- to coarse-grained sandstone with minor amounts of interbedded mudstone. The basal part is composed of sandstone containing granules and pebbles from basement rock fragments. Above this basal part, beds of cross-bedded sandstone are dominant, intercalated with bioturbated sandstone beds, clay laminae and thin mudstone beds (Fig. 21, Fig. 22). The BSU can be described as mainly quartz arenite. White, grey, brown, and red are the predominant colours. In well 6-7-65-4W4 some core intervals show greenish colours.

The basal first few meters (3–8 m) directly overlying the Precambrian basement contain granitic and metamorphic basement rock fragments and feldspar grains (Fig. 22a-c). Typically, the basement rock is overlain by a 20 cm to 40 cm thick, pebbly sandstone (Fig. 22 a-c). The average grain size of the pebbly sandstone ranges from less than 1 mm to 2 mm. The size of most pebbles is less than 30 mm, though larger pebbles are found. In the basal 1 to 2 meters, the pebbly sandstone bed is typically followed by a sequence of poorly sorted sandstone beds that can still contain basement rock fragments (smaller than 30 mm). Above the basal 1 to 2 meters the sandstone beds become better sorted, and basement fragments are only found sporadically (Fig. 22c). In some cores the sandstones are intercalated with up to 10 cm thick mudstone beds.

The overlying section of the BSU consists predominantly of cross bedded sandstone (Fig. 23a-c). Low angle cross laminae and ripple cross-laminae are also present. The bed thickness is typically less than 5 cm, although thicker beds of 10 cm or more are present locally. Grain size in the sandstone beds is mostly fine sand to medium sand, with minor amounts of coarse sand (Fig. 23c). Some examples of thin graded beds (fining upwards) exist (Fig. 23a). Convolute bedding structures and ripple bedding were observed in well 6-7-65-4W4. Very thin (less than 1 mm) to thick (up to 20 mm) laminae of clay are intercalated between the sandstone beds (Fig. 23b). The sandstone mostly occurs in cosets of planar- or cross-bedded strata which are between 1 m and 5 m thick. These co-sets are separated by thin mudstone beds that are between 5 cm and 50 cm thick. In the sections of interbedded sandstone and mudstone, horizontal and vertical burrows are very common (Fig. 24a-c). In some cases the primary sedimentary structures were almost completely destroyed by bioturbation (Fig. 24a).

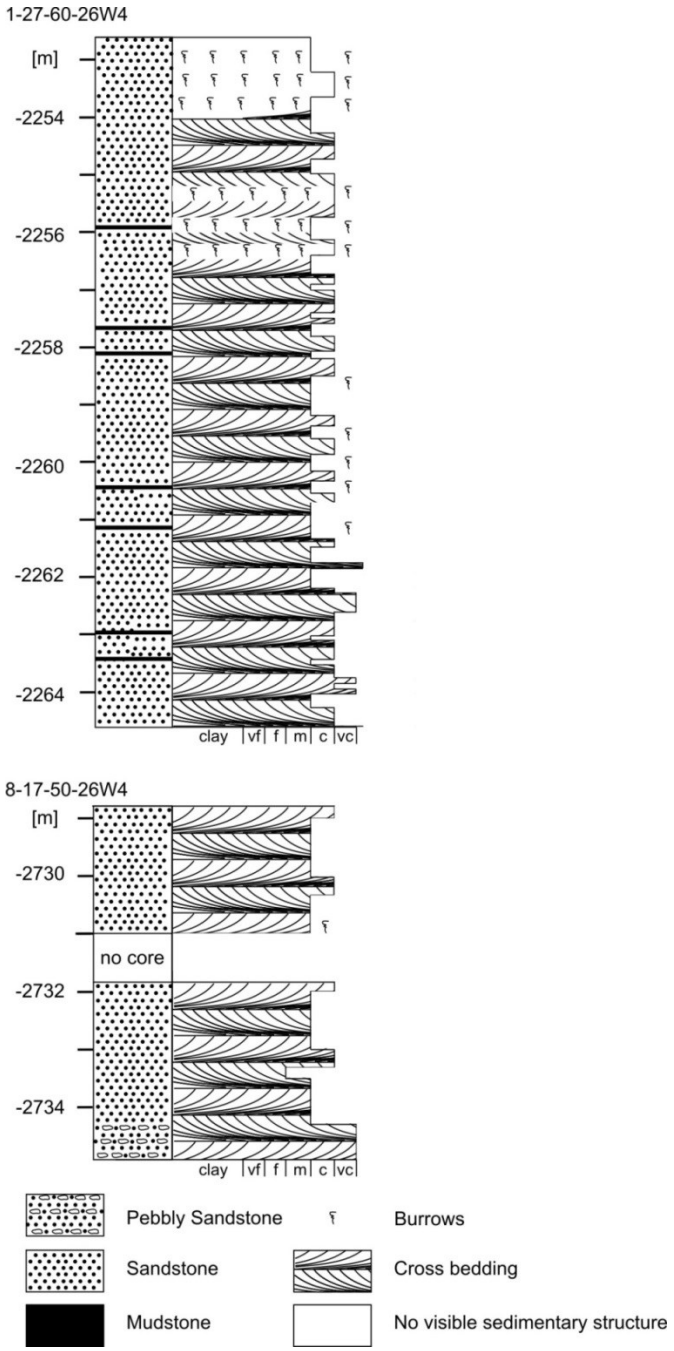

Fig. 21: Graphic representation of 2 cores from the BSU. Cores from well 8-17-50-26W4 show the bottom section, and cores from well (1-27-60-26W4) show the top section of the BSU; in well 8-17-50-26W4 the contact to the Precambrian is located at a depth of 2737.2 m, and the total thickness of the BSU is 33.3 m; in well 1-27-60-26W4 the contact to the Precambrian is located at a depth of 2288.4 m, and the total thickness of the BSU is 34.9 m.

No consistent lateral facies trend could be identified from the core material. A vertical coarsening-upward trend exists for the basal part of the BSU, where the pebbly sandstone with feldspar and granitic grains gradually develop into quartz arenite. The top part of the BSU (5.5 m in well 5-29-62-1W5 and 2 m in well 1-27-60-26W4) consists of strongly bioturbated sandstone with intercalated mud/clay laminae.

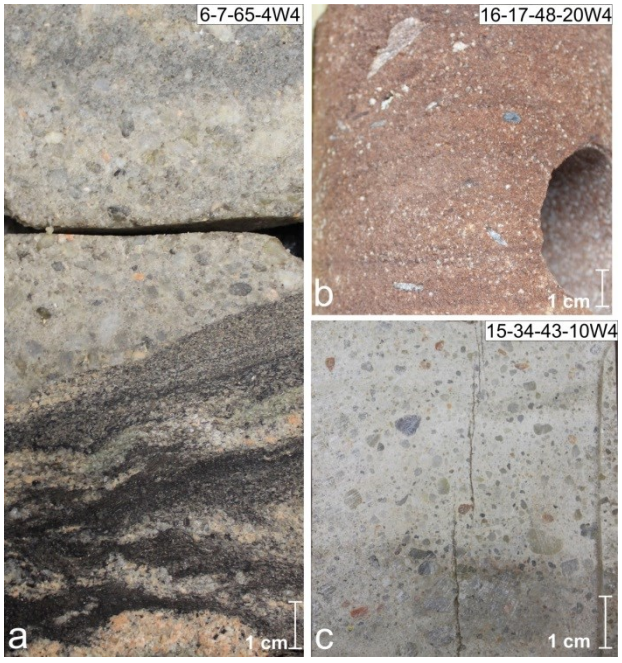

Fig. 22: Photographs of core segments representative of the basal interval of the BSU. *a*: contact between granitic basement and the basal pebbly sandstone bed of the BSU (6-7-65-4W4); *b*: feldspathic arenite containing basement rock fragments of various grain sizes (16-17-48-20W4); *c*: basal lithic arenite (15-34-43-10W4).

Modal analysis of the samples (which where all taken from cores sections above the basal pebbly sandstone) indicates that the BSU has a quartz content of at least 95 % and thus can be classified as a quartz arenite (Fig. 25a-f). Monocrystalline quartz grains dominate, the amount of polycrystalline and undulatory quartz grains is less than a few percent. Microcline, plagioclase, glauconite (Fig. 25c), chlorite, muscovite, biotite, amphibole, pyroxene, zircon, and tourmaline are found as accessory detrital minerals. In samples from wells 5-29-62-1W5, 1-27-60-26W4, 8-17-50-26W4 and 16-17-48-20W4, the cement is composed of silica which occurs as quartz overgrowths around and in optical continuity with the original detrital quartz grains (Fig. 25a, d, f). In some cases the original grain shape can be identified from iron mineral coatings, which mark the grain boundaries (Fig. 25a, d, f). In other cases the boundary between grain and overgrowth cannot be discerned with the petrographic microscope; in these cases the rock structure appears as a tight mosaic of interlocking crystals. Structures resulting from pressure dissolution are frequently found in the BSU thin sections. Fig. 25 (b, e) shows sutured contacts between quartz grains in a sample from well 5-29-62-1W5. Iron minerals are present at the original grain boundaries, and often also in the pore space (Fig. 25a, e). The type of iron mineral could not be identified with the petrographic microscope. Thin clay lamina, and less often hydrocarbons and flakes of mica, are present between the quartz grains.

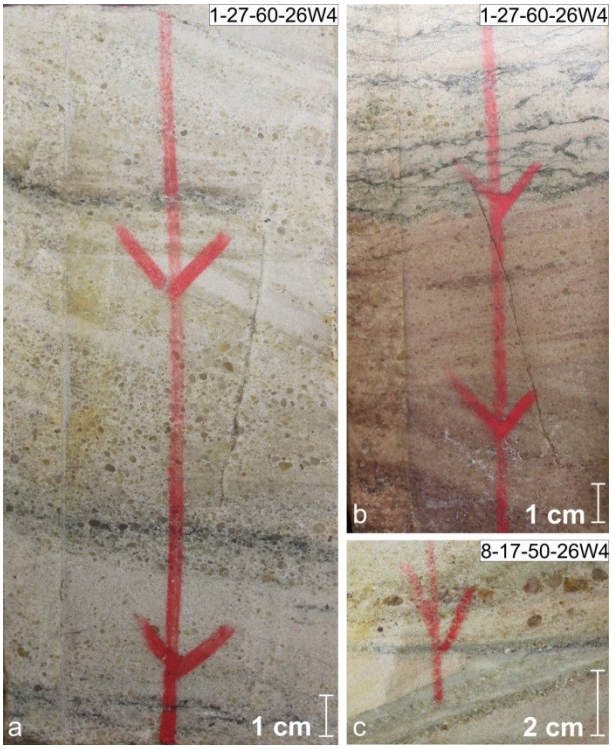

Fig. 23: Photographs of core segments representative for the cross bedded intervals of the BSU. *a*: low–angle laminae in the planar-bedded sandstone in the lower beds; upper beds consisting of cross–bedded sandstone; grain size fines upward in the middle and upper beds (1-27-60-26W4); *b*: cross-bedded sandstone; thin laminae of clay intercalated in the upper bed (1-27-60-26W4); *c*: fine-grained sandstone bed, cut off by a fine- to coarse-grained sandstone with white to brownish quartz granules (8-17-50-26W4).

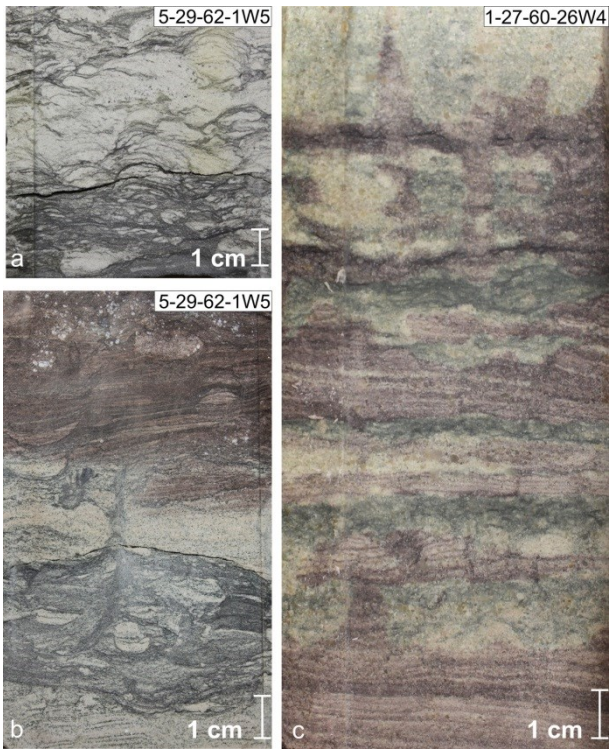

Fig. 24: Photographs of core segments representative of bioturbated intervals of the BSU. *a*: intensely bioturbated muddy sandstone (5-29-62-1W5); *b*: planar-bedded sandstone with clay laminae and vertical burrow (5-29-62-1W5); *c*: planar-bedded sandstone with horizontal and vertical burrows (1-27-60-26W4).

The BSU in well 15-34-43-10W4, located approximately 50 km southeast of the study area is cemented with clay and carbonate. Some quartz grains exhibit evidence of earlier quartz overgrowth. The grain size analysis showed that on average the BSU is composed of fine (57 %) to medium sand (30 %), with minor amounts of coarse sand (7 %) and silt (6 %). The majority of BSU samples can be classified as moderately well sorted with most of the grains being sub–rounded to rounded.

Interpretation and discussion sedimentological and petrographic analyses

The analysis of the BSU samples indicates a transgressive marine depositional environment. The basal part contains basement lithic fragments, which were weathered under subaerial exposure. Overlying planar- and cross-stratified sandstones were deposited in a marine shoreface environment at a depth where sedimentation was influenced by current and wave action. The bioturbated sandstone and intercalated mudstone beds indicate deposition in the deeper offshore transitional zone.

In some samples glauconite is present, which is an important indicator of a marine depositional environment at depths of a few tens to hundreds of meters (Tucker 2009).

Thin-section analysis showed that the BSU is a very mature quartz arenite, with rounded and moderately well sorted grains, typical of sediments deposited in a shoreline depositional environment (Tucker 2009).

Previous studies came to a similar interpretation of the BSU depositional setting. Dixon (2008) interpreted a “marine depositional environment… within water depths where wave and current action were prevalent”. The authors of the Shell Quest report suggested that the BSU was “deposited in a tide-dominated bay margin…in which sand, originally deposited by rivers, was reworked into tidal dunes…” (Shell 2010a).

It is possible that there is a general vertical facies trend of increasing bioturbation and intercalation with mud/clay laminae towards the top of the BSU; this trend could be interpreted as a result of a gradual deepening of the depositional environment. However, due to the limited amount of core material from the upper part of the BSU (only wells 5-29-62-1W5 and 1-27-60-26W4) a definite conclusion cannot be drawn.

Silica cementation appears to have significantly reduced the initial porosity of the sandstone in parts of the BSU (Fig. 25d). The origin of the silica for quartz overgrowth cementation frequently has been attributed to pressure dissolution (Tucker 2009). In this process dissolution of feldspars, amphiboles and pyroxenes (which all occur in the granite of the underlying basement) would provide silica, as would the mineral transformation

from feldspar to kaolinite (Tucker 2009). Pore solutions become enriched in silica, which is then reprecipitated as overgrowth when supersaturation is achieved (Tucker 2009). Fig. 25 (b,e) shows sutured contacts between quartz grains in a sample from well 5-29-62-1W5, as they form in the early stage of pressure solution.

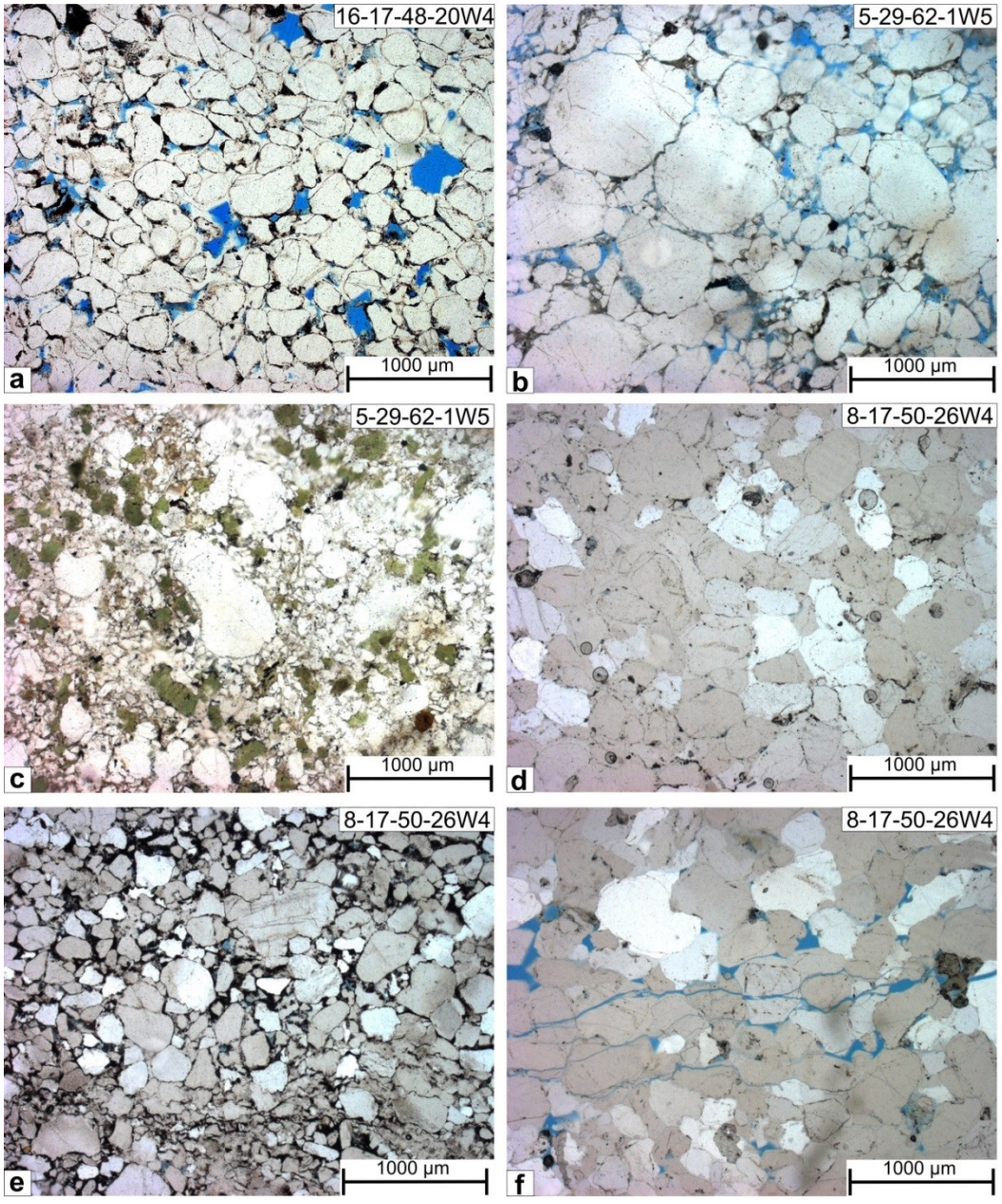

Fig. 25: Photographs of thin sections from the BSU. *a*: quartz arenite with well-developed overgrowth on rounded quartz grains; iron mineral coating around grains marks the original grain boundaries; rock impregnated with blue resin to show porosity (16-17-48-20W4); *b*: interpenetrating quartz grains as a result of pressure solution (5-29-62-1W5); *c*: glauconite grains in a tightly interlocked texture dominated by quartz; porosity is reduced by cementation and pressure solution (5-29-62-1W5); *d*: rounded quartz grains tightly interlocked by silica cementation; quartz overgrowth has eliminated initial porosity (8-17-50-26W4); *e*: porosity is reduced by pressure solution; iron minerals are abundant on grain contacts (8-17-50-26W4); *f*: sample showing quartz overgrowth, pressure solution and fracturing (8-17-50-26W4).

3.2 Porosity and permeability

Porosity of the 10 core plug samples ranges from 5.3 % to 19.6 %, with a geometric average of 9.9 % (Tab. 5). In the classification of Levorsen (1967) the porosity of the BSU samples can be described as poor to good. The small number of samples and the relatively large spread of test results do not allow us to clearly identify a well which has the highest porosity (Tab. 5). The majority of the 96 horizontal permeability measurements have results between 1×10^{-16} m^2 and 1×10^{-14} m^2 and can be classified as fair (after Levorsen 1967) (Fig. 27). However, three measurements which were conducted in a 50 cm thick interval of well 1-27-60-26W4 showed comparatively high permeability values larger than 1×10^{-13} m^2 (very good), with a maximum at 1.1×10^{-12} m^2 (Fig. 27). For comparison with the porosity measurements, nine out of these 96 permeability tests were conducted at the location from where the core plug samples were taken. These samples have a permeability of 7×10^{-16} m^2 to 1.5×10^{-15} m^2 (Tab. 5). For comparison between the different wells average values were calculated (Tab. 6). Geometric averages of horizontal permeability range from 5×10^{-16} m^2 (wells 8-17-50-26W4 and 15-34-43-10W4) to 3.4×10^{-15} m^2 (5-29-62-1W5). The box plot and the histogram shown in Fig. 27 give a good pictorial representation of the variability of the BSU permeability data.

Interpretation and discussion of porosity and permeability results

The average porosity of the BSU in central Alberta is lower than earlier studies from the shallower WCSB of eastern Alberta and Saskatchewan have reported, and consistent with the band of lower porosity south and southeast of Edmonton which had been suggested by

Sample ID	UWI	Depth [m]	Density [kg/m^3]	Porosity [%]	Khor [$\times 10^{-15}$ m^2]
A6	5-29-62-1W5	2262.9	2.69	10.02	1.66
A7	5-29-62-1W5	2264.8	2.70	19.28	6.45
B7	1-27-60-26W4	2254.2	2.62	7.97	14.94
B8	1-27-60-26W4	2252.9	2.69	11.08	2.38
B9	1-27-60-26W4	2261.3	2.68	13.00	1.32
B10	1-27-60-26W4	2263.2	2.70	5.41	0.65
C8	8-17-50-26W4	2731.6	2.67	7.38	0.66
C9	8-17-50-26W4	2733.3	2.67	19.57	1.80
C10	8-17-50-26W4	2730.4	2.66	5.25	2.36
E4	15-34-43-10W4	2111.1	2.67	9.51	-

Tab. 5: Hydraulic properties of the BSU; porosity was measured on core plugs using helium pycnometry; horizontal permeability Khor was measured using a probe permeameter; the permeability measurements were conducted on the core section at the same location where the plugs were sampled.

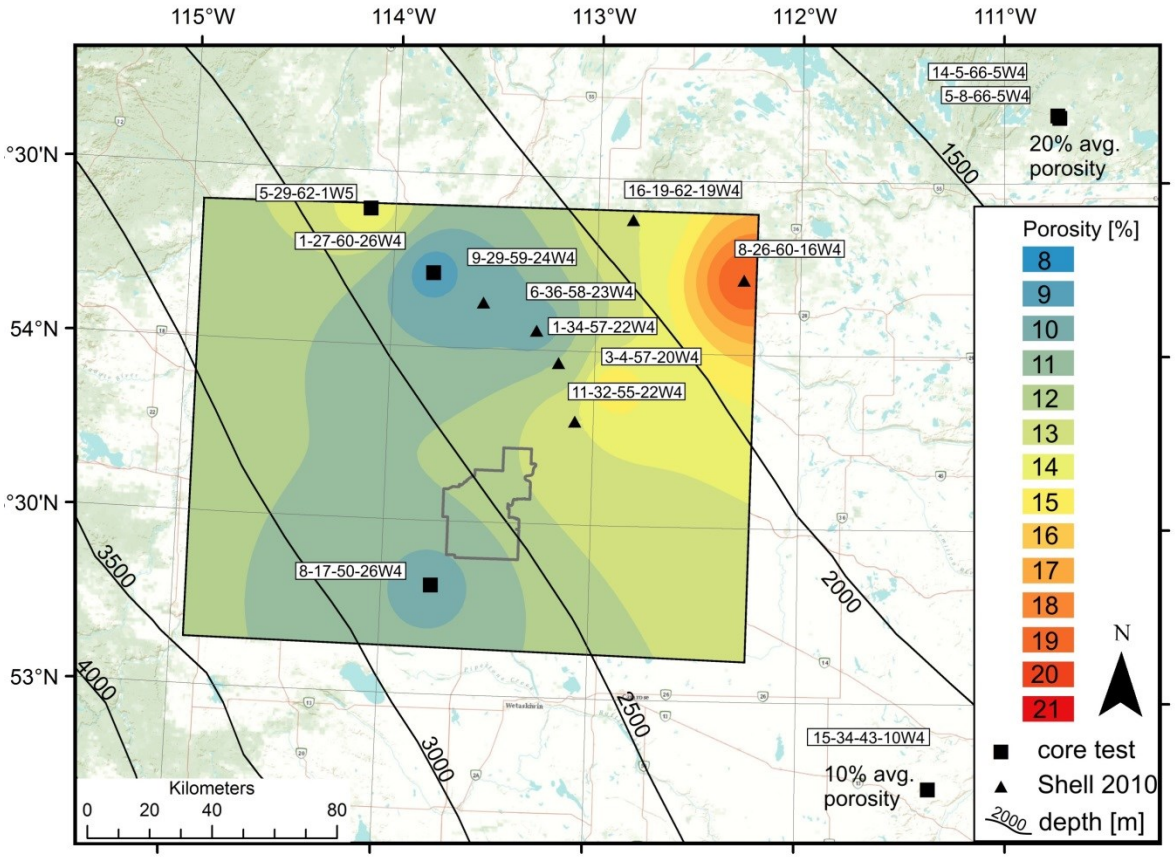

Fig. 26: Porosity map for the BSU in the study area. Inverse Distance Weighting was used for interpolation. Porosity data includes core analysis results presented in this study (black rectangles) and porosity values from well log interpretation from Shell (2010a) (black triangles). Core analysis data from wells 14-5-66-5W4 and 5-8-66-5W4 is from the IHS Accumap (IHS 2012).

Pugh (1971).

When comparing porosity data from the BSU, a general trend of decreasing porosity with depth can be identified. Fig. 26 shows the porosity of the BSU in the study area, based on the new core test results presented in this study and on porosity values from well log interpretation from Shell (2010a). The two wells located northeast of the study area (14-5-66-5W4 and 5-8-66-5W4) confirm the trend of decreasing porosity with depth, having average porosities above 20 % (core analysis results; IHS 2012). One reason for the lower porosity in the deeper basin of central Alberta could be higher compaction of the sediments. Secondly, it is observed in this study that quartz overgrowth and pressure solution have reduced the porosity of the samples. In well 15-34-43-10W4 the BSU is cemented with clay, which additionally decreases porosity. Determination of the factors causing the lower porosity of the BSU in central Alberta compared to the shallower basin was beyond the scope of this study, but could be achieved through a detailed investigation

of grain size distribution, sorting of grains, cementation, and porosity of the BSU in both the deeper and the shallower parts of the basin.

While the permeability in most samples is generally less than 1×10^{-14} m^2, three measurements conducted in a 50 cm thick part of well 1-27-60-26W4 showed permeability larger than 1×10^{-13} m^2. Semi-quantitative thin section analysis of a sample from this interval showed that the porosity is more than 30 %. Sutured grain boundaries resulting from pressure solution are present. This exceptionally high permeability may have been caused by dissolution and/or alteration of an early-formed non-silica cement (carbonate?) or unstable minerals (such as feldspar).

		horizontal permeability [× 10 $^{-15}$ m^2]			
UWI	# Samples	Minimum	Maximum	arithm. Average	geomtr. Average
5-29-62-1W5	15	0.1	42.5	8.8	3.4
1-27-60-26W4	37	0.1	1148.1	45.8	1.6
8-17-50-26W4	27	0.1	25.6	1.9	0.5
16-17-48-20W4	4	0.6	1.9	1	0.9
15-34-43-10W4	13	0.2	1	0.6	0.5

Tab. 6: Horizontal permeability of BSU obtained from probe permeametry measurements.

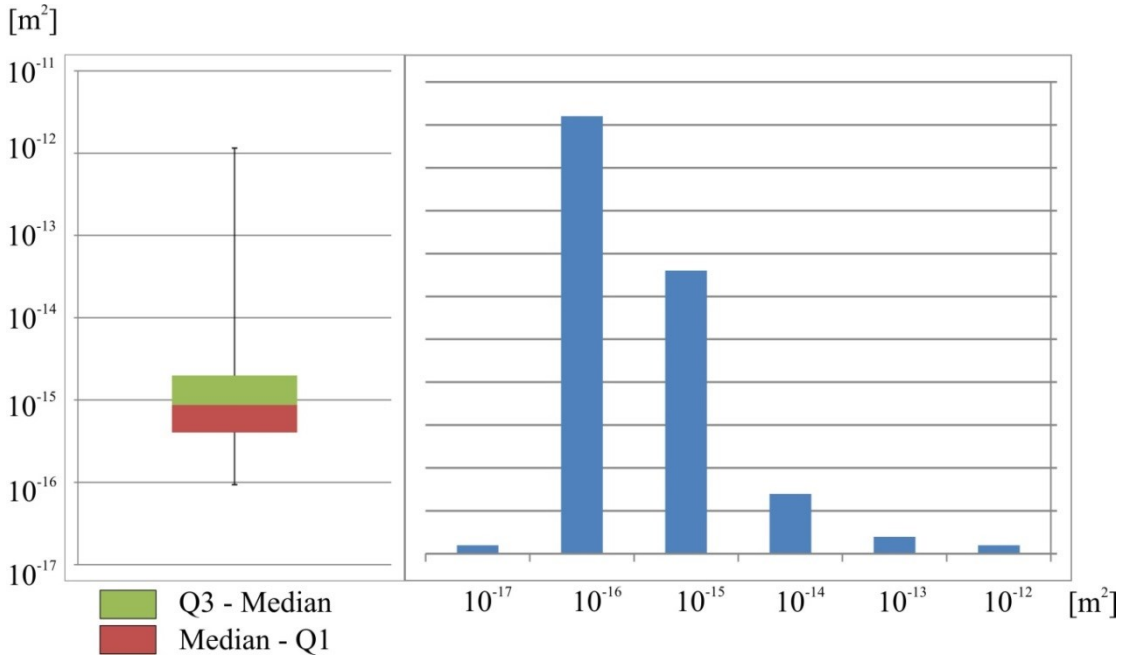

Fig. 27: *left*: box plot of horizontal permeability of BSU from 96 probe permeametry samples; *right*: lognormal histogram of probe permeametry data.

3.3 Geomechanical properties

The unconfined compressive strength (UCS) of the tested BSU specimens ranges from 22.9 MPa to 97.7 MPa (Tab. 7). Young´s moduli of the three BSU specimens range from 3.9 GPa to 21.6 GPa (Tab. 7). The friction coefficients of the six BSU specimens tested range from 0.6–1.22, with an average value of 0.96 (friction angle 31° to 50.7°) (Tab. 7). The cohesion of the BSU specimens varies from 9.4 MPa to 69.8 MPa, with an average value of 31.9 MPa. The values for tensile strength of the two test specimen are 2.1 MPa and 4.9 MPa (Tab. 7).

Interpretation and discussion of geomechanical test results

According to the UCS classification of Anon (1977) the BSU samples can be classified as moderately strong (12.5–50 MPa) to strong (50–100 MPa). Generally the UCS of sandstone has a wide spread and can range from 10 MPa to more than 200 MPa (Johnson and DeGraff 1988). The Berea sandstone, a medium grained low-rank greywacke with 20 % porosity, which is often used as a standard test rock by the petroleum industry, has a UCS of 74 MPa (Fjar et al. 2008).

Young´s moduli of the BSU samples (3.9–21.6 GPa) are within the typical sandstone range of 0.1 GPa to 30 GPa (Fjar et al. 2008). The value of Young`s modulus for the Berea sandstone is 20 GPa.

The friction coefficients of the BSU samples (0.6–1.22) are remarkably high in comparison to other sandstones, which typically range from 0.51 to 0.68 (Jaeger et al. 2007). The friction coefficient of the Berea sandstone is 0.52 (friction angle is 27.8°) (Schön 2011).

The BSU samples also show a very high cohesion (9.4–69.8 MPa) compared to other sandstones which commonly have values between 8.0 MPa and 37 MPa (Zang and Stephansson 2008; Schön 2011;). Cohesion of the Berea Sandstone is 27.2 MPa (Schön 2011).

The tensile strength of the BSU samples (2.1–4.9 MPa) is rather low. Commonly the tensile strength of sandstones is between 2.8 MPa and 8.7 MPa (Siegesmund and Snethlage 2011).

3.4 Thickness and depth

The depth of the BSU ranges from about 1900 m in the northeast to more than 3400 m in the southwest (Fig. 28a). The thickness ranges from 28–47 m with an average of 38 m (Fig. 28b). A trend of decreasing thickness with depth towards the southwest can be recognized.

Sample ID	UWI	Sample depth [m]	Unconfined compressive strength [MPa]	Young`s modulus [GPa]	Tensile strength [MPa]	Cohesion [MPa)	Friction angle [°]	Friction coefficient
A6	5-29-62-1W5	2262.9	-	-	-	27.1	31	0.6
A7	5-29-62-1W5	2264.75	-	-	2.1	-	-	-
B7	1-27-60-26W4	2254.15	-	-	-	9.4	50.4	1.21
B8	1-27-60-26W4	2252.9	-	-	4.9	25.7	42.9	0.93
B9	1-27-60-26W4	2261.25	51.5	9.9	-	-	-	-
B10	1-27-60-26W4	2263.8	97.7	21.6	-	-	-	-
C8	8-17-50-26W4	2731.55	-	-	-	30.9	50.7	1.22
C9	8-17-50-26W4	2733.3	22.9	3.9	-	-	-	-
C10	8-17-50-26W4	2730.4	-	-	-	69.8	45	1
E4	15-34-43-10W4	2111.1	-	-	-	28.7	38.7	0.8

Tab. 7: Geomechanical properties of the BSU samples.

3.5 Thermal gradient and temperature distribution

The average geothermal gradient in the study area is 35.6 °C/km (calculated from the kriging map Fig. 28c). A high-gradient zone exists in the southwestern portion of the study area, where the gradient exceeds 40 °C/km (Fig. 28c). A second zone of higher gradient exists in the northwestern corner of the area (Fig. 28c). In a band striking from the northern to the western part of the study area, the gradient is relatively low, with values smaller than 30 °C/km (Fig. 28c). Apart from this lateral variation of the geothermal gradient, the temperature distribution in the BSU is mainly controlled by depth (Fig. 28a, d). Following the general southwestward dip direction of the sedimentary strata in central Alberta the temperature in the BSU increases from about 65 °C in the shallow northeast to more than 120 °C in the deepest southwestern part (Fig. 28d).

Interpretation and discussion of the thermal data

The observed variations in the geothermal gradient (dT/dz) in the study area (Fig. 28c) can be inferred to be differences in heat flow (Q), controlled by changes in the thermal conductivity (k) of the rock units. Heat conduction is estimated to be the main force of heat transfer in this system, which is not affected by convective heat transfer due to the low Darcy flow velocities in the basin (Majorowicz et al. 1999). The variations in heat flow (Q), which control the variations of the geothermal gradient (dT/dz=Q/k), depend also on variations in heat contribution from heat production in the crust and from the mantle heat flow. As the variability in mantle heat flow in northern Alberta is low (15 mW/m^2; S.D. 5 mW/m^2) according to the recent study by Majorowicz et al. (2014), we assume that

the heat flow-heat generation relationship for the large upper crustal Precambrian domains is the major control on the heat flow (Majorowicz et al. 2014).

Variations in the BSU temperature (Fig. 28d) depend on the geothermal gradient and the depth to the Precambrian surface. For calculation of the BSU temperature a ground surface temperature of 0 °C was assumed to be in thermal equilibrium with the temperature at depth (Majorowicz et al. 2012).

From the newly established maps of the geothermal gradient and the temperature distribution in the BSU (Fig. 28c, d) regional variations can be identified. This is an improvement in comparison to earlier temperature maps which were only based on one regional geothermal gradient (see Weides et al. 2013), while for this map about 2000 individual temperature measurements from 615 wells were used.

4. Discussion

Combining the results of the different analyses enables a more detailed characterization of the geothermal system in central Alberta with the BSU as potential geothermal reservoir. The key findings of this study are: (1) the BSU in central Alberta is a very mature, well cemented quartz arenite. The initial porosity of the BSU has been significantly reduced by a combination of pressure solution and quartz overgrowth. The relatively low values from the porosity and permeability tests confirm this. Porosity of the BSU decreases from northeast to southwest. (2) The BSU is sandstone with high rock strength. (3) The temperature in the BSU is between 60 ° and 120 °C which means that in most of the area the temperature requirements for geothermal district heating are met, while in the southwestern part the temperature in the BSU is high enough to allow for electricity production. (4) The average thickness of the BSU is 38 m.

When these findings are compared to other geothermal systems in deep foreland basins it is apparent that the matrix permeability and the thickness of the BSU are too low to be used for geothermal heat production without hydraulic stimulation treatments. Aquifer transmissivity is a good way to compare different sites. The BSU in central Alberta has a vertical transmissivity of 5.3×10^{-14} m^3. Generally a transmissivity above $0.5–1 \times 10^{-11}$ m^3 is seen as a minimum requirement for direct use (Rollin 2003; Pluymaekers et al. 2012; Mathiesen et al. 2013), which is several magnitudes higher. Even if the BSU reservoir was accessed by a 1000 m long horizontal well section, the transmissivity (0.16×10^{-11} m^3) would be below the minimum requirements. Flow rate is another possible factor which can be used to compare between different sites. When drilled into the BSU, a vertical well in a

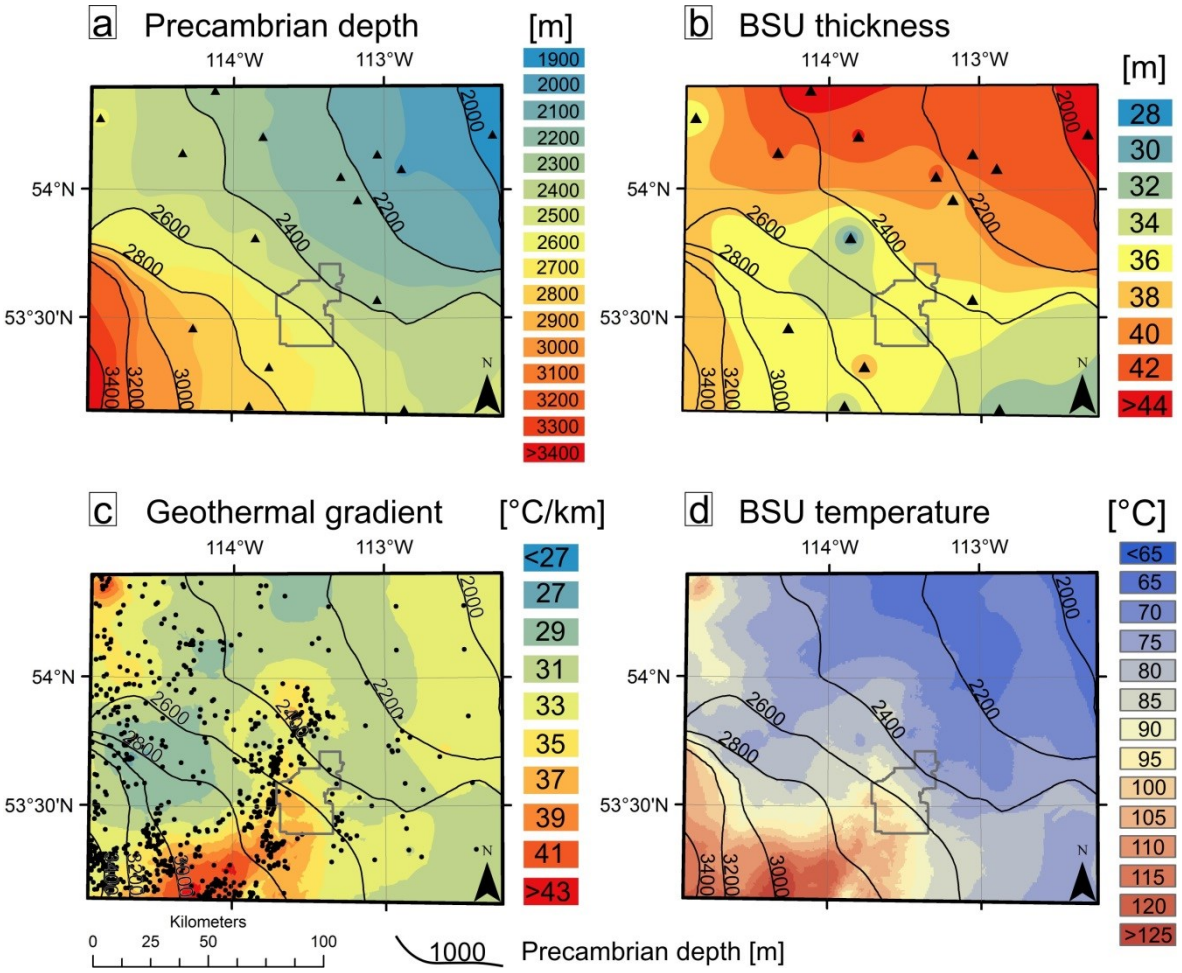

Fig. 28: *a*: Map showing the depth from ground surface to the top of the Precambrian basement (i.e., the base of the BSU), based on 15 wells; inverse distance weighting method (IDW) was used for interpolation; *b*: Thickness map of the BSU, based on 15 wells, calculated with IDW; *c*: Geothermal gradient map of the Phanerozoic succession, based on approximately 2000 temperature values from 615 wells; map was calculated using the simple kriging method; *d*: Map of the temperature distribution at the base of the BSU; map was calculated by multiplication of raster maps a and b, assuming a surface temperature of 0 °C to be in equilibrium with the deeper Basin (see Majorowicz et al. 2012).

doublet system (one producer and one injector) would have a flow rate less than 1 L/s, while 9 L/s would be possible with a system of three horizontal wells with a 1000 m long open hole section in the BSU (two producers and one injector) (see Hofmann et al. 2014). In the Dogger aquifer of France, which has been exploited for direct use of geothermal heat for more than 40 years (Lopez et al. 2010), production rates typically range from 14–167 L/s. The geothermal sites of Landau and Unterhaching in Germany have flow rates of 50–70 L/s and 100–150 L/s respectively (Geox 2014, Geothermie Unterhaching 2014). Brine disposal wells injecting into the basal clastics in Saskatchewan (which are considered as a geothermal reservoir) have flow rates between 30–40 L/s (Ferguson and Grasby 2014). Therefore the permeability of the BSU reservoirs would need to be

increased by hydraulic stimulation treatments. Results from Hofmann et al. (2014) show that the average production of more than 25 L/s per well can be obtained, when the reservoir is accessed with horizontal wells that are connected by vertical hydraulic fractures.

5. Conclusions

Due to its depth and related high temperature and its extension throughout central Alberta the BSU is a potential geothermal target formation. The BSU in central Alberta has relatively low thickness of 38 m and a relatively low matrix porosity and matrix permeability, which makes horizontal drilling and hydraulic stimulation treatments necessary for geothermal heat production.

For most of the study area the temperature is higher than 70 °C, which is sufficient for direct use of geothermal heat for district heating (Líndal 1973). The temperature in the BSU increases towards the southwest, where up to 120 °C is reached.

The geomechanical tests showed that the BSU has relatively high unconfined compressive strength (up to 97.7 MPa), high cohesion (up to 69.8 MPa) and remarkably high values for the friction coefficient (up to 1.22), while the tensile strength is rather low (less than 5 MPa).

Acknowledgements

The probe permeameter, access to core material and well data was provided by the Alberta Geological Survey (AGS). Special thanks to Gordon Jean (AGS) for supervision of the probe permeameter measurements.

The geomechanical tests were conducted at the GFZ Potsdam by Tobias Backers and Tobias Meier from Geomecon GmbH, Potsdam.

Thanks to my colleagues Fiorenza Deon and Stefan Klapperer from GFZ Potsdam and to Torsten Steiger from GeoTec Consult for fruitful discussions on the thin sections.

The maps were created using ArcGIS® software by Esri Inc.

This study is part of the Helmholtz–Alberta Initiative (HAI), which is a research collaboration between the Helmholtz Association of German Research Centres and the University of Alberta.

The authors would like to acknowledge helpful reviews by Dr. Stephen Grasby and an anonymous reviewer, and the useful comments by the Associate Editor Dr. Michael Rygel.

Chapter 4

Originally published in *Environmental Earth Sciences*,
published online first, 10 May 2014

An integrative geothermal resource assessment study for the siliciclastic Granite Wash Unit, northwestern Alberta (Canada)

Simon Weides, Inga Moeck, Douglas Schmitt, Jacek Majorowicz

Abstract

This study explores the siliciclastic Granite Wash Unit in northwestern Alberta as a potential geothermal reservoir. The approach covers regional 3D structural geological modelling of a 90 km × 70 km area based on well log and legacy 2D seismic data. The fault strike was interpreted from lineaments, which were identified with the refined trend surface analysis method. The stress state of the Granite Wash reservoirs was determined by an integrated approach of 3D fault modelling, stress ratio definition based on frictional constraints, and slip tendency analysis.

The results show that the best site for a geothermal application is located in the southwestern study area, where the highest temperatures (above 70°C) coincide with the largest thickness (above 20 m) and zones of elevated porosity and permeability. The integrated stress analysis indicates an in-situ stress regime from normal to strike-slip faulting maintaining a non-critically stressed reservoir or faults therein, assuming a friction coefficient of 0.7. The granite wash reservoirs could be used for heating of greenhouses, domestic warm water provision and district heating.

1. Introduction

The Western Canada Sedimentary Basin (WCSB) is known for its resources of oil, gas and coal. Although traditional exploration in the WCSB is focused on hydrocarbons, recently renewed interest in the geothermal energy potential of the WCSB has risen as renewable energy technologies are regarded to play a larger role in future energy production (Majorowicz and Moore 2008; Bell and Weis 2009; Grasby et al. 2011; Weides et al. 2013). Alberta, located in the central WCSB, has been characterized as a low enthalpy region with an average geothermal gradient of 25–35 °C/km and a heat flow of 50–70 mW/m^2 (Majorowicz and Grasby 2010a; Grasby et al. 2011; Weides and Majorowicz 2014). Due to the cold climatic conditions (average annual temperature in Edmonton is 2.4 °C, average temperature in January is -13.5 °C; from National Climate Data and Information Archive 2000), large amounts of energy are needed simply for heating and warm water provision in Alberta. Geothermal energy could serve as an energy

source for domestic heating and warm water provision, and reduce fossil-fuel generated heat energy used within industrial processes, e.g. in the heating of greenhouses.

1.1 Study area

This study focuses on an area of approximately 90 km × 70 km in northwestern Alberta, around the town of Peace River (Fig. 29). This area was chosen for mainly two reasons: (1) The Granite Wash reservoirs in the Red Earth field, located 60 km northeast of the study area, are known to have high porosities and high permeabilities (Balshaw 2010) at lower depths (less than 1 km). The idea of this study was to investigate whether the Granite Wash Unit in the deeper basin (where temperatures are higher) is also characterized by zones of high porosity and high permeability. (2) Although the area is densely populated, a high heat demand exists from the local greenhouse operations (at low temperatures > 40 °C) and from the oil sands industry (at high temperatures > 250 °C), which means there are potential applications for geothermal heat production.

The sedimentary succession thickness in the study area is between 1.7–2.3 km. Six siliciclastic and carbonate units form the major Paleozoic aquifer systems, any of which could theoretically be used for geothermal heat production (Fig. 30). In the deepest of these rock units—the siliciclastic Granite Wash Unit—temperatures are estimated to be high enough to be used for greenhouse heating and domestic warm water provision (both > 40 °C, Lindal 1973) or district heating (> 70 °C, Laplaige et al. 2000).

1.2 Previous work

Heat flow, thermal gradient, and radiogenic heat production in the WCSB has been investigated in numerous studies during the last decades (Garland and Lennox 1962; Majorowicz and Jessop 1981; Jessop et al. 1984; Majorowicz et al. 1985; Burwash and Burwash 1989; Bachu 1993; Bachu and Burwash 1994; Jessop et al. 2005; Majorowicz 1996; Majorowicz et al. 1999; Grasby et al. 2009; Majorowicz and Grasby 2010b).

Several studies estimated the geothermal potential of different regions in the WCSB, most of them using preexisting data from hydrocarbon exploration to investigate properties of deeper sedimentary units. Early regional studies have been conducted for Regina in eastern Saskatchewan (Vigrass 1979; Jessop and Vigrass 1989;), Hinton-Edson in western Alberta (Lam and Jones 1985) and Calgary in southern Alberta (Lam and Jones 1986). A report published by the Geological Survey of Canada (Grasby et al. 2011) synthesized previous geothermal studies and delineated the potential of the different geothermal resource types

in Canada. Recent studies focused on the geothermal anomaly of the Clarke Lake gas field in northeastern British Columbia (Walsh 2013), on the geothermal exploration of the Paleozoic aquifers in the Edmonton metropolitan area in central Alberta (Weides et al. 2013), and on the geothermal potential of the basal clastics of Saskatchewan (Ferguson and Grasby 2014).

The sedimentology of the Granite Wash Unit in northwestern Alberta has been described by Trotter (1989), Dec et al. (1996) and Balshaw (2010). Bachu and Burwash (1991) investigated regional scale porosity and permeability variations in the sedimentary succession in the Peace River Arch area (PRA). Relevant recent studies from other regions in the world, which focused on the geothermal exploration and on the assessment of geothermal potential) of a region were conducted for instance in southern Tunisia (Brahim et al. 2013), in northern Germany (Huenges et al. 2013; Sippel et al. 2013), in the Netherlands (Pluymaekers et al. 2012) and in Denmark (Mathiesen et al. 2013).

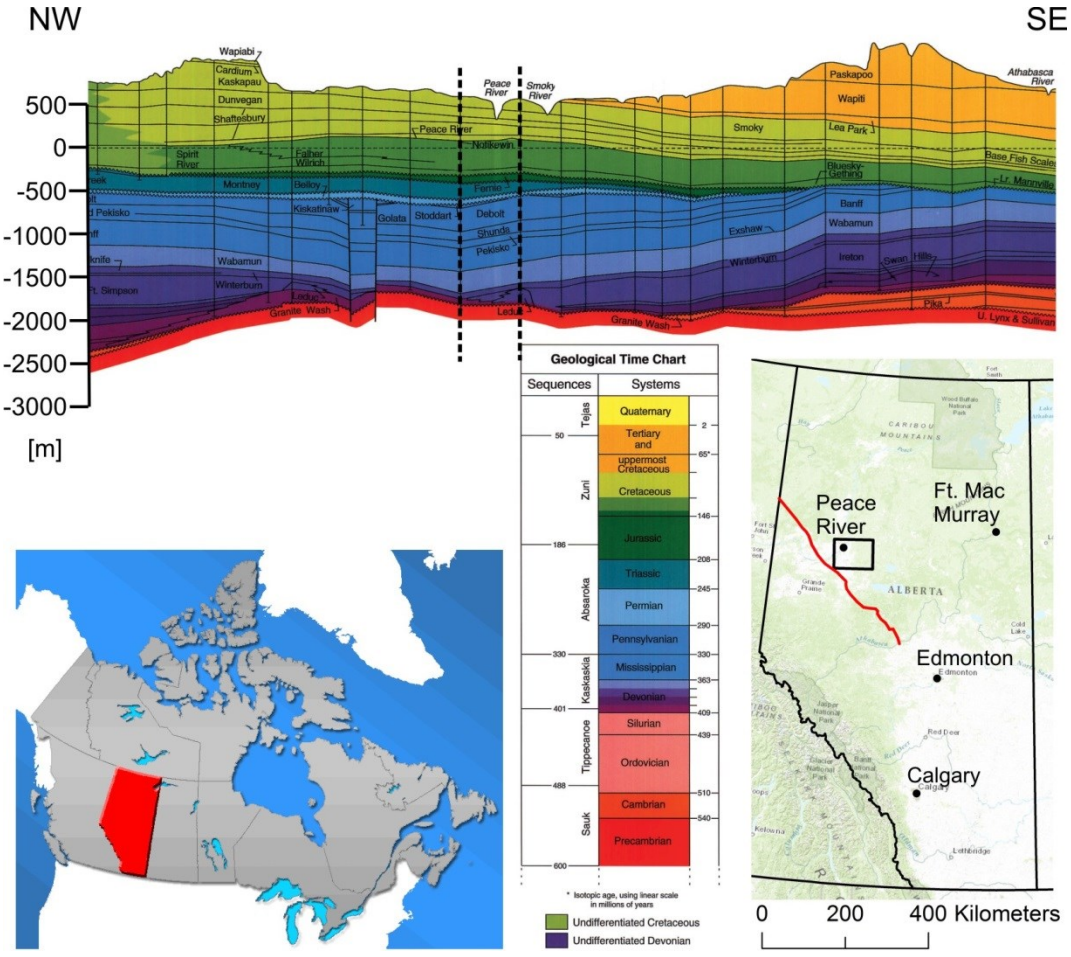

Fig. 29: Location of the study area with cross section; cross section is modified from Wright et al. (1994); dotted lines indicate the approximate location of the study area.

1.3 Focus of the study

The aim of this geological reconnaissance study was to analyze the distribution of relevant rock parameters of the Granite Wash Unit on a regional scale, and to identify locations where favorable conditions for geothermal heat extraction exist. For direct use application of the heat from the Granite Wash reservoirs, high flow rates are required. Therefore porosity and permeability are (among reservoir thickness, extent and temperature distribution) the most important parameters which were investigated and mapped. In geothermal heat production, high injection rates change the stress conditions in the reservoir, which can result in activity on critically stressed faults. A 3D fault model was developed based on reinterpreted 2D seismic data, which considered lineaments identified from refined trend surface analysis. The stress state of the faults at the depth of the Granite Wash reservoirs was determined with the slip- and dilation tendency analysis. The results of this study may help to guide future exploration and field development in the Granite Wash sediments of northwestern Alberta.

1.4 Geological Setting

The study focussed on an area in the eastern part of the Peace River Arch region, which is located in northwestern Alberta. The PRA represents one of the few large-scale tectonic elements in the WCSB that has significantly disturbed the Phanerozoic cover of the craton (O'Connell 1994) and possibly originated from an uplift over a failed rift system in the early Paleozoic (Cant 1988). During the late and Middle Devonian, the emergent Arch landmass was progressively onlapped by siliciclastics, evaporites and shallow marine carbonate sediments. The arch collapsed, perhaps due to a later phase of rifting, and was buried by the end of the Devonian (Cant 1988; Michael and Buschkuehle 2008). During the early Carboniferous a series of northeast–southwest trending interlinked grabens and half-grabens, known as the Dawsons Creek Graben Complex (Barclay et al. 1990), were formed along the crest of the Devonian Arch (Michael and Buschkuehle 2008). The grabens indicate the onset of a period of local extension, possibly related orogenesis along the western coast of the North American continent (O'Connell et al. 1990).

The depositional environment of the WCSB from the late Proterozoic to the Middle Jurassic was characterized as a passive margin, which gradually developed into a foreland basin from the Middle Jurassic until today (Porter et al. 1982). Referring to heat transfer, the WCSB belongs to the conduction dominated geothermal systems (Moeck and Beardsmore 2014). Within this classification scheme the foreland basin type is controlled

by both faults, and lithological-diagenetic characteristics influencing permeability and porosity.

1.5 The Granite Wash Unit

The lithological term "Granite Wash" was first applied by the petroleum industry to describe a lithological zone comprised of diachronous clastic wedges, sourced from Precambrian granite and gneiss, which unconformably overlie these same source rocks in the subsurface Peace River Arch (Dec et al. 1996). Intercalation of the Granite Wash clastics with Middle and Upper Devonian strata in the Peace River area allows for an approximate age determination; however, in the absence of this relationship, the age determination is uncertain (Pugh 1971; Cant 1988; Dec et al. 1996; Balshaw 2010). In the past, the Granite Wash classification has been applied to the clastic sediments of different stratigraphy: Basal Red Beds (Lower Elk Point Gr.), Contact Rapids clastics (Lower Elk Point Gr.), Keg River clastics (Upper Elk Point Gr.), and also to the Gilwood Member Sandstone (Upper Elk Point Gr.) and Beaverhill Lake clastics (Barclay et al. 1985; Balshaw 2010).

The Granite Wash Unit consists of reworked material of the predominantly granitic and metasedimentary rocks of the uplifted basement. Sandstone and conglomeratic sandstone are dominant, and the composition varies from arkosic to arenitic (Trotter 1989). Conglomerates and shales are present but less common (Trotter 1989). Depositional facies of the Granite Wash Unit ranges from alluvial fans to fan deltas to tidal environments (Dec et al. 1996). The Granite Wash Unit was deposited along the crest of the PRA, and along its northern, southern and eastern flanks (Dec et al. 1996). On the crest the Granite Wash Unit thickness is up to 100 m, and in areas south and north of the Arch 60–100 m of thickness is described (Dec et al. 1996). Earlier isopach maps of the Granite Wash Unit indicate a thickness of 0–60 m in the study area, with a large zone of no distribution of Granite Wash Unit sediments in the northern and northwestern part (Dec et al. 1996). The Granite Wash Unit typically blankets the pre-existing paleotopography of the PRA, onlapping onto basement ridges with characteristic drape and pinch-out geometries (Dec et al. 1996). Prolific oil production from the Granite Wash Unit has fueled exploration since the 1950s, and as a result, substantial drill core and wireline well log data are available. The major oil fields in the Granite Wash Unit are located about 50–100 km east of the study area, with smaller oil fields existing 40–60 km south of the study area.

2. 3D structural geological modeling

A 3D structural geological model (Fig. 30) was developed to analyze thickness and spatial distribution of the potential geothermal reservoir units (such as the Granite Wash Unit) and for investigation of geological structures. The 3D structural geological model can be subdivided into two separate models: a lithostratigraphic model (2.1), and a fault model (2.2).

2.1 Lithostratigraphic model

The lithostratigraphic model was developed by using stratigraphic tops of more than 1000 wells from the IHS AccuMap database (IHS Energy 2012). These tops were originally interpreted from geophysical well logs. Despite being a large dataset, it is also biased towards hydrocarbon-rich strata and areas, since most data come from hydrocarbon exploration and production wells. Significant data exists for the Mesozoic and Upper Devonian sediments (> 650 wells in the Lower Cretaceous Banff Formation and in the Upper Devonian Wabamun Group), while only 416 wells are penetrating the Precambrian basement at depths between 1554–2427 m. Most of the wells are located in the southern and eastern part of the study area, while less than 5 % of the wells are located in the northwestern quarter.

Modelling approach

The dataset was checked for outliers by using the inverse distance weighted interpolation method in ArcGIS, where outliers can be easily identified as they appear as a bulls eye. Few stratigraphic tops were identified as outliers as their z-value differed markedly in relation to tops from other wells in the vicinity (in some cases the difference in depth to other tops in the direct surrounding of less than 5 km was more than 100 m). These obvious data errors, probably resulting from erroneous kelly bushing elevations, were removed from the dataset. The development of the 3D geological model used EarthVision® modelling software (Dynamic Graphics Inc.). Formation top surface grids were calculated using minimum tension gridding, an interpolation algorithm based on the nearest neighbour weighted average method (Dynamic Graphics Inc. 2009). The large scale of the model (90 km × 70 km) allowed only modelling of regionally extensive formations. In the final lithostratigraphic 3D model, 14 different geological units are distinguished, of which 10 represent Paleozoic sediments Fig. 30).

2.2 3D fault model

Existing 2D seismic data from hydrocarbon exploration were re-interpreted for the development of a 3D fault model. Eight seismic lines with a total length of 177 km were used for this reconnaissance study. The orientation of the lines is E–W (line PRA_1 and PRA_3; Fig. 31), N–S (lines PRA_2 and PRA_4) and SW–NE (lines PRA_5, PRA_6, PRA_7 and PRA_8). Tie points exist between the northern W–E line and the northern N–S line and the northern W–E line and the southernmost part of the SW–NE lines. Small data gaps exist between the southern N–S line and the southern W–E line (800 m), and between the two N–S lines (4 km).

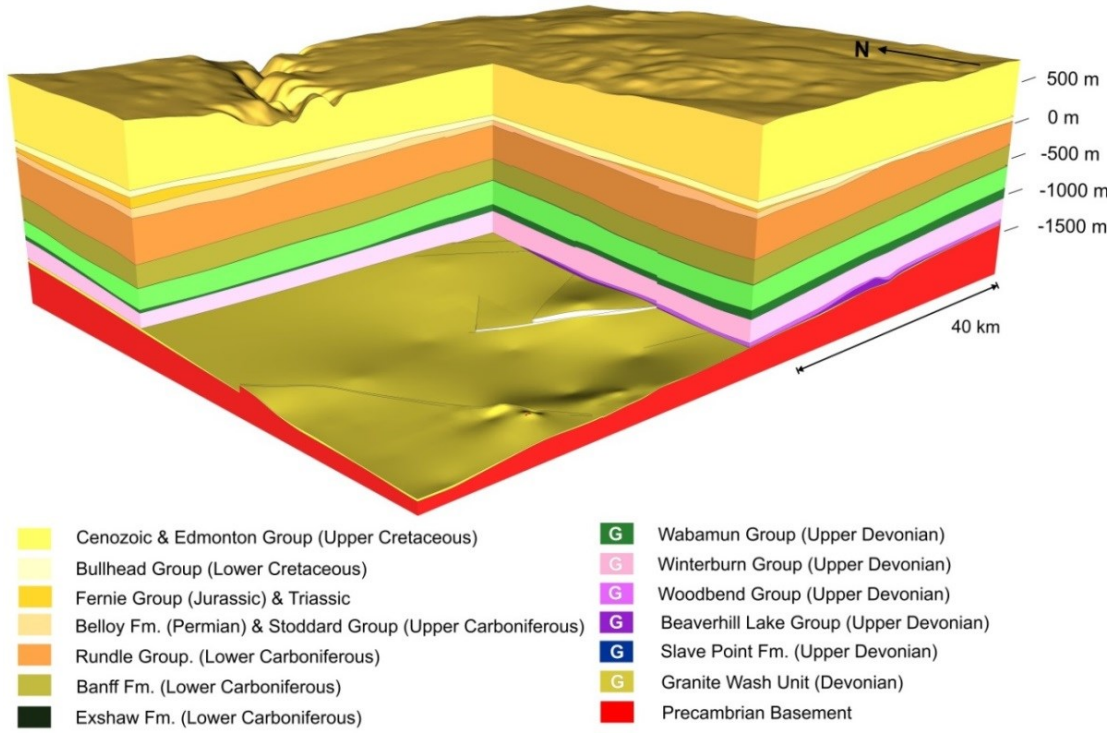

Fig. 30: 3D structural geological model of the study area, based on seismic data and well log data from more than 1000 wells. Potential geothermal target formations are marked with the letter "G" in the legend.

Seismic interpretation

The dominant seismic markers were picked in the time sections and comprise the Late Carboniferous Stoddard Group, the Early Carboniferous Banff Fm., Upper Devonian Wabamun Group and Ireton Fm., and the Precambrian Basement. In total, nine normal fault zones were identified by the seismic data. The largest vertical offset (45–70 ms) exists in the NW–SE trending fault in the southwestern part of the study area (described as „Tangent" fault by Richards et al. 1994), which is crossed by E–W striking line PRA_1.

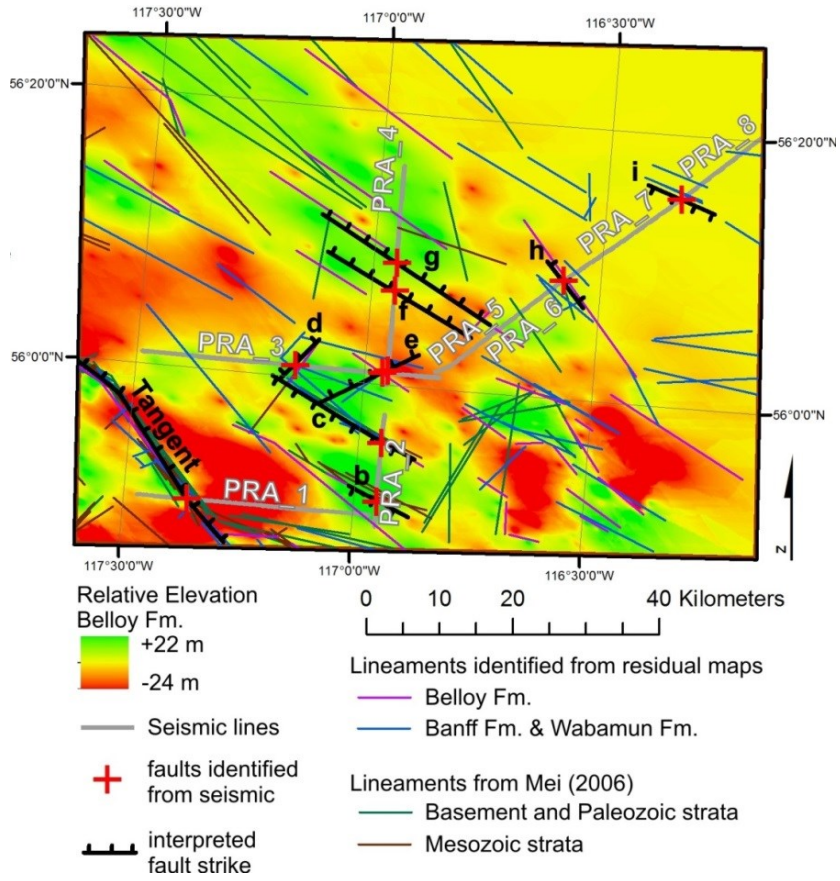

Fig. 31: Residual map for the Belloy Fm (calculated with the approach of Mei, 2009a). Superimposed are newly identified lineaments of Belloy, Banff and Wabamun formations, the lineaments from Mei (2006) and the location of the 2D seismic lines with the identified faults. The strike of the faults was interpreted in consideration of the lineaments.

Here faulting is observed in the basement, Devonian units and Lower Mississippian Banff Fm., while the younger sediments of overlying Mississippian Rundle Group (Fig. 32) are folded without a displacement visible. This indicates that the main movement of the fault occurred during or shortly after the sedimentation of the Rundle Group. The sediments of the late Carboniferous Stoddard Group thicken towards the fault and form a half-graben indicating syn-sedimentary normal faulting activity in the Carboniferous. Although most of the fault displacement in the region occurred during the deposition of the late Carboniferous Stoddard Group (e.g. Tangent fault), evidence for periods of younger activity exists. One example in the study area is the fault “c” (crossed by the N–S striking line PRA_2), where faulting is observed in the Lower Cretaceous. Existence of more potential faults in the basement and Paleozoic strata is indicated by diffraction patterns in the unmigrated seismic sections.

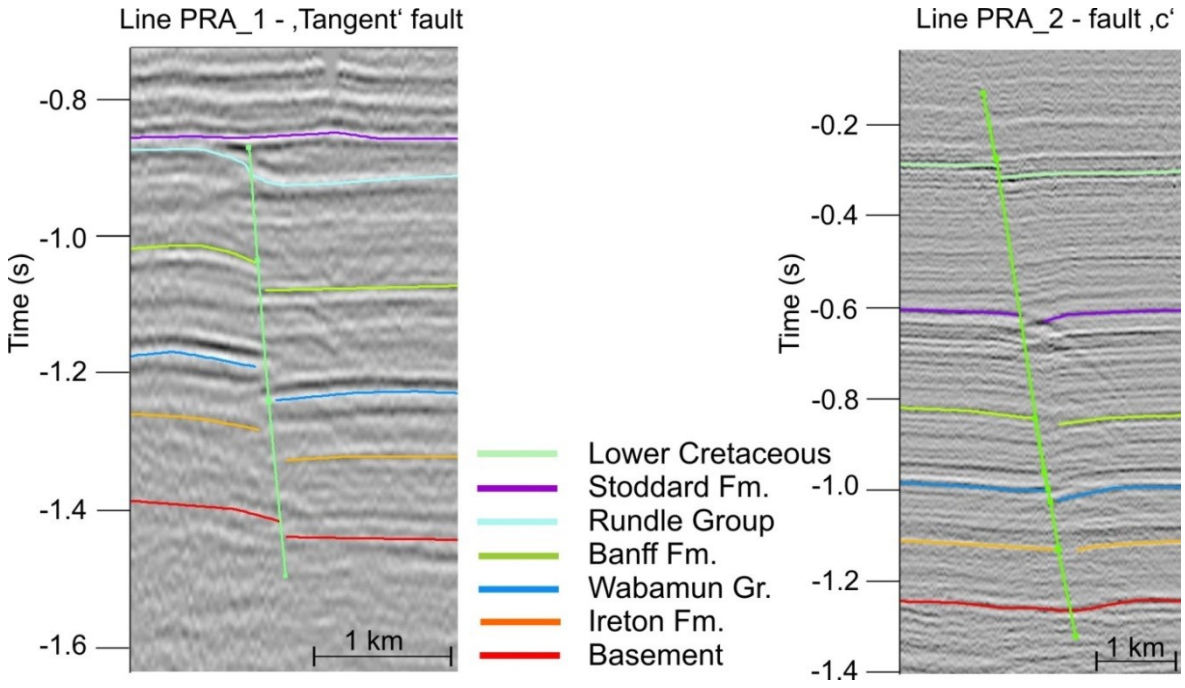

Fig. 32: Examples of the seismic expression of normal faults crossed by the 2D seismic transects. On the left, a crossing of the tangent fault shows folding of Rundle Group strata and faulting in the underlying sediments and basement. On the right, in the seismic expression of fault "c" faulting can be observed in Lower Cretaceous and underlying strata. See Fig. 31 for location of the seismic lines.

The observations on style of normal faults in this study are consistently with earlier studies in the PRA region from Eaton et al. (1999) and Hope et al. (1999).

Fault strike

Previous studies show that the general structural pattern of the PRA region consists of northeasterly and northwesterly striking normal faults (Richards et al. 1994). However, information on faults and fault orientation in the study area is rare, with exception of the NW–SE striking „Tangent" fault, which is one of the major normal faults of the PRA region with a length of more than 40 km (Richards et al. 1994). The strike direction of the other faults was interpreted in consideration of lineaments from the literature (Mei 2006, 2009b), and by identification of lineaments in the dataset by applying the refined trend surface analysis method by Mei (2009a). Using this approach, small-scale formation-top offsets were extracted from the database of formation-top picks by using geostatistical analysis and trend surface analysis (Mei 2009a). After removal of a geologist-controlled trend (Mei 2009a) from the data, a residual map for selected formation tops was generated. Linear trends were identified on this residual map which could be caused by faults, or by a change in slope. Using this approach from Mei (2009a), residual maps for the Permian

Belloy Fm., the Carboniferous Banff Fm. and the Devonian Wabamun Fm. were generated and lineaments were mapped. Fig. 31 shows the residual map for the Belloy Fm., with the newly identified lineaments of Belloy, Banff and Wabamun formations. Also included are lineaments from Mei (2006), the seismic lines, and the identified faults with the interpreted fault strike. Based on the seismic interpretation of the 2D seismic data and the interpreted lineaments, the 3D fault model was developed using EarthVision® modelling software (Dynamic Graphics Inc.).

3. Stress regime in the Granite Wash reservoirs

The knowledge of in-situ stress conditions is important for reservoir operations because the initial stress state is changed through injection and production (Moeck 2012). While injection causes an increase of the pore fluid pressure, production causes a drop of pore fluid pressure with change of effective stresses. After the concept of effective stresses, the increase of pore fluid pressure goes together with the drop of normal stress acting on arbitrary surfaces in the reservoir. As a consequence, the ratio of shear to normal stress increases and can cause slip when the frictional strength of the reservoir rock is exceeded (i.e. fault activation or reactivation). With the knowledge of the in-situ stress field, the state of shear and normal stress on an arbitrary fault slip plane can be calculated to determine whether the fault is critically stressed (Moeck et al. 2009a). Critically stressed faults exhibit a high reactivation potential and can cause induced seismicity, however they can also act as preferential pathways for fluids (Moeck et al. 2009a).

In the following, a stress state determination for a Granite Wash Unit reservoir is presented following the approach of Moeck et al. (2009b). This approach has been successfully applied in the development of the geothermal site “Gross Schönebeck” in the Northeast German Basin. In this approach, 3D fault mapping, stress ratio definition based on frictional constraints and slip tendency analysis are combined to estimate the reactivation potential of a fault (Moeck et al. 2009b).

To define possible stress conditions at depth, some assumptions have to be made (following Peška and Zoback 1995; Jaeger et al. 2007; Moeck et al. 2009b): a) the in-situ stress magnitudes in the crust would not exceed the condition for frictional sliding on well-oriented faults; b) one of the principle stresses is vertical; c) the state of stress within the rocks is in frictional equilibrium. For this case, the ratio of effective principal stresses is given by Jaeger et al. (2007) as

$$\frac{(S_1-P_p)}{(S_3-P_p)} = (\sqrt{\mu^2+1}+\ \mu)^2 \qquad (1)$$

where μ is the coefficient of sliding friction and P_p is the in situ pore pressure. Byerlee (1978) showed with laboratory measurements on a broad range of common rock types that μ is best defined by a value of 0.85 if the normal stress on failure planes is less than 200 MPa, which is the case at shallower depths from 1–5 km. On the other hand, frictional coefficients of sandstones commonly range between 0.51 and 0.68 (Jaeger et al. 2007). Thus we assume a frictional coefficient of 0.7 as representative for the siliciclastic Granite Wash reservoirs. Equation (1) was used to calculate the upper and lower boundary of any possible stress regimes under the Granite Wash reservoir conditions at a depth of 2262 m. The pore pressure P_p at this depth is calculated for a fluid with a density of 1081 kg/m^3. This assumes hydrostatic pore pressure conditions and a linear increase of water density with depth from 1000 kg/m^3 at surface to 1162 kg/m^3 in the Granite Wash reservoir (from Michael and Buschkuehle 2008), resulting in a value of 24 MPa or 0.45 S_v. The vertical stress S_v at the depth of 2262 m was calculated with densities of the overlying rock strata derived from a density log and core tests, resulting in a value of 53.8 MPa (Alberta Geological Survey, personal communication).

Equation (1) was applied using a μ of 0.7:

$$\frac{(S_1-P_p)}{(S_3-P_p)} = \left(\sqrt{0.7^2+1}+\ 0.7\right)^2 \ = \ 3.69$$

$$S_1 - P_p = 3.69\,S_3 - 3.69\,P_p$$

$$S_1 + 2.69\,P_p = 3.69\,S_3 \ \big|\ P_p = 0.45\,S_v$$

$$S_1 + 1.21\,S_v = 3.69\,S_3$$

$$S_{Hmax} \leq 2.48\,S_v \quad (\text{for } S_{Hmin} = S_v), \qquad (1a)$$

$$S_{Hmin} \geq 0.60\,S_v \quad (\text{for } S_{Hmax} = S_v), \qquad (1b)$$

The values of $S_{Hmax\ and}\ S_{Hmin}$ from Eq. (1a) and (1b) represent the upper and lower boundary of any possible stress regimes allowable by frictional strength of 0.7, which is assumed for the Granite Wash reservoir rock at the depth of 2262 m. These stress boundaries are illustrated in a stress polygon, following the approach of Peška and Zoback (1995) (Fig. 33). Points at the periphery of the polygon correspond to a state of stress in which the reservoir rock is at the frictional limit. For further estimation of the minimum

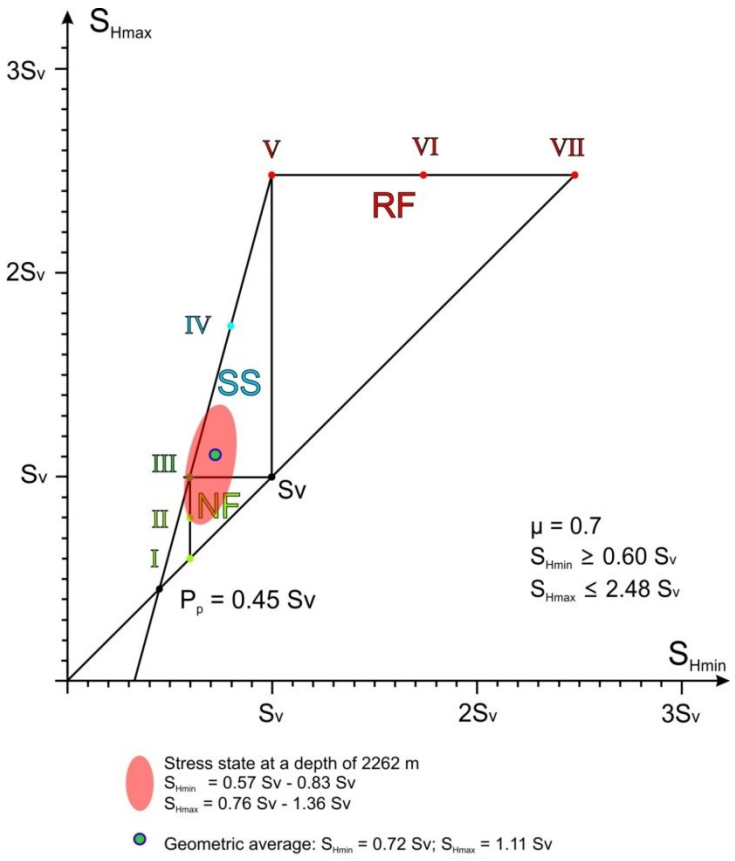

Fig. 33: Allowable horizontal stresses S_{Hmax} and S_{Hmin} in the crust based on the frictional equilibrium (after Peška and Zoback 1995 and Moeck 2009b). The stress polygon is normalized to S_v at the depth of 2262 m (53.8 MPa). The friction coefficient is assumed to be μ = 0.7. The pore pressure of 24.3 MPa was calculated for a Granite Wash brine with a density of 1162 kg/m^3 (from Michael and Buschkühle, 2008) assuming a constant increase of brine salinity with depth. NF normal faulting, SS strike slip, RF reverse faulting. I–VII cases of stress regimes defined by certain stress ratios. I radial extension, II normal faulting, III transition normal–strike slip faulting (hybrid case), IV strike slip faulting, V transition strike slip–reverse faulting, VI reverse faulting, VII radial compression.

and maximum horizontal stresses and the possible stress regimes, existing stress magnitude data from previous studies were considered. Wyman et al. (1980) and Kry and Gronseth (1983) have determined 15 magnitudes of S_{Hmin} from micro-frac treatments in a depth between 2021–2765 m in Elmworth, located 150 km southwest of the study area. In this dataset, the gradient of S_{Hmin} ranges from 13.6–19.7 MPa/km. Calculated for the reservoir depth of 2262 m, S_{Hmin} is between 30.8–44.6 MPa or 0.57–0.83 S_v. The average magnitude of S_{Hmin} at the reservoir depth is 38.7 MPa or 0.72 S_v. For 11 of these values, the magnitude of S_{Hmax} was estimated from hydraulic pressure data and pore pressure estimates (Wyman et al. 1980; Kry and Gronseth 1983; Barclay et al. 1990; Bell et al. 1994). In addition, two values of S_{Hmax} magnitude were determined by overcoring in a depth less than 200 m in

southern Alberta (Kaiser et al. 1982). From these 13 values the gradient of S_{Hmax} was calculated, which ranges from 18.1–32.3 MPa/km. At the reservoir depth of 2262 m S_{Hmax} is 40.9–73.1 MPa or 0.76–1.36 S_v, with an average of 59.7 MPa or 1.11 S_v. In the stress polygon, the possible regimes from these stress magnitudes range from normal faulting to strike-slip faulting, with the average of S_{Hmax} and S_{Hmin} plotting in the strike-slip field (Fig. 33). The normal faults identified from seismic data are compatible with these possible stress regimes.

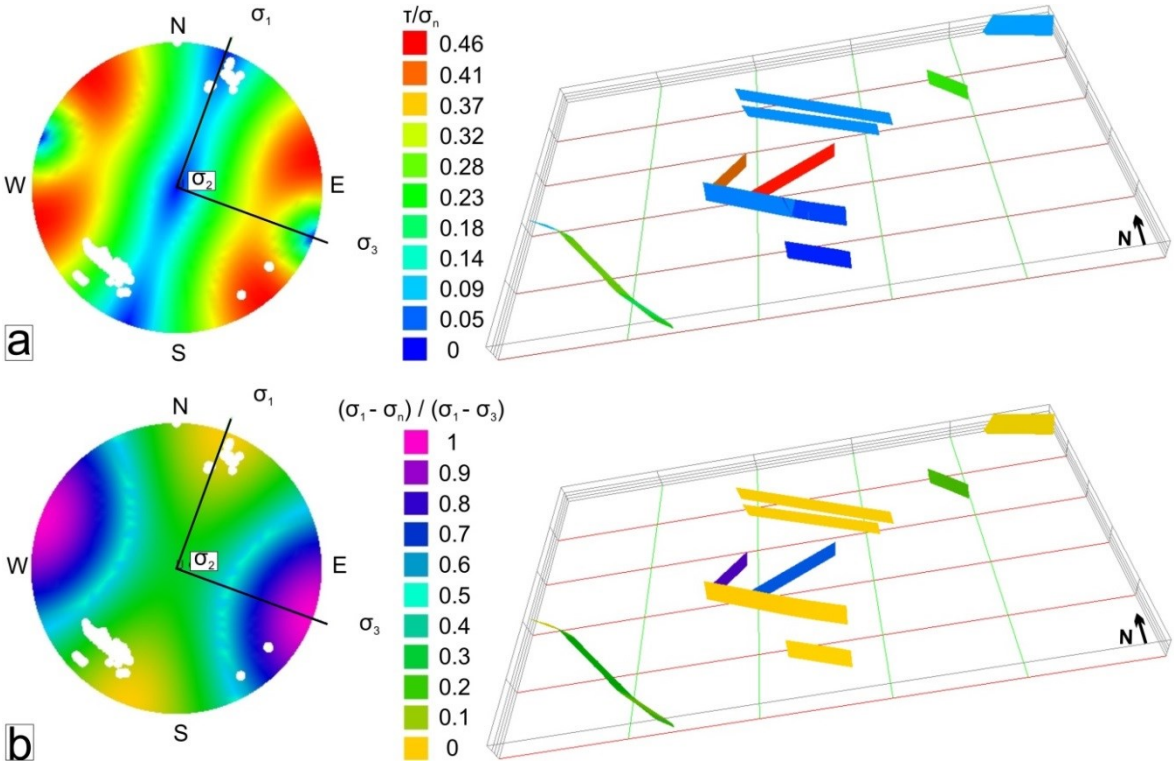

Fig. 34: Slip and dilation tendency plots for the fault planes from the 3D structural model *a: (left side)* the slip tendency and fault poles are displayed in the lower hemisphere projection; *(right side)* the spatial extension of the fault system and slip tendency along the faults are visualized in the 3D fault model. The slip tendency for a given fault is indicated on the color scale. Red indicates a relatively high slip tendency and blue indicates a relatively low slip tendency. b: (left side): the dilation tendency and fault poles are displayed in the lower hemisphere projection; *(right side)*: dilation tendency along the faults is visualized in the 3D fault model. The dilation tendency for a given fault is indicated on the color scale where purple indicates a relatively high dilation tendency and yellow indicates a relatively low dilation tendency.

4. Potential stress state on faults

The slip-tendency analysis (Morris et al. 1996) was used to identify critically stressed and dilational segments along the faults from the 3D model (Fig. 34). Fault segments are regarded as being critically stressed when the ratio of shear to normal stress acting on the fault plane exceeds the frictional strength of reservoir rock. The pore pressure reduces the

total stress, and is therefore reconsidered in the stress ratio calculation. The effective stresses used are S_{veff} = 29.8 MPa, $S_{Hmaxeff}$ = 35.7 MPa and $S_{Hmineff}$ = 14.7 MPa. The azimuth of S_{Hmax} is assumed to be 20°, as data from the World Stress Map (Heidbach et al. 2008) measured approximately 70 km east of the study area indicate. The slip-tendency analysis shows that none of the faults in the study area is critically stressed, as none of faults has a slip-tendency that is close to the friction coefficient of 0.7. The highest slip-tendency exists for the NE–SW striking faults (0.4–0.46) (Fig. 34a).

The dilation tendency describes the relative probability for a fault to dilate in the present stress field and is defined as $(\sigma_1-\sigma_n) / (\sigma_1-\sigma_3)$. The highest dilation tendency exists for faults which have a strike close to the azimuth of S_{Hmax} and perpendicular to S_{Hmin} respectively. In the study area these are the NE–SW striking faults (strike is 46° and 65°), which are close to the 20° azimuth of S_{Hmax} (Fig. 34b).

5. Thickness and distribution of the Granite Wash Unit

Well data and the resulting 3D lithostratigraphic model indicate that the Granite Wash Unit sediments are distributed over the entire study area. The thickness of the Granite Wash Unit was analyzed based on well log interpretation from 282 wells. The thickness of theGranite Wash Unit was mapped using the inverse distance weighting algorithm (Fig. 35a). The average thickness of the unit is 9.0 m. In the eastern part the thickness of the Granite Wash Unit ranges from 1 m to 10 m, with a zone of higher thickness up to 15 m (Fig. 35a). Towards the west and southwest the thickness increases and ranges from 10 m to 37.8 m. In the northwestern part 2 wells indicate a zone where the Granite Wash Unit thickness is up to 29 m.

6. Porosity and permeability analysis of the Granite Wash Unit

Porosity is the main parameter to identify domains with high storage capacity hosting producible fluids. High porosity domains therefore represent potential geothermal reservoirs. Permeability of the formation controls the flow in the reservoir and the productivity of wells.

6.1 Data set

Porosity and permeability of the Granite Wash Unit were investigated by core analysis data from IHS AccuMap (IHS Energy 2012). Core analysis data represent volume-averaged values corresponding to the sample size, which means they represent matrix properties and

not larger scale features such as fractures or vugs. As porosity and permeability of rocks may vary within short distances both vertically and laterally, the individual results from core analyses are only representative on the cm-scale. To investigate regional-scale (km-scale) trends in the data, the small-scale core analysis data were scaled up to well scale by calculating average values for each well. Following the approach of Bachu and Underschultz (1992), the arithmetic average was used for porosity values (which show a normal distribution) and the geometric average was used for permeability values (which show a lognormal distribution). Up-scaling to average regional-scale values was conducted by calculation of the geometric average of the well-scale values. For the calculation, only datasets from wells which contain at least 5 single core tests where used. In total, data from 336 Granite Wash Unit rock samples (plugs) from 21 wells were used in this study. These data are unevenly distributed: most core test data are concentrated in the southern and eastern parts of the study area, while in the central and northwestern parts no data exist.

The average regional scale porosity of the Granite Wash Unit is 7.4 %, and thus would be classified as poor (5–10 %; classification after Levorsen 1967). The maximum well-scale porosity of 19.4 %—found in the southeast—would be classified as good (15–20 %). Regional scale permeability of the Granite Wash Unit is 4×10^{-15} m^2, and would be classified as fair (1×10^{-15} m^2 – 1×10^{-14} m^2). The maximum well scale permeability found in the southeast exceeds 1×10^{-13} m^2 and would be classified as very good.

6.2 Regional distribution of porosity and permeability

The upscaled porosity and permeability data (i.e. well-scale) were mapped using inverse distance weighting, to detect zones where these properties are elevated. Fig. 35b shows the distribution of well-scale porosity in the Granite Wash Unit. In the southeastern and southwestern parts of the study area two zones with porosities larger than 10 % exist. Porosity in the northeastern part of the study area is rather low, ranging from 3–7 % on average. The distribution of maximum horizontal permeability (Kmax) is shown in Fig. 35c. The highest permeability is found in the southeastern part of the study area with a second zone of elevated permeability in the southwestern part. In the northeastern part of the study area the permeability is low.

7. Subsurface temperatures

Recent work on the thermal field covered most of central and northern Alberta (Gray et al. 2012; Majorowicz et al. 2012) and the WCSB (Weides and Majorowicz 2014). These

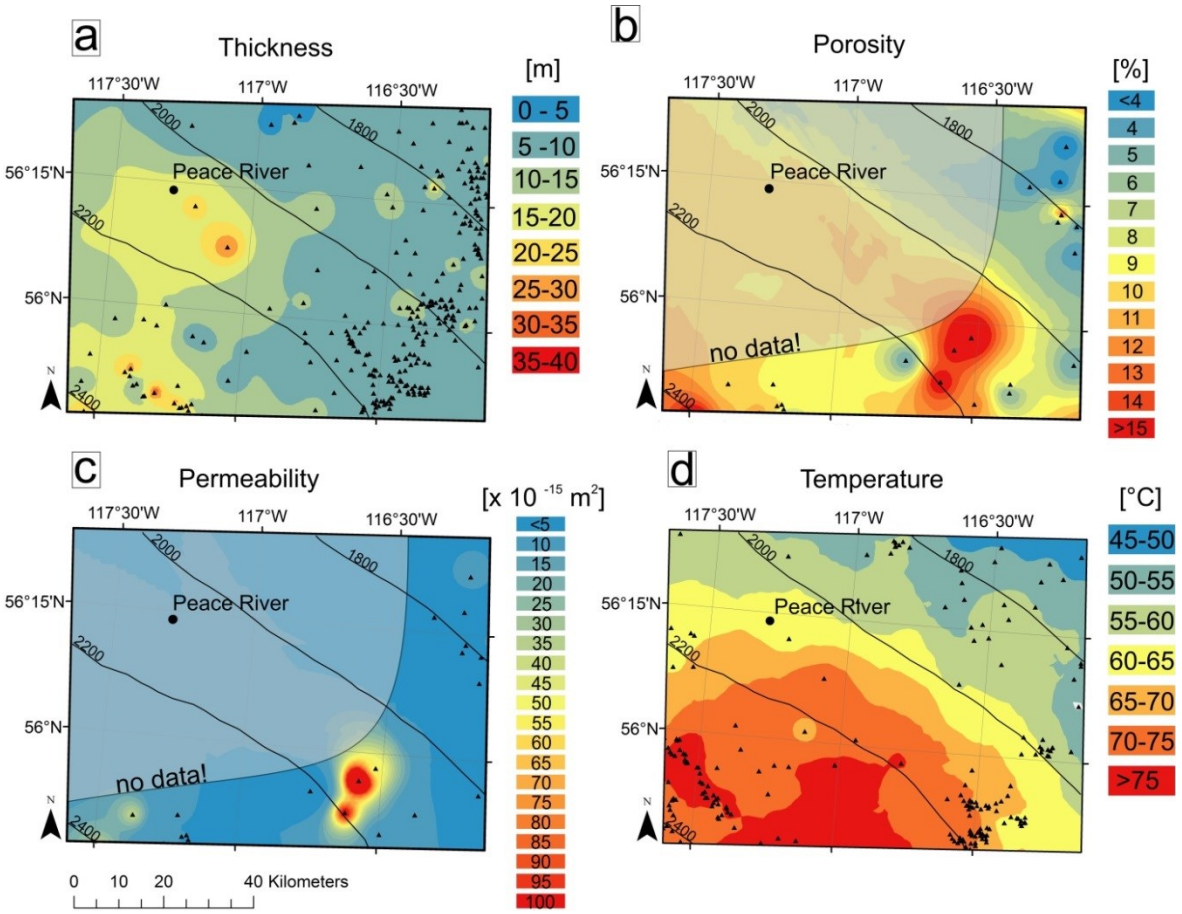

Fig. 35: Properties of the Granite Wash Unit. *a*: thickness distribution based on well log data and mapped with inverse distance weighting (IDW) *b*: porosity distribution based on upscaled core analysis data and mapped with IDW; for the northwestern part of the study area no core analysis data was available *c*: distribution of maximum horizontal permeability (Kmax) based on upscaled core analysis data and mapped with IDW; for the northwestern part of the study area no core analysis data was available. *d*: temperature map based on the geothermal gradient from 265 wells and on depth distribution (from well log data); contours are in metres below ground surface; black triangles represent wells with well log data (*a*), wells with core analysis data (*b* & *c*) or wells with temperature measurements (*d*).

thermal field studies were based on an extensive database, which included data from bottom hole temperature measurements (BHT), temperatures taken during drill stem tests (DST) and data from annual pressure and temperature (P/T) tests. A paleoclimatic correction was applied to the data (see Majorowicz et al. 2012). From this data base 510 temperature values (from 265 wells) were extracted and statistically approximated, resulting in an average geothermal gradient of 31.8 °C/km (standard deviation is 4.5 °C/km). This regional scale geothermal gradient is rather high considering the basin formed on the top of an old Precambrian craton. It can largely be explained by a thermal blanketing effect of very low effective thermal conductivity of the Phanerozoic sediments (from the surface to the Precambrian basement), which is assessed to be 1.6–1.8 W/mK

(+/- 0.2 W/mK). This is low in the context of thermal conductivity spatial variations in the WCSB, which are in the range of 1.5–2.3 W/m K. The heat flow in the study area generally ranges from 50–60 mW/m^2.

For mean ground temperature, which is required to calculate temperature at depth from the geothermal gradient, we estimate 0 °C. While present surface temperature is approximately 4 °C higher, we know that the deep sediment thermal field is still in equilibrium with sub-glacial temperature of 0 °C +/- 1 °C (see Majorowicz et al. 2012 for the discussion of equilibrium conditions in the postglacial environment of this study area).

Temperatures at the base of the Granite Wash Unit were calculated by combining the thermal gradient values and the basin depth (based on interpolation of stratigraphic tops). Fig. 35d shows the resulting temperature map for the Granite Wash Unit. Temperatures range from 51 °C in the northeastern part of the study area to more than 75 °C in the southwestern part.

8. **Discussion**

The stress magnitude data (Wyman et al. 1980; Kry and Gronseth 1983) used for the determination of the in-situ stress regime, show a high variability. The 15 stress gradients for S_{Hmin} range from 13.6–19.7 MPa/km, with a standard deviation of ±1.6 MPa/km or ±0.06 S_v. These values are slightly lower than the S_{Hmin} gradients presented in the more recent publication of Bell and Grasby (2012), which are between 16–22 MPa/km. In their study, which focuses on the larger scale of the WCSB, the S_{Hmin} gradients in the Peace River area were largely derived from hydraulic fracture treatments conducted at depths between 1–2 km (Bell and Grasby 2012). The magnitudes from Wyman et al. (1980) and Kry and Gronseth (1983) used in this study were derived from microfracturing treatments conducted at a depth of 2–2.7 km, closer to the Granite Wash reservoir depth of 2162 m. Beyond this, microfracturing is the most accurate subsurface determination of the smallest principal in situ stress (Bell and Grasby 2012; Schmitt et al. 2012). For these reasons the authors decided to use the magnitude data from Wyman et al. (1980) and Kry and Gronseth (1983).

The 13 stress gradients for S_{Hmax} range from 18.1–32.3 MPa/km, with a standard deviation of ±4.1 MPa/km or ±0.19 S_v. As a result the stress ratios of S_{Hmin} and S_{Hmax} plot in both the normal faulting and the strike slip faulting fields of the stress polygon, with the average in the strike slip field (Fig. 33). Considering the relatively large standard deviation of S_{Hmax}, a normal faulting regime as average stress regime in the Granite Wash reservoirs could also

be possible (see Fig. 33). Generally the results from this study indicate that this approach of calculating upper and lower boundaries (based on μ and S_v) for the possible minimum and maximum horizontal stress magnitudes is applicable for an estimation of the stress regime, as the majority of the stress magnitudes from the literature are located within the stress polygon. The magnitude data from literature possibly were determined in reservoirs in which production is ongoing, or in reservoirs which have already been depleted. In production affected reservoirs, the pore pressure is reduced and as a consequence, the effective stresses increase (Zoback 2007). Therefore we have to assume that the stress magnitude data likely do not represent the initial stress state of a virgin reservoir.

As fault strike was estimated using the refined trend surface analysis and is not based on 3D seismic data, the 3D fault model has a large uncertainty, which as a consequence is also true for the slip tendency analysis. However, for all possible fault orientations the maximum slip tendency under the assumed in-situ stress regime is 0.46 which is clearly below the frictional strength of the reservoir rock which we assume to be 0.7.

The stress state on faults was investigated with the slip- and dilation tendency method because various studies have shown that the state of stress along geological structures and the potential fluid flow along these structures are in close relation to each other (Barton et al. 1995; Wong et al. 1997; Ito and Zoback 2000; Gudmundsson et al. 2002; Zhang et al. 2002; Zhang et al. 2007). For reservoirs in a depth of less than 2 km, dilational faults can be important fluid pathways (Ferrill and Morris 2003). In a depth of more than 2 km, dilational failure is unlikely due to the high normal stress acting on a failure plane (Moeck et al. 2009a). In this depth critically stressed faults are considered as potential fluid pathways (Barton et al. 1995; Moeck et al. 2009a; Moeck et al. 2009b). The NE–SW striking faults identified in the study area, which have the highest dilation tendency, intersect the Granite Wash reservoir at a depth less than 2 km.

Porosity and permeability of the Granite Wash Unit were investigated with core plugs, which only reflect matrix properties but not the influence of fractures. Analysis of well logs could help to better understand the contribution of fractures to the well scale porosity. For a successful geothermal well high flow rates must be achieved, which do not necessarily follow from high porosity and permeability. Therefore future exploration of the Granite Wash Unit should include analysis of flow rates from DST`s.

Results from the 3D lithostratigraphic model indicate that the Granite Wash Unit sediments are distributed over the entire study area, which contradicts earlier studies (e.g. Dec et al.

1996). However, this result is based on information on two wells in the northeastern part of the study area (see Fig. 35a).

Results from this study indicate that the most promising area for a detailed geothermal exploration of the Granite Wash reservoirs is located in the southwestern part of the study area. In this part zones of elevated porosity (10–12 %) and permeability (1–4 × 10^{-14} m^2) exist, and temperatures in the Granite Wash Unit exceed 75 °C (Fig. 35d). Fluids with a temperature > 40 °C can be used for heating of greenhouses and domestic water provision, while temperatures > 70 °C can be used for district heating (Líndal 1973; Laplaige et al. 2000). In the southwestern part of the study area the Granite Wash Unit is located in a depth of approximately 2200–2350 m with a thickness between 15–25 m. A vertically drilled geothermal doublet system drilled in the southwestern part of the study area would have a productivity index of approximately 10 m^3/(h MPa) (calculated for a reservoir thickness of 20 m and a permeability of 2.5 × 10^{-14} m^2, a well spacing of 500 m and a 6" diameter). The productivity index is mainly dependent on the reservoir transmissivity, which is rather low (5 × 10^{-13} m^3) due to the small thickness of the Granite Wash Unit. For direct heat use, generally a transmissivity above 0.5–1 × 10^{-11} m^3 is seen as a minimum requirement (Rollin 2003; Pluymaekers et al. 2012; Mathiesen et al. 2013). Accessing the reservoir by horizontally drilled wells would result in higher transmissivity values. Assuming a permeability of 2.5 × 10^{-14} m^2, the reservoir would need to be accessed over a distance of 400 m to obtain a transmissivity of 1 × 10^{-11} m^3. This 400 m long well section in the Granite Wash Unit would have a productivity index of approximately 63 m^3/(h MPa). However, drilling and completing a horizontal well is cost intensive too, and can cost up to 300 per cent more than a vertical well directed to the same target (Helms 2008). Therefore the economic use of accessing the Granite Wash reservoirs by horizontal drilling has to be evaluated.

9. Conclusion

The most promising zone for geothermal applications is located in the southwestern part of the study area, where elevated porosity (10–12 %) and permeability (1–4 × 10^{-14} m^2) coincide with temperatures of more than 75 °C. Thickness of the Granite Wash Unit in this part of the study area is 15–25 m, while the average thickness is 9 m. There is an indication that the Granite Wash Unit is distributed in the whole study area, other than earlier studies had reported. The relatively low thickness of the Granite Wash Unit in the area is problematic for the utilization as a geothermal reservoir because it implies a low

reservoir transmissivity. The average well-scale porosity of the Granite Wash Unit is 7.4 %, the average well-scale permeability is 4×10^{-15} m^2. The temperature in the Granite Wash Unit gradually decreases towards 51 °C in the northeastern, shallower part of the study area.

The general strike pattern of the nine normal faults identified from seismic interpretation is NW–SE and NE–SW. The in-situ stress state at the depth of the Granite Wash Unit is a strike-slip regime with S_{Hmax} is 1.11 S_v (±0.19 S_v) and S_{Hmin} = 0.72 S_v (±0.06). The vertical stress S_v in the reservoir depth of 2262 m is 53.8 MPa. None of the nine interpreted faults is critically stressed with the highest slip tendency existing for the NE–SW striking faults (0.4–0.46). Faults striking in this direction also have the highest dilation tendency (0.7–0.9). These stress analyses, however, could be greatly improved by carefully conducted stress determinations in the target zone itself.

Acknowledgements

Well data and access to IHS AccuMap were provided by the Energy Resources Conservation Board and Alberta Geological Survey. Special thanks to Matt Grobe, Dan Palombi and Dave Bechtel.

The authors have benefited greatly from the input of collegues from U of A and GFZ. Particular thanks are due to Elahe A. Poureslamie, Brendan Snow and Judith Chan for their support on handling the 2D seismic data, and to Karsten Reiter for interesting and fruitful discussions on stress data. Special thanks to Nate Walsh from the University of Toronto reviewing the writing of the manuscript.

The seismic interpretation was performed with the software package „Petrel“, Schlumberger.

The 3D geological model was processed with the software package „earthVision“, Dynamic Graphics Inc. (DGI).

This study is part of the Helmholtz–Alberta Initiative (HAI), which is a research collaboration between the Helmholtz Association of German Research Centres and the University of Alberta.

The authors would like to acknowledge helpful reviews by Dr. Stephen Grasby and an anonymous reviewer.

Chapter 5

Originally published in *Energies,2014,7: 2573-2594*

Implications of spatial variability in heat flow for geothermal resource evaluation in large foreland basins: the case of the Western Canada Sedimentary Basin

Simon Weides & Jacek Majorowicz

Abstract

Heat flow and geothermal gradient of the sedimentary succession of the Western Canada Sedimentary Basin (WCSB) are mapped based on a large thermal database. Heat flow in the deep part of the basin varies from 30 mW/m^2 in the south to high 100 mW/m^2 in the north. As permeable strata are required for a successful geothermal application, the most important aquifers are discussed and evaluated. Regional temperature distribution within different aquifers is mapped for the first time, enabling a delineation of the most promising areas based on thermal field and aquifer properties. Results of previous regional studies on the geothermal potential of the WCSB are newly evaluated and discussed. In parts of the WCSB temperatures as high as 100–210 °C exist at depths of 3–5 km. Fluids from deep aquifers in these "hot" regions of the WCSB could be used in geothermal power plants to produce electricity. The geothermal resources of the shallower parts of the WCSB (> 2 km) could be used for warm water provision (> 50 °C) or district heating (> 70 °C) in urban areas.

1. Introduction

The Western Canada Sedimentary Basin (WCSB) is known for its large reserves of oil, gas and coal. In times of public discussion on climate change and the greenhouse gas emissions that come with burning of fossil fuels, the focus of interests shifts gradually towards renewable energy production such as geothermal energy. In western Canada, geothermal energy could play a role in replacing some fossil-fuel generated heat energy used as an energy source for warm water provision, district heating, industrial processes, or even electric power production. The feasibility of producing geothermal heat is strongly dependent on the thermal and geological conditions of the subsurface. Naturally, sufficient temperature is a primary constraint. However, only in a situation where a significant amount of warm fluid is produced will a geothermal project be successful. Therefore information on reservoir properties, particularly porosity and permeability, are crucial for geothermal exploration.

In this study information on subsurface thermal conditions and geology is combined by mapping the temperature for different stratigraphic depths, and overlaying the distribution of potential geothermal target formations on these maps.

2. Previous work

2.1 Thermal field

The study of geothermal heat in the WCSB has a long history (see Majorowicz and Jessop, 1981, and Majorowicz and Grasby, 2010a, for a review of the early work). The first precise heat flow measurements were done by Garland and Lennox (1962) in shallow 300–1000 m deep wells near Leduc (67 mW/m^2) and Redwater (61 mW/m^2) in the vicinity of Edmonton. Majorowicz et al. (2012) applied a paleoclimatic correction which increased these values by 12 % to 75 mW/m^2 for the Leduc well and 68 mW/m^2 for the Redwater well.

The first regional WCSB basin analysis of geothermal patterns from industrial temperatures was done in 1981 by Majorowicz and Jessop (1981) for Alberta, Saskatchewan and the Northwest Territories (NWT). Lam and Jones (1984) and Jones and Majorowicz (1987) expanded the database available to Majorowicz and Jessop and conducted thermal conductivity, heat generation and heat flow studies of the sedimentary basin and Precambrian basement rocks. They found that heat flow patterns poorly correlate with heat generation of the Precambrian basement rocks from decay of ^{235}U-, ^{232}Th- and ^{40}K- isotopes. This has been recently confirmed by Majorowicz et al. (2013). It is contradictory with Bachu (1993) who assumed that heat flow in the basin is controlled by variability of heat generation of the basement and influence of hydrodynamics is marginal (see discussion section for more information).

The first attempt to predict and map temperature at the geological surfaces was done by Jones et al. (1985) in 1985 for the Paleozoic erosional surface and the Precambrian surface of the Alberta basin, followed by mapping of temperature at Precambrian surface for the larger area of the whole WCSB by Bachu in 1993.

Majorowicz et al. (1999) identified significant overestimation of temperatures from Alberta industrial well logs from shallow depths (< 1000 m). This has been determined from high precision temperature logs conducted in shallow wells that have been allowed to reach thermal equilibrium. These findings have been confirmed by recent studies in the northern half of Alberta using tens of thousands of industrial temperature measurements

from three independent datasets: Annual Pool Pressure surveys (APP), Drill Stem Tests (DST) and Bottom Hole Temperatures (BHT) constrained by equilibrium high precision logs coupled with 33 Thermal Conductivity wells were used to provide a more accurate prediction of the temperature gradient of the northern Alberta part of the WCSB (Gray et al. 2012; Majorowicz et al. 2013). The results of these recent northern Alberta studies showed the need for this study which covers all of the WCSB.

One of the main reasons for the overestimation of BHT`s from shallow wells are seasonal effects on analogue thermometers which were used until the 1980`s (Gray et al. 2012). These thermometers recorded the maximum temperature in a well, which was assumed to have been recorded at the bottom of the well. However, during the summer months surface air temperatures exceed the BHT and can lead to overestimation of BHT`s (Gray et al. 2012).

No high precision temperature data exists below 1000 m with the exception of one deep well on the outskirts of Fort McMurray in the shallow north eastern part of the basin, drilled 2400 m into the basement granites below 0.5 km of sediments (Majorowicz et al. 2013).

2.2 Studies on the geothermal potential of deep aquifers

The first study on the geothermal potential of deep aquifers in the WCSB was published by Lam and Jones in 1985. In their paper the authors examined aquifer porosity, thickness, water chemistry and water recovery in the area of Hinton-Edson in western Alberta, concluding that especially the Mississippian and Upper Devonian carbonate rocks have a good geothermal potential. In a second study Lam and Jones (1986) investigated the geothermal potential in the Calgary area. Despite the low geothermal gradient, the authors stated that the Calgary area is an attractive location for geothermal recovery due to the relatively thick sedimentary succession and the substantial population of the city. Similar to the results of their study of the Hinton-Edson area, the largest potential for geothermal purposes in the Calgary area was also found in Upper Devonian and Mississippian carbonate rocks. Jessop and Vigrass (1989) published a report on a geothermal well which was drilled in 1979 into the depth of 2214 m at the Campus of the University of Regina (Saskatchewan). Tests showed an excellent geothermal potential, but unfortunately the large sports building that was intended to be the load for the well was not built, so the well has only been used as a research facility.

In 2011 the Geological Survey of Canada released a report (Grasby et al. 2011) which synthesizes previous geothermal studies and delineates the potential of the different geothermal resource types in Canada. A major finding of the report is that the highest geothermal potential (for electricity production) exists in the volcanic belts of the Cordillera and in parts of the WCSB (northeastern British Columbia, northern Alberta and southern Northwest Territories). The report describes the other deeper parts of the WCSB as a very large resource for direct heat use. In 2013 the British Columbia Ministry of Energy and Mines assessed the geothermal resource in the Devonian Carbonates of the Clarke Lake gas field in northeastern British Columbia (Walsh 2013). In central Alberta Weides et al. (2013) mapped porosity, permeability and temperature of four Devonian carbonate aquifers and the Cambrian Basal Sandstone Unit (Weides et al. submitted for publication), concluding that all five formations are potentially useable for geothermal heating applications. Using a similar approach, Weides et al. (2014) investigated the geothermal potential of the siliciclastic Granite Wash Unit in northwestern Alberta. Ferguson and Grasby (2014) examined the deep clastic reservoirs of the Winnipeg and Deadwood formations (Basal Clastics) in Saskatchewan, finding that these formations have "geothermal potential for development of direct use and electricity generation systems". Besides depth, thickness and temperatures of the Basal Clastics, Ferguson and Grasby focused on injection rates from existing disposal wells, most of which operate at flow rates between 30 and 140 L/s.

3. Methods

3.1 Temperature database

In this paper heat flow and geothermal gradient data for the WCSB were compiled from previous research. The heat flow and geothermal gradient data base from Majorowicz and Grasby for western and Northern Canada (Majorowicz and Grasby 2010a) has been expanded by additional heat flow and geothermal gradient studies which were conducted as part of Helmholtz-Alberta Initiative for the northern half of the Alberta territory (Gray et al. 2012; Majorowicz et al. 2012; Majorowicz and Grasby 2010a; Majorowicz et al. 2013). The recent compilation done by the Geological Survey of Canada for all of Canada includes this dataset (Grasby et al. 2011). The Majorowicz and Grasby (Majorowicz and Grasby 2010a) compilation mainly was based on the corrected bottom hole temperatures (BHTs) and drill stem test (DST) temperature records, with few (5) precise temperature

depth logs in equilibrium wells. This compilation has been expanded with a dataset containing estimates of the geothermal gradient from temperatures taken by industry and reported to the Alberta Energy Conservation Board. The same dataset has been used by Majorowicz and Moore (2008) for their first Canadian evaluation of feasibility of EGS in the Alberta basin. The resulting dataset used in this study consists of about 70,000 single values (from APP`s, DST`and BHT`s) from more than 26,400 wells. The data were carefully filtered and corrected for equilibrium conditions. More detailed information on data quality and handling of the dataset is found in Gray et al. (2012). The heat flow data used in this article is based on conductivities of the main 13 rock types in the WCSB, which were determined from about 1,405 measurements (Beach et al. 1987).

3.2 Mapping of geothermal data

The distribution of geothermal gradient and heat flow were mapped for the whole sedimentary succession deeper than 1 km. For calculation of the maps the ArcGIS 10.1 Geostatistical Analyst extension was used. In a first step, the dataset was checked for outliers. All heat flow values which were unusually high (above 100 mW/m^2) or low (below 30 mW/m^2) have been removed from the dataset. In total 462 values were identified as outliers, of which the majority showed no spatial consistency. These extreme values probably are the result of measurement or notation errors and do not represent the real thermal conditions. The resulting heat flow dataset includes 74,728 heat flow values from 26,421 wells. For those wells for which more than one heat flow value exists, the arithmetic average was calculated. The heat flow map was calculated using the simple kriging algorithm. The data were declustered to adjust for preferential sampling. A stable omnidirectional semivariogram was modelled, using 25 lags with a length of 10,000 m each, a nugget of 0.11, a range of 165 km and a partial sill of 0.50 (Fig. 36a).

A similar approach was applied to map the geothermal gradient. First, all geothermal gradient values which were unusually high (above 80 °C/km) or low (below 10 °C/km) have been removed (37 values), resulting in a dataset of 68,377 gradient values from 26,492 wells. For those wells for which more than one gradient value exists, the arithmetic average was calculated. The geothermal gradient was mapped applying the simple kriging algorithm. A tetraspherical omnidirectional semivariogram was modelled, using 25 lags with a length of 10,000 m each, a nugget of 0.13, a range of 230 km and a partial sill of 0.39 (Fig. 36b).

The geothermal gradient map was then used to calculate the temperature distribution for different stratigraphic units. The benefit of this approach over mapping temperature at a constant depth is that the resulting maps combine two key aspects relevant for geothermal exploration: temperature and geology. Five stratigraphic units where chosen for the maps: the top of the Precambrian basement, the Devonian Beaverhill Lake Group, the Devonian Winterburn Group and the Mississippian succession, and the bottom of the Cretaceous succession (sub-Mannville unconformity). First, structure depth maps were calculated for the five stratigraphic units using the well control data of the Geological Atlas of the Western Canada Sedimentary Basin (Mossop and Shetsen 1994b), applying the ordinary kriging algorithm. To obtain the temperature distribution at depth, the raster of the geothermal gradient map was then multiplied with the raster of the depth distribution. Because at shallow depths less than 1 km subsurface temperatures are generally too low for geothermal applications, and as temperature measurements from shallow wells (less than 1 km) tend to be biased (Gray et al. 2012), the depth range shallower than 1 km is not displayed on the temperature distribution maps.

In addition to the temperature and depth information, the geographical extension of potential geothermal target formations was added to the maps. These formations were either chosen because they have already been in the focus of earlier geothermal exploration

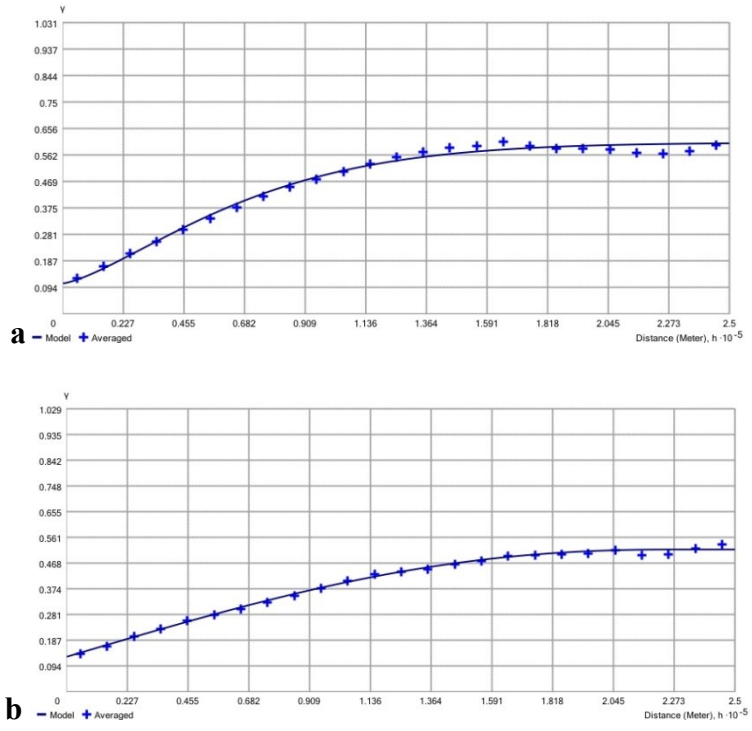

Fig. 36: Sample variograms and variogram models for heat flow (a) and geothermal gradient (b).

Period	Group	Formation	Lithology	References	Figure
Cretaceous	Mannville		sandstone	[1]	8
Cretaceous	Mannville	Cadomin	sandstone & congl.	[1]	8
Mississippian	Rundle		carbonates	[1],[2];[5]	7
Mississippian	-	Charles	carbonates	-	7
Mississippian	-	Banff	limestone	-	6
Devonian	Wabamun	Wabamun	dolomite	[1]; [2]; [5]	6
Devonian	Winterburn	Nisku	carbonates	[1]; [2]; [5]	6
Devonian	Woodbend	Grosmont	dolomite	-	5
Devonian	Woodbend	Leduc	dolomite	[1]; [5]	5
Devonian	Woodbend	Cooking Lake	reefal carbonates	[5]	5
Devonian	Beaverhill Lake	Slave Point	reefal carbonates	[1]; [4]; [7]	5
Devonian	Beaverhill Lake	Swan Hills	reefal carbonates	[7]	5
Devonian	Elk Point	Pine Point	dolostone	-	5
Devonian	-	Granite Wash Unit	sandstone	[7]	4
Ordovician	Basal Clastics	Winnipeg	sandstone	[3]; [8]: [9]	4
Cambrian		Deadwood	sandstone		
Cambrian	-	Basal Sandstone Unit	sandstone	[2]; [5]; [6]	4

Tab. 8: Potential geothermal target formations in the WCSB. References: [1] = Lam and Jones (1985), [2] = Lam and Jones (1986), [3] = Jessop and Vigrass (1989), [4] = Walsh (2013), [5] = Weides et al. (2013), [6] = Weides et al. (submitted for publication), [7] = Weides et al. (2014), [8] = Ferguson and Grasby (2014). [9] = Dixon (2008).

Fig. 37: Core samples from potential geothermal target formations.

studies, or because they have been described in the literature as porous (and permeable) and therefore could host larger amount of warm fluids. It has to be pointed out that the potential geothermal target formations in most cases do not have the same depth as the particular temperature map (and as the depth contours), but rather are located a few hundred meters above or below, because the maps report the temperature at the top or bottom of a specified formation. A brief overview on the potential geothermal target formations is given in Tab. 8. Fig. 37 shows examples of core samples from some of the formations.

4. Results

4.1 Heat flow and geothermal gradient

The heat flow in the WCSB generally ranges from 30–100 mW/m^2, being 60.4 mW/m^2 on average (Fig. 38b). The highest heat flow is found in the northern part of the WCSB in the Northwest Territories, and adjacent northeastern British Columbia (B.C.) and northwestern Alberta. Other larger positive anomalies exist at the southeastern margin of the WCSB in the area of Regina (Saskatchewan) and Brandon (Manitoba), and in the western part of central Alberta (Fig. 38b). Larger negative heat flow anomalies are found in northeastern Alberta (south of Fort McMurray) and in southern Alberta in the area of Calgary. Generally a northerly trend of increasing heat flow exists.

The geothermal gradient in the WCSB ranges from 20–55 °C/km, with an average value of 33.2 °C/km (Fig. 39). The distribution of the thermal gradient follows the same trend of increasing values towards the northern WCSB.

4.2. Temperature at depth and distribution of potential geothermal target formations

At the base of the sedimentary column the highest temperatures are found in the deepest parts of the basin close to the Cordillera, reaching values above 180 °C at a depth of 4.5 km and more (Fig. 40). In the deeper half of the WCSB, at depth below 2–2.5 km, temperatures are above 70°C, thus sufficient for district heating (see also discussion section). Potential geothermal target formations at the basal part of the basin fill are the siliciclastic deposits of the Cambrian Basal Sandstone Unit in central Alberta and western Saskatchewan, the Cambro-Ordovician Basal Clastics in eastern Saskatchewan, and the Devonian Granite Wash Unit in northwestern Alberta.

At the stratigraphic depth of the Devonian, the porous deposits from the carbonate platforms and reefal buildups in the Alberta and B.C. part of the WCSB are the potential targets formations (see Fig. 41 & Fig. 42). Porous carbonate formations from the Carboniferous succession are deposited throughout the major part of the deeper WCSB (Fig. 43). The temperature distribution at the sub-Mannville unconformity is the shallowest map presented in this study (Fig. 44). Potential geothermal target formations are the sandstones and conglomerates of the Mannville Group above the unconformity, which reach temperatures above 60 °C in the cities of Red Deer and Great Prairie at a depth of about 2 km, and are naturally warmer at greater depths closer to the Cordillera.

a)

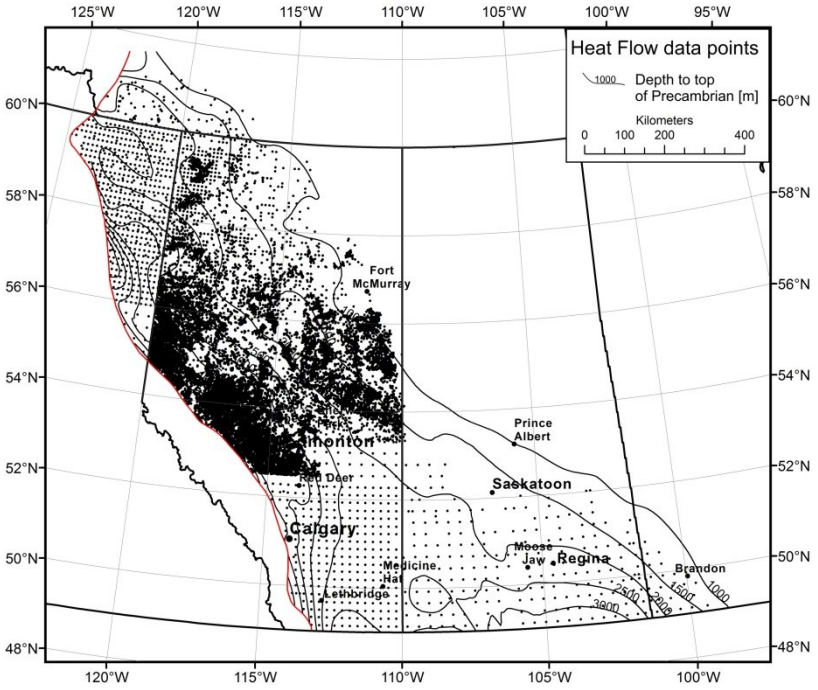

b)

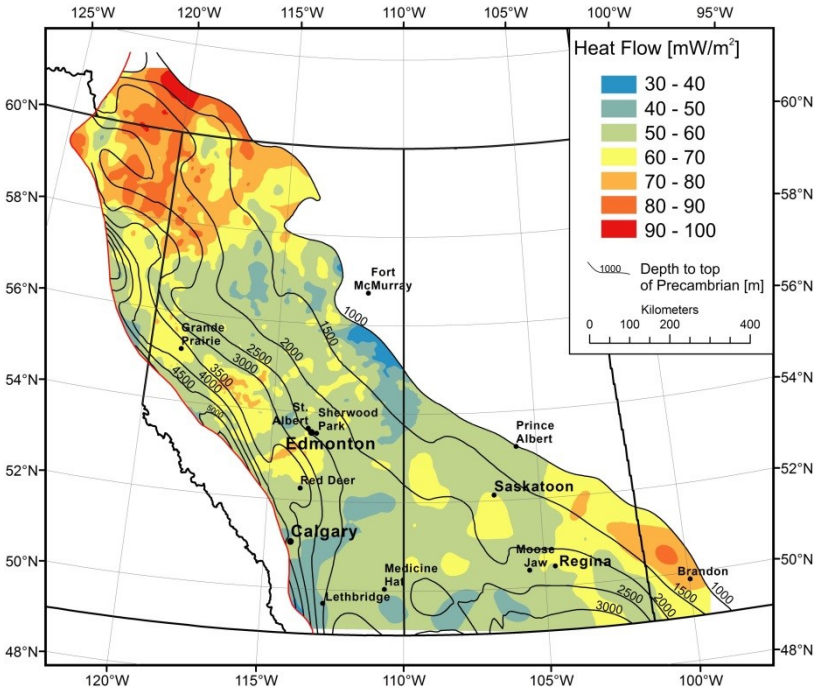

Fig. 38: a: Data points used for mapping of heat flow; dataset consists of on 74,728 values at 26,421 locations; b: Heat flow of the WCSB; map was calculated using the simple kriging algorithm.

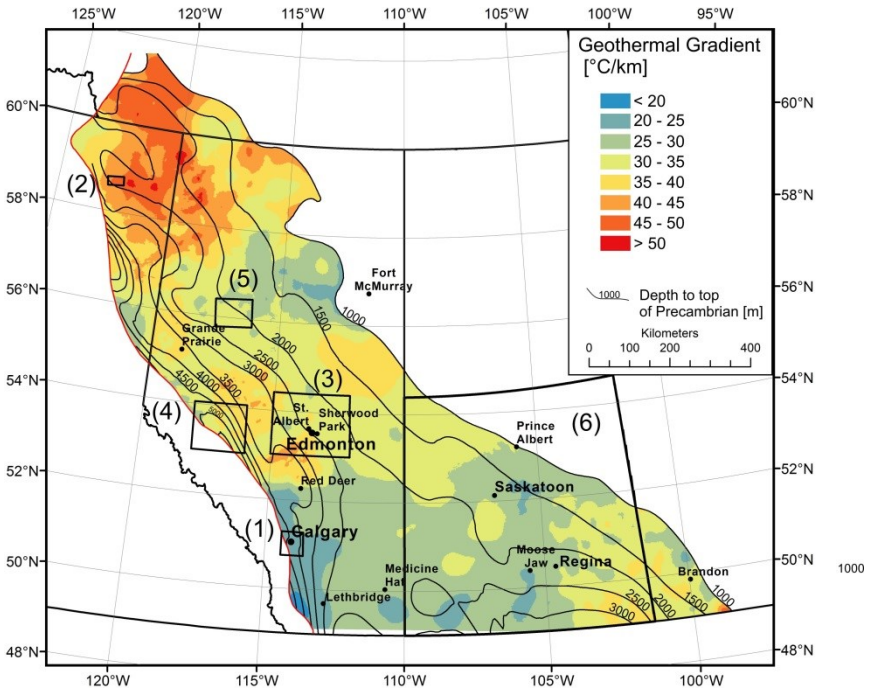

Fig. 39: Geothermal gradient of the WCSB based on 68,377 gradient values from 26,492 wells; map was calculated using the simple kriging algorithm. Black boxes represent the location of previous geothermal studies (see Tab. 9).

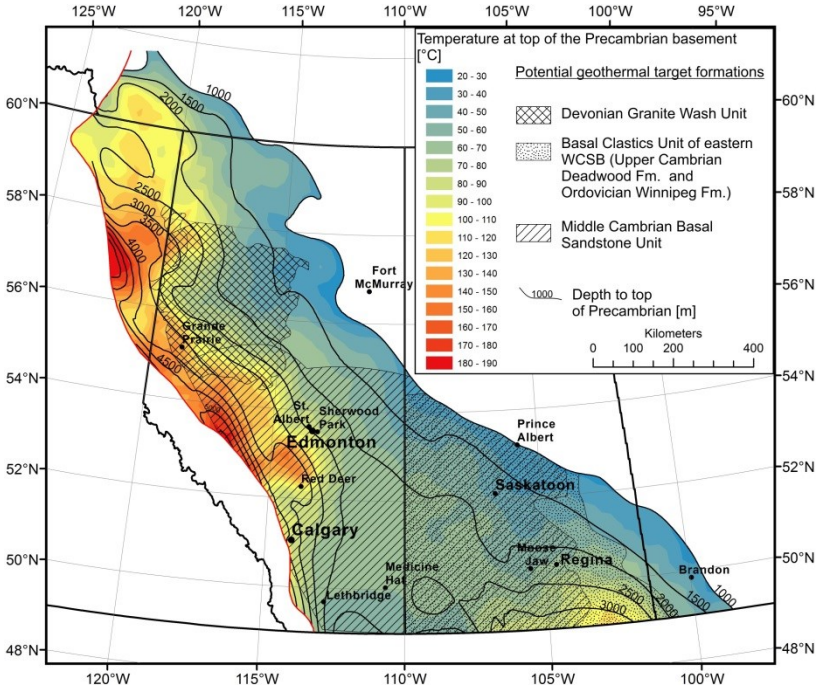

Fig. 40: Temperature at the top of the Precambrian basement with potential geothermal target formations; formations outline from Trotter (1989) for the Granite Wash Unit, from Slind et al. (1994) and Dixon (2008) for the Basal Clastics, and from Pugh (1971; 1973) for the Cambrian Basal Sandstone Unit (BSU).

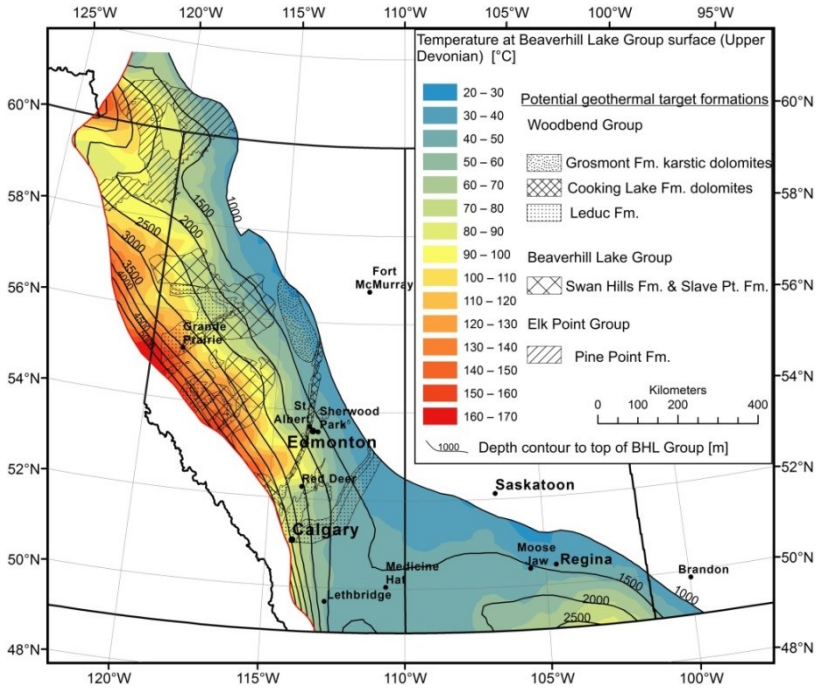

Fig. 41: Temperature at the base of Beaverhill Lake Group; formations outline from Switzer et al. (1994) for the Woodbend Group, from Oldale and Munday (1994) for the Beaverhill Lake Group and from Meijer Drees (1994) for the Elk Point Group.

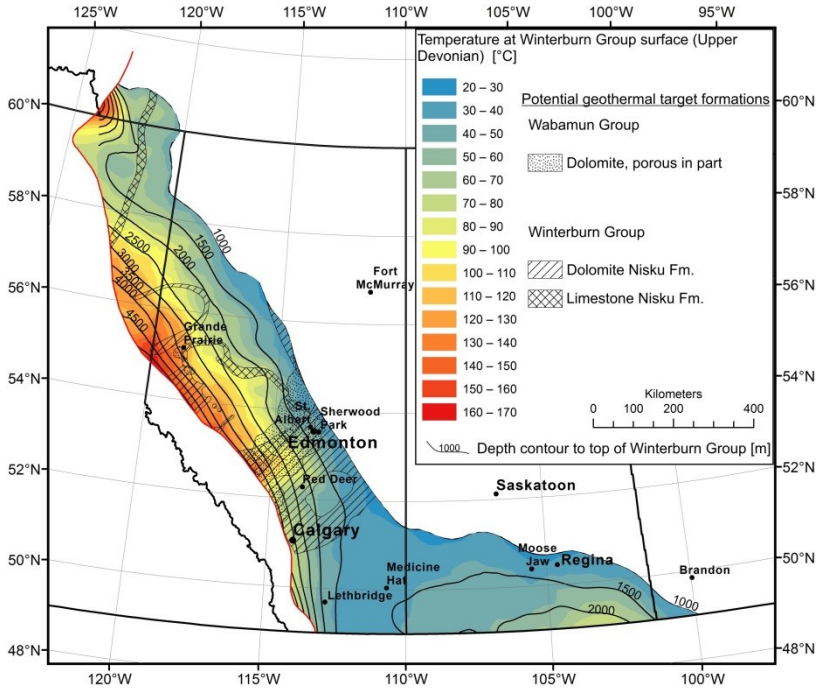

Fig. 42: Temperature at the top of the Winterburn Group; formations outline from Switzer et al.(1994) for the Winterburn Group and from Halbertsma (1994) for the Wabamun Group.

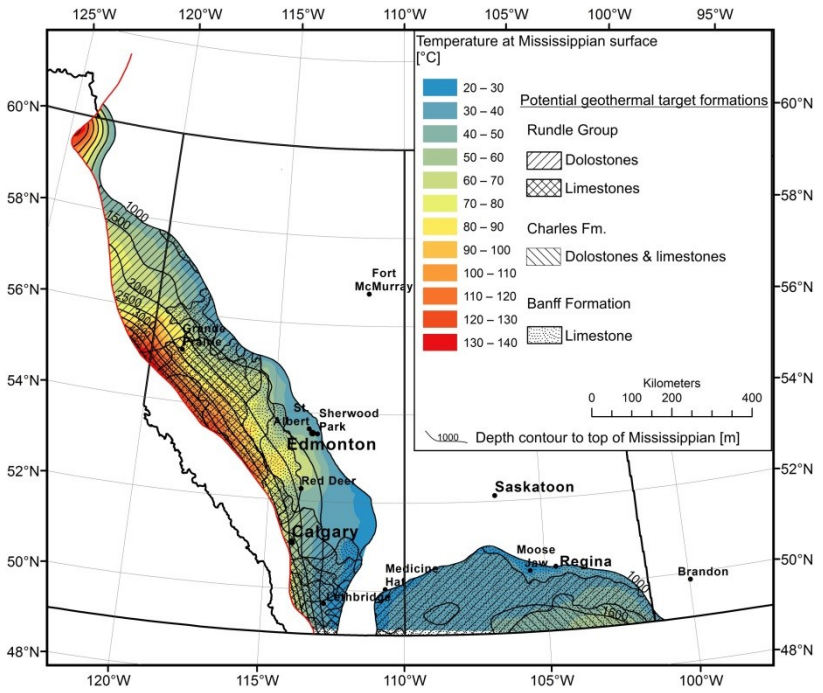

Fig. 43: Temperature at the top of the Mississippian; formations outline from Richards et al. (1994).

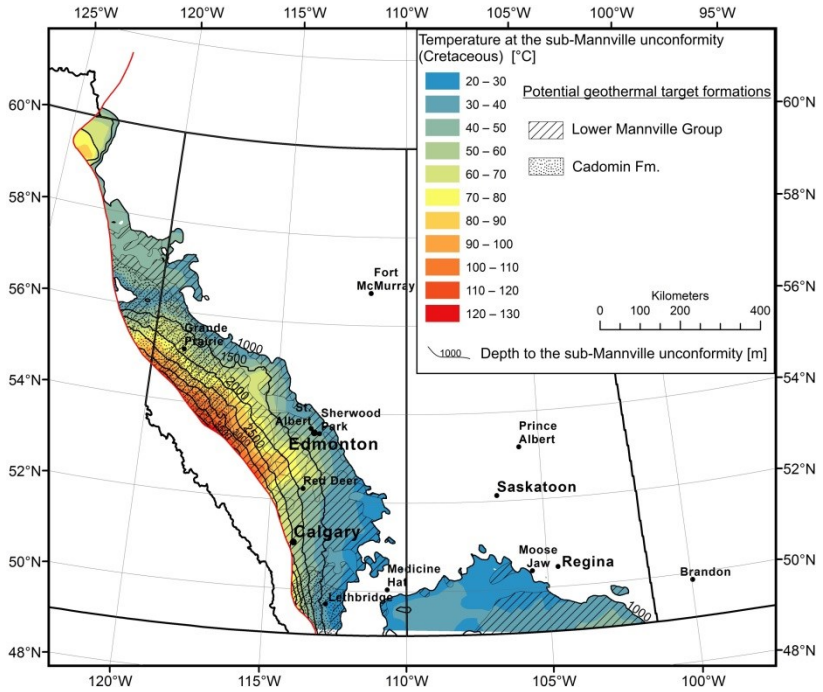

Fig. 44: Temperature at the sub-Mannville unconformity; formations outline from Hayes et al. (1994).

5. Discussion

5.1 Controls upon thermal field

It is noticed that the thermal field in the WCSB is highly variable. Heat flow in the deep part of the basin varies from 30 mW/m^2 in the south to 100 mW/m^2 in the north; the geothermal gradient varies from as low as 20 °C/km to over 55°C/km. While values in the range of 30–60 mW/m^2 and 20–30 °C/km are typical for the Precambrian basement platform filled with sediment, values of 70–100 mW/m^2 and 40–55 °C/km can be considered as high respectively anomalous.

There are several controlling factors for geothermal gradient:

1. Thermal conductivity
2. Heat flow
3. Gravity driven convectional heat transport

Thermal conductivity k controls the geothermal gradient at constant heat flow Q. The Q/k relationship for any depth along the vertical z axis of the well follows Fourier's law:

$$Q/k=dT/dz \quad (1)$$

where: T is the temperature at depth, z is the vertical depth, dT/dz is the temperature gradient and Q is the heat flow.

Thermal conductivity k for the crust for Canada is given by Jessop (1990) and Beach et al. (1987). Beach et al. (1987) based their statistic on 1,405 values measured on core samples from Alberta basin rocks with use of the divided bar method. Typically, thermal conductivity is 3 W/mK for crystalline rocks, and 2 W/mK for sediments, which serve as a thermal blanket over the top of the crystalline crust. Fig. 45 shows a good example of the control of k upon heat flow for a constant Q=70 mW/m^2 and a mean thermal gradient approximation for the sedimentary succession in this paper.

Heat flow at the surface is composed of the heat generation in the sediments (10^{-1} $\mu W/m^3$), in the granitic upper crust (1–10 $\mu W/m^3$), in the basaltic crust (10^{-2} $\mu W/m^3$), and of the contribution from below the crust, which consists of input from transient sources and radiogenic heat production at a very low rate (10^{-3} $\mu W/m^3$) (Majorowicz et al. 2013). While for several regions in the world a heat flow–heat generation relationship has been established (mainly for the measurements taken in the granitic batholiths; Jessop 1990), it is difficult to find one for the heat flow estimates vs. heat generation of the basement of the

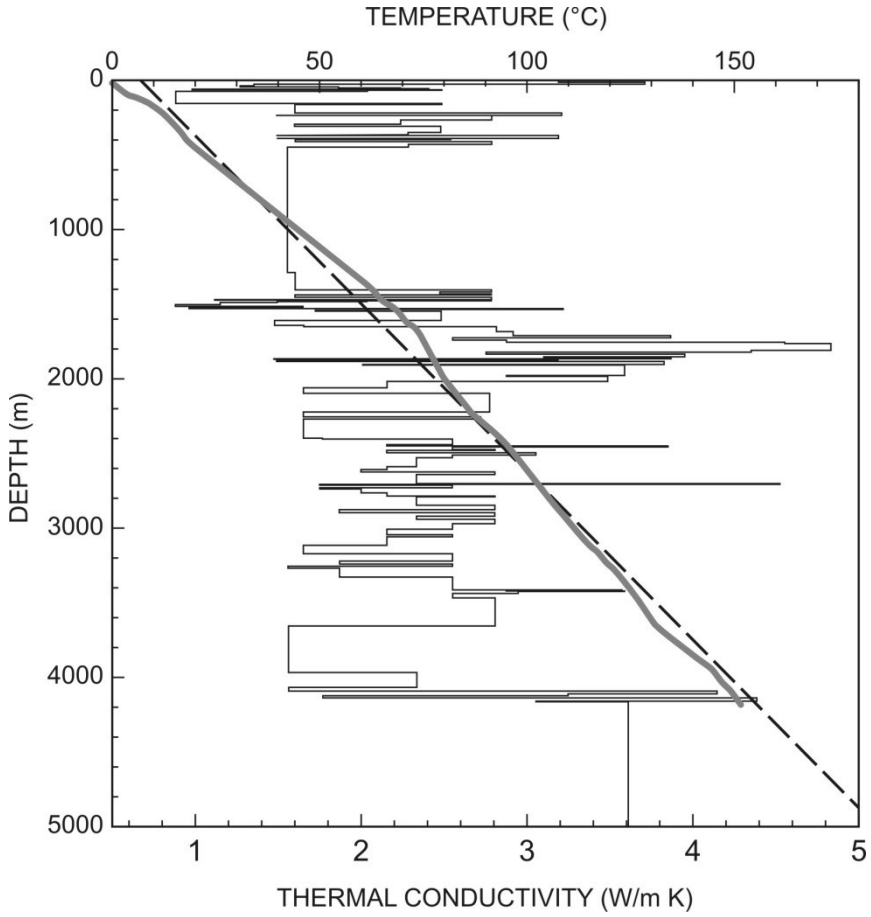

Fig. 45: Temperature depth (gray continuous profile) and thermal conductivity k (step line) control based on an example of a location in the deep foreland basin in British Columbia part (123°W 57°N; see Fig. 38 for location). Approximation of the mean thermal gradient is also shown by a broken line.

WCSB (Jones and Majorowicz 1987). In case of WCSB estimate of contribution from the upper crust can be based on ^{235}U, ^{232}Th and ^{40}K radiogenic elements contribution (Jones and Majorowicz 1987; Jessop 1992) and lower crust and mantle contribution (Jessop 1992). This shows that the so called „reduced heat flow“ from the mantle and the lower crust is 37 mW/m^2 (S.D. =2 mW/m^2) (Jessop 1992). The upper crustal contribution varies in much wider range due to much larger variability of heat production of the „granitic“ crust (Jones and Majorowicz 1987). Its contribution will depend on the thickness the upper crustal high heat generating („granitic“) part and the mean heat generation which differs between 1.1 µW/m^3 (Precambrian shield) and 2.4 µW/m^3 (WCSB) (Jessop 1992).

In the WCSB Burwash and Burwash (1989) have provided data on uranium and thorium concentrations for 182 samples from the Precambrian basement in Alberta, Saskatchewan, Manitoba and British Columbia, and for the southern part of the Mackenzie Corridor of the southern Northwestern Territories. The measurements were made by the delayed neutron activation method. Jones and Majorowicz (1987) included additional data from the Peace

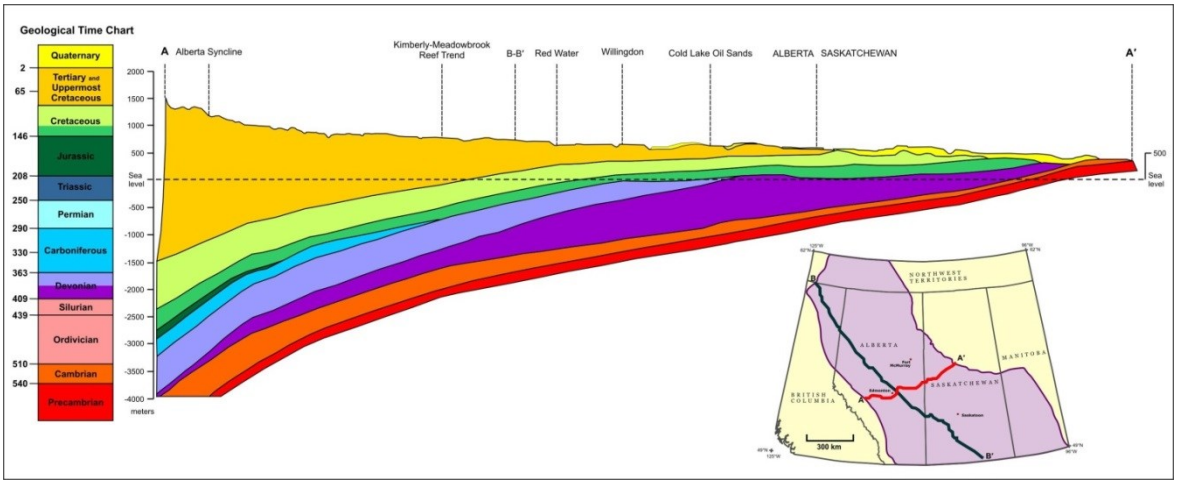

Fig. 46: Geological cross section used for the thermal model (see Fig. 47); modified from Wright et al. (1994).

River area in northwestern Alberta (total of 229 samples analyzed in a nuclear reactor facility at the University of McMaster in Ontario). First analysis and mapping of the heat generation trends across the WCSB was reported by Jones and Majorowicz (1987) who delineated three major high heat generation trends across the basement underlying the basin and concluded that these do not correlate with heat flow for the same study area (based on their heat flow data). Burwash and Burwash (1989) and Bachu and Burwash (1991) also did further analysis and mapping for Alberta and the WCSB, respectively. It has been noticed that the mean heat production for the WCSB is 2.4 $\mu W/m^3$ (Jones and Majorowicz 1987; Jessop 1992) which is more than two times higher that of the eastern Canada for the shield 1.1 $\mu W/m^3$ (Jessop 1992). This can to some extent explain the elevated high heat flow in the WCSB based on the data which was used for the heat flow map (Fig. 38b). The average heat flow for the WCSB is 60 mW/m^2, with a standard deviation of 9 mW/m^2, calculated from 74,728 determinations. If the average heat flow is calculated from the geostatistical interpolation grid presented in Fig. 38b, the result is almost the same (61 mW/m^2). This is much higher than the heat flow examined for the Precambrian shield which is closer to 42 mW/m^2 (S.D. 9 mW/m^2) (Jessop 1992). There is a difference of approx. 18–19 mW/m^2 which cannot be explained by the contribution of radiogenic elements in the sediments. It can be explained by the difference in mean heat generation between the shield and the WCSB, which differs from 1.1 $\mu W/m^3$ to 2.4 $\mu W/m^3$ respectively (Jessop 1992). If the upper high heat productive „granitic“ crust is about 15 km thick, the difference of 1.3 $\mu W/m^3$in heat generation will explain the difference of about 20 mW/m^2.

A study based on gamma spectroscopy and API gamma logs from a 2.4 km deep well in the NE Alberta part of the WCSB (Majorowicz et al. 2013) shows a large contrast in the contribution of radiogenic elements to heat production in the sedimentary succession (0.6 $\mu W/m^3$) and in the Precambrian granites of the upper crust (3.2 $\mu W/m^3$).

Temperatures in sedimentary rocks of the foreland basin can be influenced to some extent by non-conductive mechanisms, such as fluid flow. This occurs mainly through flow through porous aquifer conduits in the sedimentary succession above the westward deepening basement (Fig. 46), however, flow through faults in the basement cannot be excluded. It was shown by previous research that in these porous sedimentary rocks the calculated surface Q values are significantly different (up to 50%) from the conductive Q, depending upon the nature of the hydrogeological system and its geometry which has been changing over time (Majorowicz and Jessop 1981; Majorowicz et al. 1999). This was later questioned by Bachu and Burwash (1991) who speculated on the relation of heat flow and heat generation as the main factor controlling distribution of thermal field in the WCSB. They argued that Darcy flow rates are too small to make an impact on regional-scale heat flow. Also hydraulic heads and Darcy fluid flow rates with reducing hydrodynamic influence upon heat flow have been diminishing over time due to the erosional change in topography. In the area towards the deep basin foothills of the Rocky Mountains about 2 km of erosion has taken place since the uplift during the Laramide orogeny (Majorowicz et al. 1990).

Majorowicz et al. (1999) numerically tested the extent of hydrodynamic influence across the basin using a 2D numerical model constrained by revised thermal data. For this model a finite element mesh was generated which rebuilds the geometry of the cross section shown in Fig. 46 (model is shown in lower panel of Fig. 47). For the major fluid conduits like the Devonian carbonates or the Cambrian Basal Sandstone Unit the range of hydraulic conductivities was estimated. The Tertiary and Cretaceous shale units were assumed to have minimal permeability. Topography controls gravity driven flow patterns. Analysis shown in Fig. 47 demonstrates that Darcy velocities of 0.01 to 1 m/yr can explain only 10–15 °C/km of thermal gradient elevation, and consequently cannot alone explain observations of temperature gradients elevated 30–40 °C/km above typical values for the basin. From the thermal gradient map (Fig. 39) some reduction of gradients can be observed in high topography areas in the western part of the foreland basin, while some positive anomalies are located further east at a distance of 100 km and more, as predicted

by the simple model which was made along the cross section through the central foreland basin (Fig. 47).

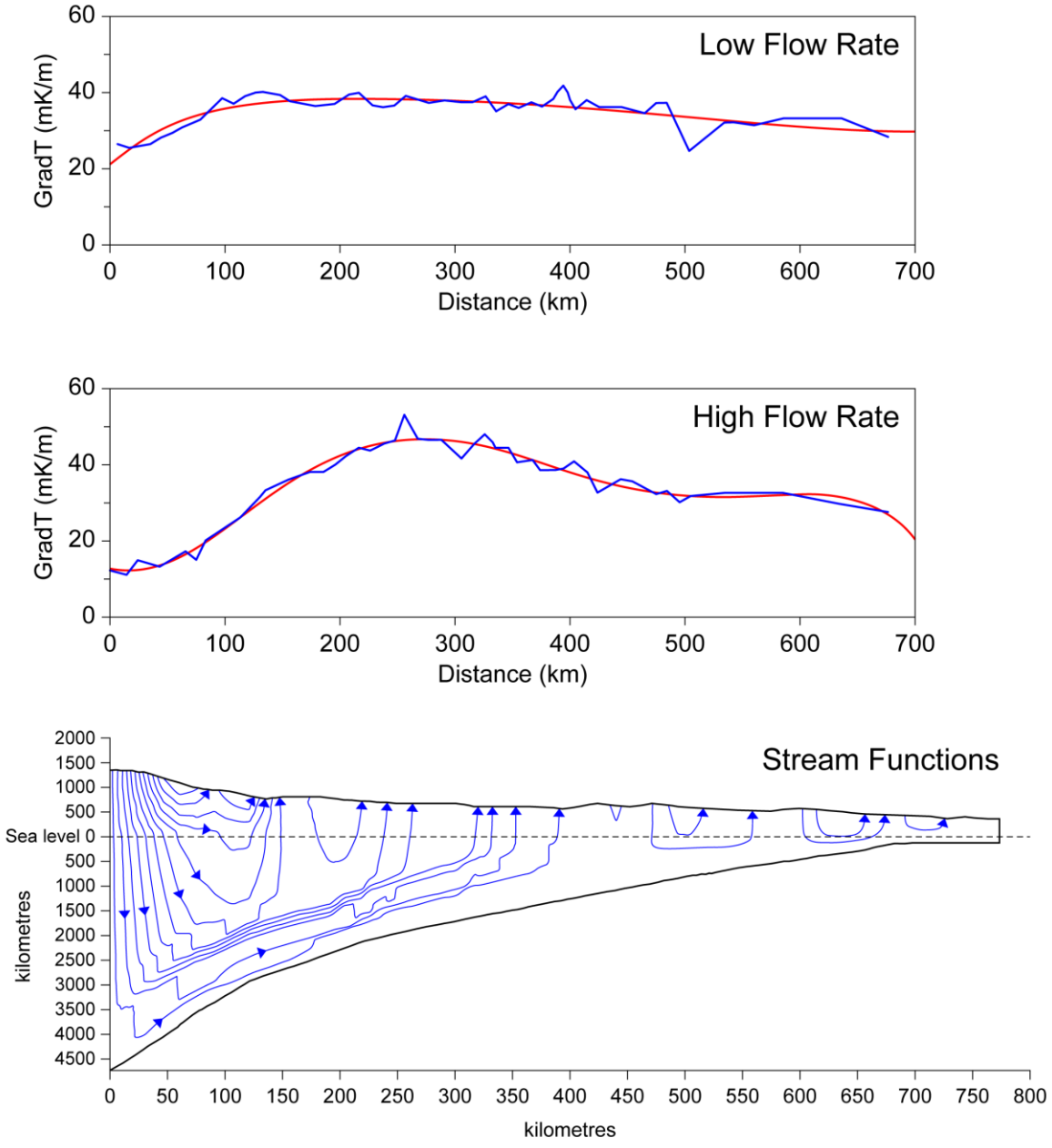

Fig. 47: Geothermal gradient across the WCSB profile from numerical modeling (Majorowicz et al. 1999) for a base heat flow of 70 mW/m^2, a thermal conductivity model of the sedimentary cover and a surface temperature constrained by 0^{o}C for two scenarios of gravity driven regional fluid flow (upper panel – low velocity of 10^{-2} m/yr and mid-panel- 10^2 m/yr. The surface temperature of 0°C was chosen because the thermal field in the deeper sediments is still in equilibrium with this temperature (Majorowicz et al. 2012). The red curve shows the smoothed thermal gradient. Assumed flow paths are shown in the lower panel; modified from Majorowicz et al. (1999).

5.2 Geothermal potential zones

Other than previous studies on the geothermal potential of deep aquifers which all focused on a scale of several 10 km to few 100 km, this paper investigates temperatures and extension of potential geothermal target formations on the scale of the whole WCSB. With help of the maps presented in this paper the best locations for geothermal energy utilization can be identified both laterally and in the rock column on the WCSB scale. However, besides temperature, an appropriate (porous and permeable) reservoir is mandatory for a successful geothermal project. Though the extension of geological formations can be mapped over large distances with manageable effort, the facies of the formations, which controls the distribution of porosity and permeability, must always be investigated on a smaller scale. It is possible to map facies or reservoir properties such as porosity on a large scale, using well logs and core analysis data for example (see Weides et al. 2013 & 2014). However, to obtain a reliable facies map for the scale of the WCSB, an enormous amount of well data would need to be collected, interpreted, classified and mapped, which is beyond the scope of this paper. Previous studies on geothermal reservoir parameters, though they are fragmented throughout the WCSB, can help to increase our knowledge on formation properties at a regional scale. Tab. 9 summarizes the major findings of these previous studies, and Fig. 39 gives the location of these studies projected on the geothermal gradient map. Tab. 9 gives information on porosity and permeability which are important properties for reservoir evaluation. However, it must be emphasized that high porosities and permeabilities do not necessarily result in high flow rates, which are crucial for the success of a geothermal well. As a result of the large scale of this study, it was not possible to estimate of flow rates from single well tests for all formations presented. Lam and Jones (1985 & 1986) calculated flow rates from DST`s for some aquifers in their geothermal exploration studies. For the Leduc Fm. in the central part of the Hinton-Edson area (area 4 in Fig. 39; for formation properties see Tab. 9) flow rates of more than 400 m^3/h are reached (Lam and Jones 1985). This value is high and can be compared to the wells at the geothermal power plants of Landau and Unterhaching in Germany, which produce at rates of 180–540 m^3/h from siliciclastic and carbonatic aquifers at a depth of 3–3.4 km (Geox GmbH 2007; Geothermie Neubrandenburg GmbH 2011).

Depending on subsurface temperature and the heat demand at the surface, different applications for using geothermal resources are possible. In Fig. 48 different geothermal potential zones are presented for the WCSB, depending on the Precambrian surface temperature, after a classification of Líndal (1973): (1) potential for warm water provision

(> 40 °C), (2) potential for domestic heating (> 70 °C), (3) marginal potential for electrical power production (> 100 °C) and (4) good potential for electrical power production (> 150 °C). For the major part of the WCSB the temperatures at depths below 1.3 km are high enough to be used for warm water provision or balneological use. Underneath the large urban areas of Edmonton and Calgary, fluid temperatures are sufficient to be used for district heating purposes. Here geothermal heat production appears as a feasible option for a green, sustainable and economic way to reduce dependency on fossil fuels and decrease greenhouse gas emissions. For the southern part of Saskatchewan, Ferguson and Grasby (2014) found that direct use of geothermal energy could be quite successful due to the high injection rates and sufficiently high temperatures.

Replacement of gas heating with geothermal systems could form part of a long range target for industrial emissions reduction. Based on the calculations from Majorowicz and Moore (2014) 1,000 heat generating systems (with 2 wells each) across Alberta drawing 100 °C from deep wells in deep sedimentary basin can save about 30 MT CO_2 per year. For a comparison, the oil sands industry generates some 34.7 MT CO_2 and other greenhouse gases (Biello 2013). 1,000 wells is a small number compared to > 300,000 oil and gas wells drilled in Alberta.

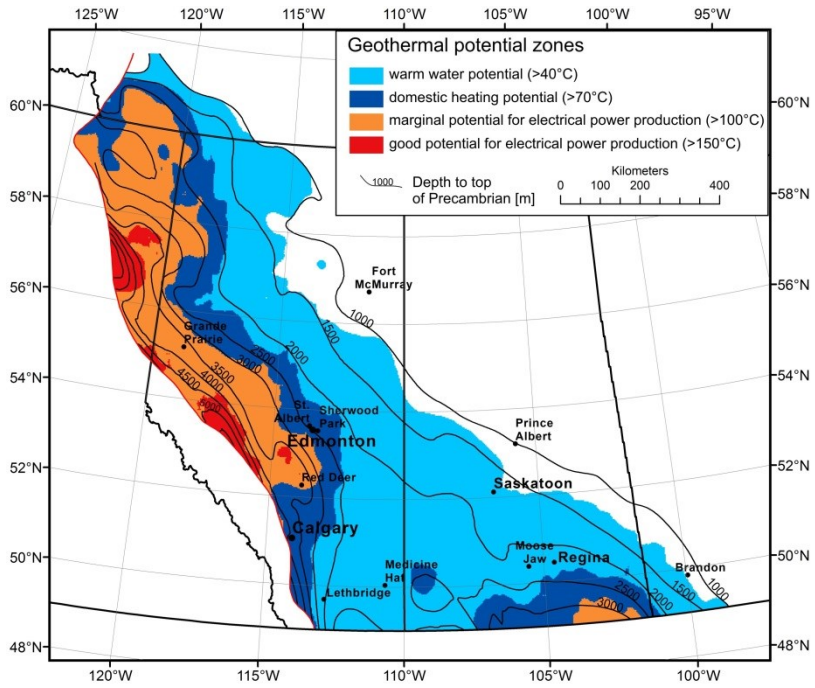

Fig. 48: Possible geothermal applications based on the temperature at the top of the Precambrian basement.

Area & basin depth	Geothermal gradient [°C/km]	Best aquifer	Lithology	Aquifer depth [km]	Thickness [m]	Porosity [%]	Permeability [mD]	Temp. [°C]	Other potential aquifers
Calgary (1) 3.4–4.2 km	23.6	Leduc	reefal carbonate, dolomitized	3.7–4.0	up to 300	-	-	87–94	BSU, Nisku, Wabamun, Elkton
Clarke Lake (2) 2.4–2.6 km	up to 50–55	Slave Point & Keg River	reefal carbonate, dolomitized	2.0–2.1	up to 200	up to 25	-	110–123	-
Edmonton (3) 1.8–3.5 km	34.6	BSU	sandstone	1.8–3.5	28–45	7–9	1- > 1000 (avg. ~1)	62–122	Cooking Lake, Leduc, Nisku, Wabamun
Hinton – Edson (4) 4–6 km	29.2	Leduc	reefal carbonate, dolomitized	3.4–5.4	up to 250	6–12	-	99–158	Slave Point, Nisku, Wabamun, Elkton, Belloy
Peace River (5) 1.7–2.3 km	33	Granite Wash Unit	sandstone	1.7–2.4	< 30	2–19	1– >200 (avg ~1–10)	50–75	Slave Point
Saskatchewan (6) 2.2 km	28.1	Basal Clastics	sandstone	0.4–3.0	50–550	11–17	100–200	40–100	-

Tab. 9: Results from previous regional geothermal studies in the WCSB; See Fig. 39 for location of the study areas; data is taken from Lam & Jones (1986) for Calgary, Walsh (2013) for Clarke Lake, Weides et al. (2013) for Edmonton, Lam & Jones (1985) for Hinton-Edson, Weides et al., (2014) for Peace River, and Jessop & Vigrass (1989) & Ferguson & Grasby (2014) for Saskatchewan.

Electrical power production from geothermal heat is generally possible in the deepest part of the basin in vicinity of the Cordillera. A suitable spot for a geothermal power plant would be the geothermal anomaly around the hamlet of Winfield, located 100 km southwest of Edmonton and in direct vicinity of the Altalink transmission line. Here temperatures above 150 °C are found in the Basal Cambrian Sandstone Unit at a depth of 3.7 km. Another good location for a geothermal power plant is found in the area near Hinton in western Alberta, where temperatures in the Leduc Fm. at a depth of 5 km are above 150 °C (Lam and Jones 1985). Marginal potential for electrical power production exists at the Clarke Lake gas field near Ft. Nelson in northeastern B.C., where temperatures above 110 °C are found in 2.1 km deep Middle Devonian porous reefal carbonates (Walsh 2013), and in southeastern Saskatchewan in the highly permeable Basal Clastics aquifer, where temperatures are around 100 °C at depth of 3 km (Ferguson and Grasby 2014).

Generally it has to be emphasized that all locations presented here as favorable for geothermal utilizations represent locations with technical geothermal potential, based on the distribution of temperatures and potentially permeable formations. However, besides temperature the critical point in the development of a geothermal project is to achieve high flow rates. Hence, in the first phase of a local scale exploration study flow rates from DST`s should be analyzed to evaluate whether a site has an economic geothermal potential. In some cases, depending on the geological and economic situation, stimulation techniques like massive waterfrac treatments or acid injection could be applied to increase permeability of the reservoir.

While exploitation of geothermal resources generally can help to significantly reduce Western Canada`s CO_2 emissions, geothermal power production could also lower the power costs for remote communities and reduce their dependency on diesel fuel transports. Electricity costs in remote areas of Canada range from 0.40–1.3 $/kWh (Arriaga et al. 2013). Compared to the feed in tariffs for electricity from geothermal power plants in Germany of 0.20–0.28 $/kWh (Einspeiseverguetung.info 2014), or to the electricity generation costs from low temperature binary developments provided by the International Energy Agency (International Energy Agency 2010), which range from 0.08–0.22 $/kWh, geothermal energy production could be economically in remote areas of Canada.

6. Conclusions

The thermal field of the WCSB is highly variable. The heat flow ranges from 30 mW/m^2 in the south to high 100 mW/m^2 in the north, while the geothermal gradient varies from as low as 20 °C/km to over 55°C/km. The controlling factors of the thermal field in WCSB are poorly understood, and a heat flow–heat generation relationship cannot be established for the entire WCSB. Convective heat transport through fluid flow across the basin can partly explain observed thermal gradient variations.

For most of the WCSB potential geothermal target formations are present at sufficient depth. Especially the deep foreland basin clastic and carbonate plays offer potential for geothermal applications. In the large urban areas of Edmonton and Calgary, fluid temperatures are in the range of 80–90 °C and could be used for district heating, warm water provision, and for industrial applications. In the deepest basin, potential for electricity production by applying EGS technology exists.

Acknowledgments

The authors would like to acknowledge the helpful reviews by three anonymous reviewers. This study is part of the Helmholtz–Alberta Initiative (HAI), which is a research collaboration between the Helmholtz Association of German Research Centres and the University of Alberta.

We would like to thank HAI, and especially theme 4 “Geothermal Energy” research coordinators Prof. Martyn Unsworth (UofA Edmonton) and Prof. Ernst Huenges (GFZ Potsdam), for enabling such a in depth study which increased our knowledge on the geothermal energy potential in the area.

We would like to thank Prof. Inga Moeck (UofA) for encouraging us to further conduct and deepen this study, which at an earlier point was presented during the “Reservoirs in foreland basin” session at the “Sedimentary Basins Jena 2013” conference in Jena, Germany.

Chapter 6

Discussion and Conclusions

1. Key findings of the thesis

The goal of this thesis was to assess the geothermal potential of Paleozoic formations in the Alberta Basin, and to delineate the spots which are favorable for the development of a first geothermal site in Alberta. To achieve this goal, two regional exploration studies were conducted: a first study in central Alberta, around the city of Edmonton, and a second study in northwestern Alberta around the town of Peace River. These two studies used preexisting well log data and core analysis data to characterize potential geothermal target formations, focusing on thickness, depth, lateral extension, and on the distribution of porosity, permeability and temperature. For the characterization of the Cambrian Basal Sandstone Unit in central Alberta additional core tests were conducted to obtain values for porosity, permeability and geomechanical parameters. In the Peace River area the stress state of faults was analyzed with the 3D structural geological modelling and conduction of the slip tendency method. The distribution of heat flow, geothermal gradient and temperature was analyzed at the large scale across the WCSB and on a smaller regional scale covering the two study areas. The key findings of the previous thesis chapters are briefly summarized in the following.

1.1 Potential geothermal target formations in Alberta

Central Alberta

In central Alberta five Paleozoic formations were identified as potentially usable for geothermal applications: The Cambrian Basal Sandstone Unit (BSU), the Devonian Cooking Lake, Leduc, and Nisku formations, and the Devonian Wabamun Group.

Due to its depth related high temperature and its extension throughout central Alberta, the BSU is the most favorable formation for further geothermal prospection in central Alberta. The unit is distributed throughout the entire study area at a depth of 1785–3490 m, and has a thickness of 28–45 m. The temperature of the BSU in the study area ranges from 65–120 °C. Beneath the Edmonton metropolitan area the BSU is located at a depth of 2.4–2.6 km and has a temperature of 79–93 °C. Porosity (measured from core samples) is between 5.3–19.6 %. A general trend of increasing porosity with decreasing depth is

identified for the BSU in central Alberta and is interpreted as typical diagenetic effect in sandstones exhibiting a linear relationship of porosity-permeability ratio versus depth (Moeck 2014). Permeability of the BSU (measured with probe permeametry) is generally low, with values less than 10×10^{-15} m^2. However, in one well a highly permeable ($> 100 \times 10^{-15}$ m^2) section was identified. Geomechanical tests showed that the BSU has relatively high unconfined compressive strength (up to 97.7 MPa), high cohesion (up to 69.8 MPa) and remarkably high values for the friction coefficient (up to 1.22), while the tensile strength is rather low (less than 5 MPa). Due to the low thickness and the relatively low matrix porosity and permeability horizontal drilling and hydraulic stimulation treatments would be required to achieve sufficient flow rates for geothermal heat production (see also results from numerical reservoir simulations from Hofmann et al. 2014).

In all four Devonian carbonate formations positive porosity- and permeability anomalies exist, with values exceeding 20 % and 100×10^{-15} m^2, respectively. In combination with the large average thickness of the units, which ranges from 60 m (Cooking Lake) to more than 300 m (Leduc), high flow rates can be expected for parts of Devonian formation. The temperature in the Devonian units ranges from 22–88 °C at a depth of 0.6–2.5 km for the whole central Alberta study area, and from 38 °C (Wabamun) to 63 °C (Cooking Lake) in the Edmonton metropolitan area.

Northwestern Alberta

In the northwestern Alberta study area the Devonian Granite Wash Unit is a potential geothermal target formation. The unit is located at a depth of 1.6–2.4 km and has a temperature ranging from 51–75 °C. The thickness of the unit is generally low, ranging from few meters to 38 m. The average porosity and permeability of the Granite Wash Unit are quite low (7.4 % porosity and less than 5×10^{-15} m^2 permeability), but positive anomalies exist in the southwestern and southeastern part of the study area. The most promising zone for geothermal applications is located in the southwestern part of the study area, where elevated porosity (10–12 %) and permeability ($1–4 \times 10^{-14}$ m^2) coincide with temperatures of more than 75 °C. Due to the low thickness of the unit, horizontal drilling would be needed to achieve economic flow rates from the Granite Wash Unit.

1.2 Stress state of faults

The stress state of faults was analyzed for the stress conditions at 2262 m depth in a Granite Wash reservoir in northwestern Alberta using an integrated approach of 3D structural geological mapping, stress ratio definition based on frictional constraints, and slip tendency analysis under consideration of existing stress magnitude data from literature. The in-situ stress state at the depth of the Granite Wash Unit is a strike-slip regime with S_{Hmax} = 1.11 S_v (±0.19 S_v) and S_{Hmin} = 0.72 S_v (±0.06 S_v). The vertical stress S_v in the reservoir depth of 2262 m is 53.8 MPa. The results from the slip tendency analysis indicate that under these stress conditions none of the interpreted faults is critically stressed. The highest slip tendency exists for the NE–SW striking faults (0.4–0.46). Faults striking in this direction also have the highest dilation tendency (0.7–0.9).

1.3 Thermal state of the Alberta Basin and temperature distribution of potential geothermal target formations in Alberta

The heat flow and thermal state of the sedimentary succession of the Western Canada Sedimentary Basin (WCSB)—of which the Alberta Basin represents the largest central part—were mapped based on a large thermal database consisting of more than 68,000 temperature values from more than 26,000 wells.

The heat flow in the Alberta Basin generally ranges from 30–90 mW/m^2, and is approximately 60 mW/m^2 on average. Generally a northerly trend of increasing heat flow exists, with the highest heat flow being found in the northwesternmost part of Alberta. Positive heat flow anomalies exist in the western central Alberta Basin (west and southwest of Edmonton), while negative heat flow anomalies are found in northeastern Alberta (south of Fort McMurray) and in southern Alberta in the area of Calgary. The distribution of the thermal gradient follows the same trend of increasing values towards the northern Alberta Basin.

The geothermal gradient in the Alberta Basin ranges from 20–55 °C/km, with an average value of about 33 °C/km.

Temperatures at the base of the Phanerozoic succession in Alberta are > 180 °C in the vicinity to the Cordillera in western Alberta. In the most urbanized area of Alberta, the Calgary-Edmonton corridor, temperatures at the base of the Phanerozoic are between 80–140 °C at a depth of 2.5–4 km. At the top of the Devonian Winterburn Group, temperatures from 51–75 °C are found in this area at a depth of 1.3–3.1 km.

1.4 Potential applications for geothermal energy in Alberta

The low (< 90 °C) to intermediate enthalpy (< 150 °C) geothermal resources of the Alberta Basin offer a good potential for different direct heat use applications (categorization from Muffler and Cataldi 1978).

In the Calgary–Edmonton corridor fluid temperatures at the base of the Phanerozoic are high enough to be used for district heating purposes. If economic flow rates can be achieved, geothermal heat production from the BSU appears as a feasible option for domestic heat provision and warm water provision in the area. Hereby fluids from overlying Devonian carbonates could be co-produced to increase the total flow rate of a geothermal well. Provision of heat for industrial applications, e.g. in the refineries of the Edmonton metropolitan area could also be an application for direct-use of geothermal resources. In the Peace River region of northwestern Alberta geothermal heat could be used to feed the large heat demand of the greenhouses farming industry.

Electrical power production from geothermal heat is generally possible if temperatures exceed 100 °C. As the efficiency of geothermal power plants is better at higher fluid temperatures, electricity production is only possible in the warmest (and deepest) part of the Alberta basin in vicinity to the Cordillera in westernmost Alberta. A good location for a geothermal power plant would be the area near Hinton in western Alberta, where temperatures in the Leduc Formation at a depth of 5 km are above 150 °C. Another favorable location is found at the western margin of the Calgary-Edmonton corridor at the geothermal anomaly around the hamlet of Winfield, located 100 km southwest of Edmonton and in direct vicinity to the Altalink transmission line, where temperatures above 150 °C are found in the BSU at a depth of 3.7 km. Geothermal power production could also be an option for remote communities in northern Alberta, which are currently dependent on expensive diesel fuel transports. Here, even electricity production from resources < 150 °C could be economically competitive.

2. How can future geothermal assessment of the Alberta Basin (and similar areas) be improved?

This assessment study benefitted from the large number of well log data and core analysis data which enabled the development of 3D geological models and the mapping of rock properties. With help of these models and maps it was possible to describe the depth, thickness and extension of potential geothermal aquifers and to investigate porosity, permeability and temperature distribution. Based on the results of these investigations it is

possible to delineate the best sites for detailed reservoir studies which could then be followed by drilling of a first geothermal well and subsequent development of a geothermal heat (or power) plant. This approach as presented in this thesis could be applied in other areas of the WCSB, or in other conduction dominated geothermal systems in the world where sufficient pre-existing data are available.

Future assessment studies in these geothermal systems would benefit from using geological well log data and results from Drill Stem Tests (DST), both of which were not available for this study. Using well logs as input data instead of or in combination with core analysis data would strengthen the analysis of porosity distribution within a formation, as well logs provide information over the whole thickness of the formation and not only at the cm-scale of the core sample. Therefore well logs account for larger scale feature such as fractures, while core tests measure matrix porosity only. Beyond this, core samples are often taken preferentially from well sections of interest to the particular study, and are not systematically sampled over the whole thickness of the formation. Well log interpretation would reduce this effect of preferential sampling. With well logs as input parameters the distribution of porosity could also be easier mapped in 3D, which would allow for better identification of vertical and lateral facies changes within a formation. DST`s could be used to investigate flow rates, which could subsequently be compared to the porosity and permeability values. High flow rates are crucial for the success of a geothermal well, and while analyzing porosity and permeability of formations is a relatively good method to delineate favorable locations for a geothermal well, it must be emphasized that high porosities and permeabilities do not necessarily result in high flow rates.

Conduction-dominated geothermal play types such as the Alberta Basin can in most cases only be developed using engineered geothermal systems (EGS), which requires knowledge of geomechanical parameters of the reservoir rock and the in-situ stress field (Moeck and Beardsmore 2014). Investigation of these parameters (and subsequent hydraulic reservoir modeling; see also Hofmann et al. 2014) as it was conducted for the BSU in central Alberta is an important part of a geothermal assessment study in any conduction-dominated geothermal system.

Knowledge of faults and on their stress state (as investigated in the Peace River area) is also an important part of a geothermal assessment study in conduction-dominated geothermal systems for two main reasons. On the one hand it is important to account for possible movement on fault planes and related seismicity that can occur when the in-situ

stress field is changed due to production or injection of fluids during geothermal heat production. On the other hand faults can also play an important role as fluid conduit (or barrier) during geothermal production (Moeck and Beardsmore 2014), and can therefore be preferential targets for a geothermal well (as for example in parts of the German Molasse Basin). For the Alberta Basin the influence of faults on the fluid flow has not been investigated as part of this study and remains an important open question for future geothermal assessment.

3. Future steps for a geothermal development in Alberta

Depending on the desired end-use a suitable location for a first geothermal development can be determined using the results of this study (see 1.4 this chapter for potential locations in Alberta). For this site, a small scale (5 km × 5 km) structural geological model of the reservoir should be developed based on 3D seismic data and pre-existing well log data. The distribution of porosity, permeability and temperature should be mapped, and the stress state of faults in the recent stress field should be analyzed to identify faults with high slip- and dilation tendency. With numerical reservoir simulations the perfect combination of well path design and hydraulic stimulation scenario for this site can then be identified. The reservoir model should continuously be updated with parameters from core testing and well logging after the first well has been drilled into the reservoir.

Alberta has a long tradition of hydrocarbon production with more than 300,000 wells drilled until today. Many of these wells penetrate the oil and gas reservoirs of the Upper Devonian carbonates of the Wabamun Group, and Nisku and Leduc formations, which were identified a potential geothermal target formations in this study. With regard to the large number of wells it would be worthwhile to investigate whether it is possible to use some of the „old“ wells from depleted oil- or gas reservoirs to produce geothermal heat.

Beyond this, the utilization of supercritical CO_2 as transport fluid might be an option to increase the efficiency of geothermal heat production from the low temperature and relatively low permeable reservoirs of Alberta. CO_2 is anticipated to be a better geothermal fluid than water with an average heat extraction rate 50% greater than that of water (Eastman and Muir 2013). With this concept, which until today has only been applied in demonstration projects, the geothermal reservoirs of Alberta could be used for both geothermal heat production and CO_2 sequestration. A combined use of CO_2 sequestration and geothermal production could reduce Alberta`s rapidly growing CO_2 emissions and lower the dependency of fossil fuel based energy sources and the related environmental

problems that exist in the province. The BSU reservoirs northeast of Edmonton, which are already used for underground CO_2 sequestration (Shell 2010a, 2011) would be an optimal site for the worldwide first combined commercial CO_2-EGS and CO_2-sequestration operation.

References

Agosta, F., Prasad, M., and Aydin, A. 2007. Physical properties of carbonate fault rocks, fucino basin (Central Italy): implications for fault seal in platform carbonates. Geofluids 7(1): 19-32.

Ahr, W.M. 2008. Geology of carbonate reservoirs. Wiley Online Library.

Airwaterland. 2007. Oilsands Consortium Examining Geothermal Energy. Available from http://www.airwaterland.ca/article.asp?id=1717 [accessed 09 May 2014].

Aitken, J.D. 1968. Cambrian sections in the easternmost southern Rocky Mountains and the adjacent subsurface, Alberta. Geological Survey of Canada, Dept. of Energy, Mines and Resources, Ottawa.

Amthor, J.E., Mountjoy, E.W., and Machel, H.G. 1994. Regional-scale porosity and permeability variations in Upper Devonian Leduc buildups: implications for reservoir development and prediction in carbonates. AAPG Bulletin-American Association of Petroleum Geologists 78(10): 1541-1559.

Andrichuk, J.M. 1958a. Cooking Lake and Duvernay (Late Devonian) sedimentation in Edmonton area of central Alberta, Canada. AAPG Bulletin-American Association of Petroleum Geologists 42: 2189-2222.

Andrichuk, J.M. 1958b. Stratigraphy and facies analysis of Upper Devonian reefs in Leduc, Stettler, and Redwater areas, Alberta. AAPG Bulletin-American Association of Petroleum Geologists 42(1): 1-93.

Anon, Q. 1977. The description of rock masses for engineering purposes. QJ Eng Geol 10: 355-388.

Arriaga, M., Cañizares, C.A., and Kazerani, M. 2013. Renewable energy alternatives for remote communities in Northern Ontario, Canada. IEEE Transactions on sustainable energy 4(3): 661-670.

Axelsson, G., and Gunnlaugsson, E. 2000. Background: Geothermal utilization, management and monitoring, in *Long-term monitoring of high-and low enthalpy fields under exploitation*. World Geothermal Congress 2000 Short Course, Japan,: 3-10.

Aydin, A. 2000. Fractures, faults, and hydrocarbon entrapment, migration and flow. Marine and Petroleum Geology 17(7): 797-814.

Bachu, S. 1993. Basement heat flow in the Western Canada sedimentary basin. Tectonophysics 222(1): 119-133.

Bachu, S. 1995. Synthesis and model of formation-water flow, Alberta Basin, Canada. AAPG Bulletin-American Association of Petroleum Geologists 79(8): 1159-1178.

Bachu, S., and Burwash, R.A. 1991. Regional-scale analysis of the geothermal regime in the Western Canada Sedimentary Basin. Geothermics 20(5): 387-407.

Bachu S., and Burwash, R. 1994. Geothermal regime in the Western Canada sedimentary basin. *In* Geological Atlas of the Western Canada Sedimentary Basin. *Edited by* G. Mossop and I. Shetsen. Canadian Society of Petroleum Geologists and Alberta Research Council, Special Report 4: 447-454.

Bachu, S., and Underschultz, J.R. 1992. Regional-scale porosity and permeability variations, Peace River Arch area, Alberta, Canada. AAPG Bulletin-American Association of Petroleum Geologists 76(4): 547-562.

Bachu, S., Brydie, J., Hauck, T., Lakeman, B., Palombi, D., Stoakes, F., Wendte, J., Lawton, D., Darvish, M.P., Hawkes, C., Chalaturnyk, R., Krawec, T., and Sawchuk, W. 2011. The Heartland Area Redwater CO2 storage project (HARP): Results of Phase I site characterization. Energy Proced 4: 4559-4566. doi: DOI 10.1016/j.egypro.2011.02.414.

Balshaw K.E. 2010. Sedimentology and stratigraphy of the Granite Wash: Contact Rapids and Keg River Sandstone (Red Earth Area). *MSc. thesis*. University of Alberta, Edmonton, Alberta, Canada.

Barclay, J.E., Hamblin, A.P., Lee, P.J., Podruski, J.A., and Taylor, G.C. 1985. Oil Resources of Western Canada Part I: Devonian and Pre-Devonian. Geological Survey of Canada, Panel Report 85-01.

Barclay, J.E., Krause, F., Campbell, R., and Utting, J. 1990. Dynamic casting and growth faulting: Dawson Creek graben complex, Carboniferous-Permian Peace River embayment, western Canada. Bulletin of canadian petroleum geology 38(1):115-145.

Barton, C.A., Zoback, M.D., and Moos, D. 1995. Fluid flow along potentially active faults in crystalline rock. Geology 23(8):683-686.

Beach, R., Jones, F., and Majorowicz, J. 1987. Heat flow and heat generation estimates for the Churchill basement of the Western Canadian Basin in Alberta, Canada. Geothermics 16(1): 1-16.

Bell, J., and Grasby, S. 2012. The stress regime of the Western Canadian Sedimentary Basin. Geofluids 12(2): 150-165.

Bell, J., and Weis, T. 2009. Greening the Grid: Powering Alberta's Future with Renewable Energy. Pembina Institute for Appropriate Development, Canada.

Bell, J., Price, P., and McLellan, P. 1994. In-situ stress in the western Canada Sedimentary Basin. *In* Geological Atlas of the Western Canada Sedimentary Basin. *Edited by* G. Mossop and I. Shetsen. Canadian Society of Petroleum Geologists and Alberta Research Council, Special Report 4: 439-446.

Benderitter, Y., and Cormy, G. 1990. Possible approach to geothermal research and relative costs. Small Geothermal Resources: A Guide to Development and Utilization, UNITAR, New York: 59-69.

Benfield, A. 1939. Terrestrial heat flow in Great Britain. Proceedings of the Royal Society of London. Series A. Mathematical and Physical Sciences 173(955): 428-450.

Bertini, G., Casini, M., Gianelli, G., and Pandeli, E. 2006. Geological structure of a long-living geothermal system, Larderello, Italy. Terra Nova 18(3): 163-169.

Biello, D. 2013. How much will tar sands oil add to global warming? Scientific American (January issue 2013).

Birner, J., Fritzer, T., Jodocy, M., Schneider, M., and Stober, I. 2009. Molassebecken. Aufbau eines geothermischen Informationssystems für Deutschland–Endbericht. R. Schulz [Hrsg.]–LIAG–Bericht, Archiv (0128452).

Blackwell, D., and Richards, M. 2004. Geothermal Map of North America: American Association of Petroleum Geologists. Tulsa, Oklahoma, scale (1:6,500,000).

Blackwell, D., Negraru, P., and Richards, M. 2006. Assessment of the enhanced geothermal system resource base of the United States. Natural Resources Research 15(4): 283-308.

Brahim, F.B., Makni, J., and Bouri, S. 2013. Properties of geothermal resources in Kebilli region, Southwestern Tunisia. Environmental Earth Sciences 69(3): 885-897.

Burwash, R., and Burwash, R. 1989. A radioactive heat generation map for the subsurface Precambrian of Alberta. Geological Survey of Canada, Paper 89: 363-368.

Burwash, R., McGregor, C., and Wilson, J. 1994. Precambrian basement beneath the Western Canada sedimentary basin. *In* Geological Atlas of the Western Canada Sedimentary Basin. *Edited by* G. Mossop and I. Shetsen. Canadian Society of Petroleum Geologists and Alberta Research Council, Special Report 4: 49-56.

Byerlee, J. 1978. Friction of rocks. Pure and applied Geophysics 116(4-5): 615-626.

Cant, D.J. 1988. Regional structure and development of the Peace River Arch, Alberta: a Paleozoic failed-rift system? Bulletin of canadian petroleum geology 36 (3): 284-295.

Chang, C. 1988. Measuring density and porosity of grain kernels using a gas pycnometer. Cereal Chem 65(1): 13-15.

Coskun, S.B., Addison, G.D., and Hein, F.J. 1995. Thin Section Image Analyis of the Cambrian Basal Sandstone, East Central Alberta. In LITHOPROBE Alberta Basement Transects #47 Report Transect Workshop April 10-11, 1995. pp. 113-164.

Cushman, J.H. 1984. On unifying the concepts of scale, instrumentation, and stochastics in the development of multiphase transport theory. Water Resources Research 20(11): 1668-1676.

Dagan, G. 1989. Flow and transport in porous formations. Springer-Verlag New York.

David, M. 1977. Geostatistical ore reserve estimation, Elsevier Scientific Publishing Company, New York.

Dec, T., Hein, F.J., and Trotter, R.J. 1996. Granite wash alluvial fans, fan-deltas and tidal environments, northwestern Alberta: implications for controls on distribution of Devonian clastic wedges associated with the Peace River Arch. Bulletin of canadian petroleum geology 44(3): 541-565.

Dembicki, E.A., and Machel, H.G. 1996. Recognition and delineation of paleokarst zones by the use of wireline logs in the bitumen-saturated Upper Devonian Grosmont Formation of northeastern Alberta, Canada. AAPG Bulletin-American Association of Petroleum Geologists 80(5): 695-712.

Deutsch, C.V., and Journel, A.G. 1998. GSLIB: Geostatistical software library and user's guide Oxford university press New York. pp. 340.

Dictionary.com. Available from http://dictionary.reference.com/browse/assess [accessed 20 November 2013].

DiPippo, R. 2012. Geothermal power plants: principles, applications, case studies and environmental impact. Butterworth-Heinemann, Oxford.

Dixon, J. 2008. Stratigraphy and facies of Cambrian to Lower Ordovician strata in Saskatchewan. Bulletin of canadian petroleum geology 56(2): 93-117.

Dynamic Graphics Inc. 2009. EarthVision 8.1 User´s Guide. Dynamic Graphics, Alameda, CA.

Eastman, A., and Muir, M. 2013. CO2 EGS and the utilization of highly pressured CO2 for purposes other than power generation. *In* Transactions of the Thirty-Eighth Workshop on Geothermal Reservoir Engineering Stanford University, Stanford, California, February 11-13, 2013.

Eaton, D.W., Ross, G.M., and Hope, J. 1999. The rise and fall of a cratonic arch: A regional seismic perspective on the Peace River Arch, Alberta. Bulletin of canadian petroleum geology 47(4):346-361.

Einspeiseverguetung.info. 2014. Einspeiseverguetung Geothermie. Available from http://www.einspeisevergütung.info/?page_id=41 [accessed 26 March 2014].

Energy Resources Conservation Board 2009. Table of Formations, Alberta; Energy Resources Conservation Board, Calgary, Alberta, Canada.

Environment Canada. 2011. National Inventory Report 1990-2009: Executive Summary http://www.ec.gc.ca/ges-ghg/default.asp?lang=En&n=72E6D4E2-1 [accessed 4 July 2012].

Ferguson, G., and Grasby, S.E. 2014. The geothermal potential of the basal clastics of Saskatchewan, Canada. Hydrogeol. J., 22: 143–150.

Ferrill, D.A., and Morris, A. 2003. Dilational Normal Faults. Journal of Structural Geology 25(2): 183-196.

Fjar, E., Holt, R.M., Raaen, A., Risnes, R., and Horsrud, P. 2008. Petroleum related rock mechanics. Elsevier, Amsterdam.

Folk, R.L., and Ward, W.C. 1957. Brazos River bar; a study in the significance of grain size parameters. J Sediment Res 27:3–26.

Fridleifsson, I.B. 1998. Direct use of geothermal energy around the world. GHC Bulletin. December 1988: 4-9.

Gando , A., Gando , Y., Ichimura, K., Ikeda, H., Inoue, K., Kibe, Y., Kishimoto, Y., Koga, M., Minekawa, Y., Mitsui, T., Morikawa, T., Nagai, N., Nakajima, K., Nakamura, K., Narita, K., Shimizu, I., Shimizu, Y., Shirai, J., Suekane, F., Suzuki, A., Takahashi, H., Takahashi, N., Takemoto, Y., Tamae, K., Watanabe, H., Xu, B., Yabumoto, H., Yoshida, H., Yoshida, S., Enomoto, S., Kozlov, A., Murayama, H., Grant, C., Keefer, G., Piepke, A., Banks, T., Bloxham, T., Detwiler, J., S., F., Fujikawa, B., Han, K., Kadel, R., O'Donnell, T., Steiner, H., Dwyer, D., McKeown, R., C., Z., Berger, B., Lane, C., Maricic, J., Miletic, T., Batygov, M., Learned, J., Matsuno, S., Sakai, M., Horton-Smith, G., Downum, K., Gratta, G., Tolich, K., Efremenko, Y., Perevozchikov, O., Karwowski, H., Markoff, D., Tornow, W., Heeger, K., and Decowski, M. 2011. Partial radiogenic heat model for Earth revealed by geoneutrino measurements. Nature Geoscience 4(9): 647-651.

Garland, G., and Lennox, D. 1962. Heat flow in western Canada. Geophys. J. Int. 6, 245–262.

Geothermie Neubrandenburg GmbH. 2011. Größtes geothermisches Kraftwerk in Süddeutschland: Wärmegeführtes Kalina-Kraftwerk in Unterhaching. Available from http://www.gtn-online.de/Projekte/TiefeGeothermie/Projektbeispiel/grotesgeothermischeskraftwerkinsuddeutschland [accessed 26 March 2014].

Geothermie Unterhaching. 2014. Geothermieprojekt Unterhaching. Available from https://www.geothermie-unterhaching.de/cms/geothermie/web.nsf/id/pa_daten_fakten.htm. [accessed 17 April 2014].

Geox GmbH. 2014. Geothermische Stromerzeugung in Landau. Available from: http://www.geox-gmbh.de/media/Downloadbereich/projekt_1407internet-x.pdf [accessed 17 April 2014].

Gosnold, W., Majorowicz, J., Klenner, R., and Hauk, S. 2011. Implications of Post-Glacial Warming for Northern Hemisphere Heat Flow. GRC Transactions, 35, 795-800.

Government of Alberta. 2011. Alberta Environment: Report on 2009 Greenhouse Gas Emissions. 27., Edmonton, Alberta.

Government of Canada. 2010. Basal Cambrian saline formation CO2 storage project. Available from http://www.climatechange.gc.ca/dialogue/default.asp?lang=En&n=774E76B0-1&offset=1&toc=show [accessed 10 April 2014].

Graham, B., Girbecca, R., Mesonjesi, A., and Aydin, A. 2005. Evolution of fluid pathways through fracture controlled faults in carbonates of the Albenides fold-and-thrust belt. AAPG Bulletin-American Association of Petroleum Geologists 90(8): 1227-1249.

Grasby, S., Majorowicz, J., and Ko, M. 2009. Geothermal maps of Canada. Geological Survey of Canada, Open File 6167:35.

Grasby, S.E., Allen, D.M., Chen, Z., Ferguson, G., Jessop, A., Kelman, M., Majorowicz, J., Moore, M., Raymond, J., and Therrien, R. 2011. Geothermal energy resource potential of Canada. Geological Survey of Canada, Calgary, Canada.

Gray, D.A., Majorowicz, J., and Unsworth, M. 2012. Investigation of the geothermal state of sedimentary basins using oil industry thermal data: case study from Northern Alberta exhibiting the need to systematically remove biased data. Journal of Geophysics and Engineering 9(5): 534-548. doi: 10.1088/1742-2132/9/5/534.

Gudmundsson, A., Fjeldskaar, I., and Brenner, S.L. 2002. Propagation pathways and fluid transport of hydrofractures in jointed and layered rocks in geothermal fields. Journal of Volcanology and Geothermal Research 116(3): 257-278.

Haenel, R., Rybach, L., and Stegena, L. 1988. Fundamentals of geothermics. *In* Handbook of terrestrial heat-flow density determination. Springer. pp. 9-57.

Halbertsma, H. 1994. Devonian Wabamun Group of the western Canada sedimentary basin. *In* Geological Atlas of the Western Canada Sedimentary Basin. *Edited by* G. Mossop and I. Shetsen. Canadian Society of Petroleum Geologists and Alberta Research Council, Special Report 4: 203-220.

Halvorsen, C., and Hurst, A. 1990. Principles, practice and applications of laboratory minipermeametry. *In* Advances in Core Evaluation: Accuracy and Precision in Reserves Estimation. *Edited by* P. F. Worthington: Gordon and Breach, London, pp. 521-549.

Harrison, W., Luza, K., Prater, M., and Chueng, P. 1983. Geothermal resource assessment of Oklahoma, Oklahoma Geological Survey Special Publication SP 83-1, Oklahoma.

Hauck, T., Peterson, J., Melnik, A., and Bachu, S. 2012. Geology and Hydrogeology of the Basal Aquifer in the Prairie Region of Canada: Characterization for CO2 Storage. *In* 2012 CSPG CSEG CWLS Conference GeoConvention 2012: Vision, Calgary, Canada.

Hayes, B., Christopher, J., Rosenthal, L., Los, G., McKercher, B., Minken, D., Tremblay, Y., Fennell, J., and Smith, D. 1994. Cretaceous Mannville Group of the Western Canada Sedimentary Basin. *In* Geological Atlas of the Western Canada Sedimentary Basin. *Edited by* G. Mossop and I. Shetsen. Canadian Society of Petroleum Geologists and Alberta Research Council, Special Report 4: 317-334.

Hebben, T. 2009. Analysis of water quality trends for the long-term river network: Athabasca River, 1960-2007. Alberta Environment, Edmonton, Alberta.

Heidbach, O., Tingay, M., Barth, A., Reinecker, J., Kurfeß, D., and Müller, B. 2008. The World Stress Map database release 2008 doi:10.1594/GFZ.WSM.Rel2008.

Helms, L. 2008. Horizontal drilling. North Dakota Department of Mineral Resources Newsletter, vol. 35(1): 1–3.

Hochstein, M.P. 1988. Assessment and modelling of geothermal reservoirs (small utilization schemes). Geothermics 17(1): 15-49.

Hofmann, H., Weides, S., Babadagli, T., Zimmermann, G., Moeck, I., Majorowicz, J., and Unsworth, M., 2014. Potential for Enhanced Geothermal Systems in Alberta, Canada. Energy. First published online. Available from http://dx.doi.org/10.1016/j.energy.2014.03.053 [accessed 24 April 2014].

Hope, J., Eaton, D.W., and Ross, G.M. 1999. Lithoprobe seismic transect of the Alberta Basin: Compilation and overview. Bulletin of canadian petroleum geology 47(4): 331-345.

Huang, X., Bandilla, K., Celia, M., Bachu, S., Rebscher, D., Zhou, Q., and Birkholzer, J. 2012. Modeling carbon dioxide storage in the Basal Aquifer of Canada. *In* AGU fall meeting, San Francisco, USA, H23A-1322.

Huenges, E. 2010. Geothermal Energy Systems: Exploration, Development, and Utilization. Wiley-VCH, Weinheim.

Huenges, E., Kohl, T., Kolditz, O., Bremer, J., Scheck-Wenderoth, M., and Vienken, T. 2013. Geothermal energy systems: research perspective for domestic energy provision. Environmental Earth Sciences 70(8):3927-3933.

IEA. 2013. IEA Geothermal annual report. http://iea-gia.org/wp-content/uploads/2013/10/2011-GIA-Annual-Report-Final-4Oct13.pdf. [accessed 24 April 2014].

IHS Energy 2012. IHS Accumap. Commercial database IHS Energy, Englewood, CO.

International Energy Agency. 2010. Renewable Energy Essentials: Geothermal. Available from https://www.iea.org/publications/freepublications/publication/Geothermal_Essentials.pdf [accessed 26 March 2014].

IPCC. 2006. IPCC guidelines for national greenhouse gas inventories, Prepared by the National Greenhouse Gas Inventories Programme, Eggleston H.S., Buendia L., Miwa K., Ngara T. and Tanabe K. (eds). Published: IGES, Japan.

IPCC. 2011. IPCC Special Report on Renewable Energy Sources and Climate Change Mitigation. *Prepared by* Working Group III of the Intergovernmental Panel on Climate Change [O. Edenhofer, R. Pichs-Madruga, Y. Sokona, K. Seyboth, P. Matschoss, S. Kadner, T. Zwickel, P. Eickemeier, G. Hansen, S. Schlömer, C. von Stechow (eds)]. Cambridge University Press, Cambridge, United Kingdom and New York, NY, USA.

Isaaks, E., and Srivastava, R. 1989. An introduction to applied geostatistics: Oxford Univ. Press, New York.

ITG. 2014. Geothermieprojekt Waren (Müritz). Available from http://www.tiefegeothermie.de/projekte/waren-mueritz [accessed 29 April 2014].

Ito, T., and Zoback, M.D. 2000. Fracture permeability and in situ stress to 7 km depth in the KTB scientific drillhole. Geophysical Research Letters 27(7):1045-1048.

Jaeger, J., Cook, N., and Zimmerman, R. 2007. Fundamentals of Rock Mechanics. Wiley-Blackwell, Oxford.

Jerram, D.A. 2001. Visual comparators for degree of grain-size sorting in two and three-dimensions. Computers & geosciences 27(4): 485-492. doi: 10.1016/S0098-3004(00)00077-7.

Jessop, A.M. 1990. Thermal geophysics. Elsevier Amsterdam.

Jessop, A.M. 1992. Thermal input from the basement of the Western Canada Sedimentary Basin. Bulletin of canadian petroleum geology 40(3): 198-206.

Jessop, A. 2008. Geological Survey of Canada, Open File 5906. Natural Resources Canada, Ottawa, Canada.

Jessop, A.M., and Vigrass, L.W. 1989. Geothermal measurements in a deep well at Regina, Saskatchewan. Journal of Volcanology and Geothermal Research 37(2): 151-166.

Jessop A., Lewis T., Judge A., Taylor A., and Drury M. 1984. Terrestrial heat flow in Canada. Tectonophysics 103(1): 239-261.

Jessop, A.M., Allen, V., Bentkowski, W., Burgess, M., Drury, M., Judge, A.S., Lewis, T., Majorowicz, J., Mareschal, J., and Taylor, A. 2005. The Canadian geothermal data compilation. Geological Survey of Canada, Open File 4887.

Johnson, R.B., and DeGraff, J.V. 1988. Principles of engineering geology. Wiley, New York.

Jones, F., and Majorowicz, J. 1987. Regional trends in radiogenic heat generation in the Precambrian basement of the Western Canadian Basin. Geophysical Research Letters 14(3): 268-271.

Jones, F., Lam, H.-L., and Majorowicz, J. 1985. Temperature distributions at the Paleozoic and Precambrian surfaces and their implications for geothermal energy recovery in Alberta. Canadian Journal of Earth Sciences 22(12): 1774-1780.

Kaiser, P., Mackay, C., and Morgenstern, N. 1982. Performance of a shaft in weak rock (Bearpa W Shale). In: Wittke W (ed) Rock Mechanics: Caverns and Pressure Shafts: ISRM Symposium. Proceedings, Aachen, pp 613-626.

Ko, J., and Donahue, W.F. 2011. Drilling Down - Groundwater risks imposed by in situ oil sands development. Water Matters Society of Alberta: 32.

Kohl, T., Signorelli, S., Engelhardt, I., Berthoud, N.A., Sellami, S., and Rybach, L. 2005. Development of a regional geothermal resource atlas. Journal of Geophysics and Engineering 2(4): 372.

Kry, P., and Gronseth, J. 1983. In situ stresses and hydraulic fracturing in the Deep Basin. Journal of Canadian Petroleum Technology 22(6): 31-35.

Lachenbruch, A.H., and Brewer, M.C. 1959. Dissipation of the temperature effect of drilling a well in Arctic Alaska. US Geol. Surv. Bull. 1083: 73-109.

Lam, H., and Jones, F. 1984. Geothermal gradients of Alberta in western Canada. Geothermics 13(3): 181-192.

Lam, H.-L., and Jones, F. 1985. Geothermal energy potential in the Hinton-Edson area of west-central Alberta. Canadian Journal of Earth Sciences 22(3): 369-383.

Lam, H., and Jones, F. 1986. An investigation of the potential for geothermal energy recovery in the Calgary area in southern Alberta, Canada, using petroleum exploration data. Geophysics 51(8): 1661-1670.

Laplaige, P., Jaudin, F., Desplan, A., and Demange, J. 2000. The French geothermal experience review and perspectives. *In* Proceedings World Geothermal Congress, Kyushu - Tohoku, Japan. pp. 283-295.

Lee, Y., Park, S., Kim, J., Kim, H., and Koo, M. 2010. Geothermal resource assessment in Korea. Renewable and Sustainable Energy Reviews 14(8): 2392-2400.

Levorsen, A. 1967. Geology of petroleum. WH Freeman, New York.

Li, D.Y., and Wong, L.N.Y. 2013. The Brazilian Disc Test for Rock Mechanics Applications: Review and New Insights. Rock Mechanics and Rock Engineering 46(2): 269-287. doi: 10.1007/s00603-012-0257-7.

Líndal, B. 1973. Industrial and other applications of geothermal energy:(except power production and district heating). *In* Geothermal Energy: Review of Research and Development. UNESCO, Paris. pp. 135-148.

Lopez, S., Hamm, V., Le Brun, M., Schaper, L., Boissier, F., Cotiche, C., and Giuglaris, E. 2010. 40 years of Dogger aquifer management in Ile-de-France, Paris Basin, France. Geothermics 39(4): 339-356.

Lund, J.W. 2010. Direct utilization of geothermal energy. Energies 3(8): 1443-1471.

Lund, J.W., Bloomquist, R.G., Boyd, T.L., and Renner, J. 2005. The United States of America Country Update. *In* Geothermal and Mineral Recources of Modern Volcanism Areas (Proceedings of the International Kuril-Kamchatka Field Workshop). pp. 25-50.

Lund, J.W., Freeston, D.H., and Boyd, T.L. 2011. Direct utilization of geothermal energy 2010 worldwide review. Geothermics 40(3): 159-180.

Machel, H.G. 2004. Concepts and models of dolomitization: a critical reappraisal. The geometry and petrogenesis of dolomite hydrocarbon reservoirs: Geological Society (London) Special Publication 235: 7-63.

Majorowicz, J.A. 1996. Anomalous heat flow regime in the western margin of the North American craton, Canada. Journal of geodynamics 21(2): 123-140.

Majorowicz, J., and Grasby, S.E. 2010a. Heat flow, depth–temperature variations and stored thermal energy for enhanced geothermal systems in Canada. Journal of Geophysics and Engineering 7(3): 232-241.

Majorowicz, J., and Grasby, S.E. 2010b. High potential regions for enhanced geothermal systems in Canada. Natural resources research 19(3): 177-188.

Majorowicz, J., and Jessop, A. 1981. Regional heat flow patterns in the western Canadian sedimentary basin. Tectonophysics 74(3): 209-238.

Majorowicz, J., and Moore, M.C. 2008. Enhanced Geothermal Systems (EGS) Potential in the Alberta Basin. University of Calgary, Institute for Sustainability, Energy, Environment and Economy, Calgary, Alberta.

Majorowicz, J., and Moore, M. 2014. The feasibility and potential of geothermal heat in the deep Alberta foreland basin-Canada for CO2 savings. Renewable Energy 66: 541-549.

Majorowicz, J., Jones, F., Lam, H., and Jessop, A. 1985. Terrestrial heat flow and geothermal gradients in relation to hydrodynamics in the Alberta Basin, Canada. Journal of geodynamics 4(1): 265-283.

Majorowicz, J., Jones, F., Ertman, M., Osadetz, K., and Stasiuk, L. 1990. Relationship between thermal maturation gradients, geothermal gradients and estimates of the thickness of the eroded foreland section, southern Alberta Plains, Canada. Marine and Petroleum Geology 7(2): 138-152.

Majorowicz, J. A., Garven, G., Jessop, A. and Jessop, C. 1999. Present heat flow along a profile across the Western Canada Sedimentary Basin: the extent of hydrodynamic influence. *In* Geothermics in Basin Analysis. *Edited by* A. Foerster and D. F. Merriam. Kluwer Acad., Norwell, Mass. pp. 61-80.

Majorowicz, J., Gosnold, W., Gray, A., Safanda, J., Klenner, R., and Unsworth, M. 2012. Implications of Post-Glacial Warming for Northern Alberta heat flow- correcting for the underestimate of the geothermal potential. *In* GRC Transactions 36: 693-698.

Majorowicz, J., Unsworth, M., Chacko, T., Gray, A., Heaman, L., Potter, D., and Schmitt, D. 2013. Geothermal energy as a source of heat for oil sands processing in northern Alberta, Canada. *In* Heavy Oil/Bitumen Petroleum Systems in Alberta and beyond. *Edited by* F.J. Hein and D.A. Leckie and J. Suter and S. Larter. AAPG Studies in Geology. pp. 725-746.

Majorowicz, J., Chan, J., Crowell, J., Gosnold, W., Heaman, L. M., Kück, J., Nieuwenhuis, G., Schmitt, D. R., Unsworth, M., Walsh, N. and Weides, S. 2014. The first deep heat flow determination in crystalline basement rocks beneath the Western Canadian Sedimentary Basin, Geophysical Journal International 197(2): 731-749. doi: 10.1093/gji/ggu065.

Marfil, R., Scherer, M., and Turrero, M.J. 1996. Diagenetic processes influencing porosity in sandstones from the Triassic Buntsandstein of the Iberian Range, Spain. Sedimentary Geology 105(3): 203-219.

Mathiesen, A., Kristensen, L., Nielsen, C., Weibel, R., Hjuler, M., Rogen, B., Mahler, A., and Nielsen, L. 2013. Assessment of sedimentary geothermal aquifer parameters in Denmark with focus on transmissivity. *In* European Geothermal Congress 3-7 June 2013. Pisa, Italy, pp 1-9.

Mei, S. 2006. Structures and Faults in the Peace River Arch Region, Alberta, 2006 (GIS Data, line features). Energy Resources Conservation Board. http://www.ags.gov.ab.ca/publications/abstracts/DIG_2007_0011.html. Accessed 28 March 2014

Mei, S. 2009a. Geologist-controlled trends versus computer-controlled trends: introducing a high-resolution approach to subsurface structural mapping using well-log data, trend surface analysis, and geospatial analysis. Canadian Journal of Earth Sciences 46(5):309-329.

Mei, S. 2009b. New insights on faults in the Peace River Arch region, northwest Alberta, based on existing well-log data and refined trend surface analysis. Canadian Journal of Earth Sciences 46(1):41-65.

Michael, K., and Buschkuehle, B. 2008. Subsurface Characterization of Acid-Gas Injection Operations in the Peace River Arch area. Energy Resources Conservation Board ERCB/AGS, Calgary, Canada, Special Report (090):186 p.

Meijer Drees, N. 1994. Devonian Elk Point Group of the Western Canada Sedimentary Basin. *In* Geological Atlas of the Western Canada Sedimentary Basin. *Edited by* G. Mossop and I. Shetsen. Canadian Society of Petroleum Geologists and Alberta Research Council, Special Report 4: 129-138.

Moeck, I. 2012. Iterative Development of Stress Models for Deep Geothermal Reservoirs. *In* 74th EAGE Conference & Exhibition, Copenhagen, Denmark, 2012.

Moeck, I. 2014. Catalog of geothermal play types based on geologic controls. Renewable & Sustainable Energy Reviews (in press).

Moeck, I., and Beardsmore, G. 2014. A new 'geothermal play type' catalog: Streamlining exploration decision making. *In* Proceedings of the Thirty-Ninth Workshop on Geothermal Reservoir Engineering, Stanford University, Stanford, California, February 24-26, 2014, SGP-TR-202.

Moeck, I., Kwiatek, G., and Zimmermann, G. 2009a. Slip tendency analysis, fault reactivation potential and induced seismicity in a deep geothermal reservoir. Journal of Structural Geology 31(10): 1174-1182.

Moeck, I., Schandelmeier, H., and Holl, H-G. 2009b. The stress regime in a Rotliegend reservoir of the Northeast German Basin. International Journal of Earth Sciences 98(7):1643-1654.

Morris, A., Ferrill, D.A., and Henderson, D.B. 1996. Slip-tendency analysis and fault reactivation. Geology 24(3): 275-278.

Mossop, G., and Shetsen, I. 1994a. Introduction to the Geological Atlas of the Western Canada Sedimentary Basin. *In* Geological Atlas of the Western Canada Sedimentary Basin. *Edited by* G. Mossop and I. Shetsen. Canadian Society of Petroleum Geologists and Alberta Research Council, Special Report 4: 1-12.

Mossop, G.D., and Shetsen, I. 1994b. Geological atlas of the Western Canada Sedimentary Basin. Canadian Society of Petroleum Geologists and Alberta Research Council.

Muffler, L.J.P. 1979. Assessment of geothermal resources of the United States--1978. U.S. Geol. Surv., Circ.

Muffler, P., and Cataldi, R. 1978. Methods for regional assessment of geothermal resources. Geothermics 7(2): 53-89.

National Climate Data and Information Archive, N. 2000. Canadian Climate Normals 1971-2000. Available from http://climate.weatheroffice.gc.ca/climate_normals [accessed 28 February 2012].

Natural Resources Canada, N. 2009. Comprehensive Energy Use Database, 1990 to 2009. Available from http://oee.nrcan.gc.ca/corporate/statistics/neud/dpa/comprehensive_tables/index.cfm [accessed June 26 2012].

Natural Resources Canada, N. 2011. Energy use data handbook tables. Available from http://oee.nrcan.gc.ca/corporate/statistics/neud/dpa/handbook_res_ca.cfm?attr=0 [accessed December 2011].

Nicholson, K. 1993. Geothermal fluids. Springer, Berlin.

Nowlan, G., Hein, F., Coskun, S., Stasiuk, L., Fowler, M., Norford, B., Palmer, B., and Addison, G. 1995. Characterization of Cambrian and Ordovician strata in the subsurface of Alberta using lithostratigraphy, biostratigraphy, organic petrology and image analysis. CSPG Special Publications, pp. 217 – 236.

Oberösterreichischer Energiesparverband. 2014. Geothermie Altheim. Available from http://www.esv.or.at/foerderungen/oekostrom/beispiele/geothermie-altheim/ [accessed 29 April 2014].

O'Connell, S. 1994. Geological history of the Peace River arch. *In* Geological Atlas of the Western Canada Sedimentary Basin. *Edited by* G. Mossop and I. Shetsen. Canadian Society of Petroleum Geologists and Alberta Research Council, Special Report 4: 431-438.

O'Connell, S.C., Dix, G.R., and Barclay, J.E. 1990. The origin, history, and regional structural development of the Peace River Arch, Western Canada. Bulletin of canadian petroleum geology 38(1): 4-24.

Oldale, H., and Munday, R. 1994. Devonian Beaverhill Lake Group of the western Canada sedimentary basin. *In* Geological Atlas of the Western Canada Sedimentary Basin. *Edited by* G. Mossop and I. Shetsen. Canadian Society of Petroleum Geologists and Alberta Research Council, Special Report 4: 149-163.

Peška, P., and Zoback, M.D. 1995. Compressive and tensile failure of inclined well bores and determination of in situ stress and rock strength. J. Geophys. Res., 100: 12791–12811.

Pettijohn, F.F.J. 1987. Sand and sandstone. Springer, Heidelberg.

Pluymaekers, M., Kramers, L., van Wees, J., Kronimus, A., Nelskamp, S., Boxem, T., and Bonté, D. 2012. Reservoir characterisation of aquifers for direct heat production: Methodology and screening of the potential reservoirs for the Netherlands. Netherlands Journal of Geosciences-Geologie en Mijnbouw 91(4): 621-636.

Porter, J., Price, R., and McCrossan, R. 1982. The western Canada sedimentary basin. Philosophical Transactions of the Royal Society of London. Series A, Mathematical and Physical Sciences 305(1489): 169-192.

Price, R. 1994. Cordilleran tectonics and the evolution of the Western Canada Sedimentary Basin. *In* Geological Atlas of the Western Canada Sedimentary Basin. *Edited by* G. Mossop and I. Shetsen. Canadian Society of Petroleum Geologists and Alberta Research Council, Special Report 4: 13-24.

Pugh, D.C. 1971. Subsurface Cambrian stratigraphy in southern and central Alberta. Geological Survey of Canada, Dept. of Energy, Mines and Resources, Ottawa.

Pugh, D.C. 1973. Subsurface lower Paleozoic stratigraphy in northern and central Alberta. Geological Survey of Canada, Dept. of Energy, Mines and Resources, Ottawa.

Rebscher, D., Zhou, Q., and Birkholzer, J.T. 2012. Simulation of CO2 storage in the Basal Aquifer in the Northern Plains - Prairie region of North America. *In* TOUGH2 Symposium 2012, Lawrence Berkeley National Laboratory, Berkeley, California, September 17-19, 2012.

Richards, B., Barclay, J., Bryan, D., Hartling, A., Henderson, C., and Hinds, R. 1994. Carboniferous strata of the Western Canada sedimentary basin. *In* Geological Atlas of the Western Canada Sedimentary Basin. *Edited by* G. Mossop and I. Shetsen. Canadian Society of Petroleum Geologists and Alberta Research Council, Special Report 4: 221-250.

Roduit, N. 2008. JMicroVision: Image analysis toolbox for measuring and quantifying components of high-definition images. Version 1.2.7. Available from http://www.jmicrovision.com [accessed 22 October 2013].

Rollin, K. 2003. Low-temperature geothermal energy. Earthwise Issue 19: Energy and mineral resources, British Geological Survey BGS, 24-25.

Sanyal, S.K. 2005. Classification of Geothermal Systems–A possible scheme. *In* Transactions of the Thirtieth Workshop on Geothermal Reservoir Engineering, Stanford University, Stanford, California, January 31-February 2, 2005, SGP-TR-176. p. 8.

Schellschmidt, R., Sanner, B., Jung, R., and Schulz, R. 2010. Geothermal energy use in Germany. *In* Proceedings World Geothermal Congress 2010, 25-29 April, Bali, Indonesia.

Schmitt, D.R., Currie, C.A., and Zhang, L. 2012. Crustal stress determination from boreholes and rock cores: Fundamental principles. Tectonophysics 580:1-26. doi:http://dx.doi.org/10.1016/j.tecto.2012.08.029

Schön, J. 2011. Physical Properties of Rocks: A Workbook. Elsevier, Amsterdam.

Shell. 2010a. Quest Carbon Capture and Storage Project; Directive 65: Application for a CO2 acid gas storage scheme. Available from http://s05.static-shell.com/content/dam/shell-new/local/country/can/downloads/pdf/aboutshell/our-business/oil-sands/quest/d65-main-report-appai.pdf [accessed 6 January 2014].

Shell. 2010b. Quest CCS Project. Available from http://www-static.shell.com/static/investor/downloads/news_and_library/quest_ccs_project_overview.pdf [accessed 29 August 2012].

Shell. 2011. Quest Carbon Capture and Storage Project; update to directive 65: Application for a CO2 acid gas storage scheme. Available from http://s08.static-shell.com/content/dam/shell-new/local/country/can/downloads/pdf/aboutshell/our-business/oil-sands/quest/quest-d65-updatejune2011.pdf [accessed 6 January 2014].

Siegesmund, S., and Snethlage, R. 2011. Stone in architecture: properties, durability. Springer, Heidelberg.

Sippel, J., Fuchs, S., Cacace, M., Braatz, A., Kastner, O., Huenges, E., and Scheck-Wenderoth, M. 2013. Deep 3D thermal modelling for the city of Berlin (Germany). Environmental Earth Sciences 70(8):3545-3566.

Slind, O., Andrews, G., Murray, D., Norford, B., Paterson, D., Salas, C., and Tawadros, E. 1994. Middle Cambrian to Lower Ordovician strata of the Western Canada Sedimentary Basin. *In* Geological Atlas of the Western Canada Sedimentary Basin. *Edited by* G. Mossop and I. Shetsen. Canadian Society of Petroleum Geologists and Alberta Research Council, Special Report 4: 87-108.

SPE-PRMS. 2007. Society of Petroleum Geologists, Petroleum Resources Management System Guide for non-technical users, 1-4. Available from http://www.spe.org/industry/docs/PRMS_guide_non_tech.pdf [accessed 13 May 2014].

Sproule Associates Limited. 1976. Report on study of geothermal resources in western Canadian sedimentary basins from existing data, phase one, the Sproule Report. Earth Physics Branch, Energy, Mines and Resources Canada, Open File 77- 13, 110 p.

Sproule Associates Limited. 1977. Report on study of geothermal resources in western Canadian sedimentary basins from existing data, phase two, theSproule Report. Earth Physics Branch, Energy, Mines and Resources Canada, Open File 77- 14, 127 p.

Stoakes, F. 1988. Evolution of the Upper Devonian of western Canada. *In* Principles and Concepts for the Exploration of Reefs in the Western Canada Basin. *Edited by* GR Bloy and M. Charest. Short Course Notes, Canadian Society of Petroleum Geologists, Calgary, Canada.

Stober, I., and Bucher, K. 2012. Geothermie. Springer DE.

Subramanya, K. 1994. Engineering hydrology. Tata McGraw-Hill Education, New-Delhi.

Switzer, S., Holland, W., Christie, D., Graf, G., Hedinger, A., McAuley, R., Wierzbicki, R., and Packard, J. 1994. Devonian Woodbend-Winterburn strata of the Western Canada sedimentary basin. *In* Geological Atlas of the Western Canada Sedimentary Basin. *Edited by* G. Mossop and I. Shetsen. Canadian Society of Petroleum Geologists and Alberta Research Council, Special Report 4: 165-202.

Talman, S., Perkins, E., Wigston, A., Ryan, D., and Bachu, S. 2013. Geochemical Effects of Storing CO2 in the Basal Aquifer that Underlies the Prairie Region in Canada. Energy Procedia 37: 5570-5579.

Tischner, T., Pfender, M., and Teza, D. 2006. Hot Dry Rock Projekt Soultz: Erste Phase der Erstellung einer wissenschaftlichen Pilotanlage. Abschlussbericht zum Vorhaben 0327097, Bundesministerium für Umwelt, Naturschutz und Reaktorsicherheit, 1.4.2001-31.3.2005.

Trautwein, U., and Huenges, E. 2005. Poroelastic behaviour of physical properties in Rotliegend sandstones under uniaxial strain. International Journal of Rock Mechanics and Mining Sciences 42(7): 924-932.

Trotter, R.D. 1989. Sedimentology and depositional setting of the Granite Wash of the Utikuma and Red Earth areas, north-central Alberta. Dalhousie University, Halifax, Nova Scotia, Canada.

Tucker, M.E. 2009. Sedimentary petrology: an introduction to the origin of sedimentary rocks. Wiley-Blackwell, Oxford.

Turcotte, D.L., and Schubert, G. 2002. Geodynamics. Cambridge University Press.

Vigrass, L. 1979. Final well report, U or R Regina 3-8-17-19 (W.2nd.Mer.) Saskatchewan. Earth Physics Branch Open File, vol 79-9. Regina, Saskatchewan, Canada.

Vigrass, L., Kent, D., and Leibel, R. 1978. Low-grade geothermal project, geological feasibility study, Regina-Moose Jaw area, Earth Physics Branch Open File, vol 78-4. Regina, Saskatchewan, Canada.

Vigrass, L.W., Jessop, A.M., and Brunskill, B. 2007. Regina geothermal project. *In* Summary of investigations. Saskatchewan Geological Survey, Regina, SK, p A–2. Regina, Saskatchewan, Canada.

Walls, R., and Burrowes, O. 1990. Diagenesis and reservoir development in Devonian limestone and dolostone reefs of western Canada. *In* The Development of Porosity in Carbonate Reservoirs. *Edited by* GR Bloy and MG Hadley. Canadian Society of Petroleum Geologists, Continuing Education Short Course Notes, section 7: 1-13.

Walsh, W. 2013. Geothermal resource assessment of the Clarke Lake Gas Field, Fort Nelson, British Columbia. Bulletin of canadian petroleum geology 61(3): 241-251.

Weides, S. and Majorowicz, J. 2014. Implications of spatial variability in heat flow for geothermal resource evaluation in large foreland basins: the case of the Western Canada Sedimentary Basin. Energies 7(4): 2573-2594. doi:10.3390/en7042573.

Weides, S., Moeck, I., Majorowicz, J., Palombi, D., and Grobe, M. 2013. Geothermal exploration of Paleozoic formations in Central Alberta. Canadian Journal of Earth Sciences 50(5): 519-534. doi: 10.1139/cjes-2012-0137.

Weides, S., Moeck, I., Schmitt, D., and Majorowicz, J. 2014. An integrative geothermal resource assessment study for the siliciclastic Granite Wash unit, north western Alberta (Canada). Environmental Earth Sciences, published online first 10 May 2014, doi: 10.1007/s12665-014-3309-3.

Weides, S., Moeck, I., Majorowicz, J., and Grobe, M. (submitted for publication). The Cambrian Basal Sandstone Unit in central Alberta – an investigation of temperature distribution, petrography and hydraulic and geomechanical properties of a deep saline aquifer. Submitted to Canadian Journal of Earth Sciences (under revision).

Wendte, J. 1994. Cooking Lake platform evolution and its control on Late Devonian Leduc reef inception and localization, Redwater, Alberta. Bulletin of canadian petroleum geology 42(4): 499-528.

Williams, C.F. 2007. Updated methods for estimating recovery factors for geothermal resources. *In* Proceedings of the Thirty-Second Workshop on Geothermal Reservoir Engineering, Stanford University, Stanford, California, SGP-TR-183, 411–420.

Williams, C.F., Reed, M.J., and Anderson, A.F. 2011. Updating the classification of geothermal resources. *In* Proceedings of the thirty-sixth Workshop on Geothermal Reservoir Engineering Stanford University, Stanford, California, January 31 - February 2, 2011 SGP-TR-191.

Williams, C.F., Reed, M.J., and Mariner, R.H. 2008. A review of methods applied by the US Geological Survey in the assessment of identified geothermal resources. US Geological Survey Open-File Report 1296: 27.

Wong, T., David, C., and Zhu, W. 1997. The transition from brittle faulting to cataclastic flow in porous sandstones: Mechanical deformation. Journal of Geophysical Research: Solid Earth (1978–2012) 102 (B2):3009-3025.

Wright, G., McMechan, M., and Potter, D. 1994. Structure and architecture of the Western Canada sedimentary basin. *In* Geological Atlas of the Western Canada Sedimentary Basin. *Edited by* G. Mossop and I. Shetsen. Canadian Society of Petroleum Geologists and Alberta Research Council, Special Report 4: 25-40.

Wyman, R., Holditch, S., and Randolph, P. 1980. Analyses of an Elmworth hydraulic fracture in Alberta. Journal of Petroleum Technology 32(9):1621-1630.

Zang, A.H., and Stephansson, O.J. 2010. Stress field of the Earth's crust. Springer, Heidelberg.

Zhang, X., Sanderson, D.J., Barker, A.J. 2002. Numerical study of fluid flow of deforming fractured rocks using dual permeability model. Geophysical Journal International 151(2):452-468.

Zhang, X., Koutsabeloulis, N., and Heffer, K. 2007. Hydromechanical modeling of critically stressed and faulted reservoirs. AAPG Bulletin-American Association of Petroleum Geologists 91(1):31-50.

Zoback, M. 2007. Reservoir mechanics. Cambridge Press, Cambridge.